TU Delft

Delft University of Technology

Faculty of Civil Engineering
Department Hydraulic Engineering

Laboratory observations and calculations
of the depth averaged flow patterns in a
square harbor on a tidal river.

E.J. Langendoen

Report no. 8-89

Laboratory of Fluid Mechanics
Department of Civil Engineering
Delft University of Technology
Delft, The Netherlands

Contents

1. Introduction

Many harbors in the world suffer from siltation in their basins and in many cases removal of the deposited sediment leads to high costs. This siltation results from a net transport of sediment into the harbor caused by the water motion in the harbor entrance. The water motion is very complex and of a three-dimensional nature. Three main mechanisms can be distinguished: (1) exchange in consequence of water flowing along the mouth of the harbor and the resulting eddies in the harbor entrance, (2) exchange in consequence of variations in water level of the adjacent waterbody (e.g. sea, estuary or river), and (3) exchange in consequence of a density difference between harbor and adjacent waterbody. For a more extensive discussion of the problem see Langendoen (1988).

The first two mechanisms are being examined in a physical model in the Laboratory of Fluid Mechanics of the Delft University. Measurements were made to generate a dataset by which numerical models of the flow in harbor entrances can be tested. A more distant goal of this project is to obtain insight in the influence of the geometry of the entrance on siltation of the harbor. The first part of the research is discussed in this report. It concerns the water motion in a square harbor due to an oscillatory flow in the adjacent waterbody (here a tidal river). The time-varying depth averaged flow patterns in the harbor have been measured. These flow patterns are then compared to the results of preliminary calculations with a numerical model that solves the shallow water equations.

The measurements in the physical model are discussed in section two and the results of the numerical calculations in section three, while in section four the results of both models are compared. Finally in section five some conclusions follow.

Further measurements, that is local velocity measurements and the dispersion of heated water, will be dealt with in a subsequent report.

2. Physical model

2.1 Introduction

A physical model was constructed to examine the influence of the shape of the harbor entrance on the velocity field and the turbulence in the entrance due to a homogeneous oscillatory flow — representing the tide — in the river.

The model consists of a basin in which various geometries of harbor entrances can be examined, and an adjacent flume representing a river in which a tidal current is generated (see fig. 2.1). The flume has a length of 18 m and a width of 1 m. The basin has a length of 4 m and a width of 2 m. The bottom of river and basin is horizontal, the sidewalls are vertical, and the water depth was 0.11 m. The flow in the flume is generated by a constant water supply and an adjustable sharp-crested weir at each end of the flume. The angular motion of the weirs is controlled using servo-motors generating a sinusoidal flow in the flume. When the motion of the weirs is in phase there is no vertical tide in the flume. A vertical tide can be generated by introducing a difference in phase between the weirs.

If we think of the model as representing a typical harbor in the Rotterdam Harbor Area, the length and depth scales are of the order 200. Using conventional Froude law scaling would yield a velocity scale of 14. As a result, assuming a maximum water velocity in the field of 1 m/s, the maximum Reynolds number in the harbor would be 2750, which is not sufficient to maintain a turbulent flow. Scaling according to the Reynolds number criterion would yield a velocity scale of 0.0057, and a maximum Froude number in the flume of 170. As a compromise the velocity scale is chosen to be 2.5, yielding a maximum Froude number in the flume of 0.37 and a maximum Reynolds number in the harbor of 15000.

This requirement was met by supplying a constant flow rate of 65 ℓ/s at each end of the flume, and varying the discharge over the weirs between ca. 23 ℓ/s and 107 ℓ/s. As a result, the amplitude of the discharge in the flume is 42 ℓ/s.

The research reported is concerned with a square harbor of 1 m^2 with an entrance width of 1 m and vertical sidewalls (see fig. 2.2). No vertical

tide was present.

The period, T, of the semi-diurnal tide, when scaled using the Strouhal number criterion, would be of the order 1000 s. However, to speed up the experiments, shorter periods of 250 s and 500 s were also examined. The period is chosen to be at least four times the time, T_e, the flow pattern in the harbor needs to adapt to a change in the flow in the river. Based on experiments in steady flow, Booij (1986) gives for this time:

$$T_e \simeq 50b^2 \frac{L_e B}{U_r B_m}$$

where L_e is the length of the eddy in the harbor, B the width of the harbor, U_r the velocity in the river, B_m the width of the harbor entrance and b a constant varying from ca. 0.4 to 1 depending on the harbor geometry.

For a square harbor with $B_m=B=L_e=1$ m, $U_r=0.38$ m/s and b=0.59, T_e equals 46 s. Taking into account some inaccuracy, a period of 250 s should be adequate . However, since various harbor geometries are planned to be examined, a larger period of 500 s was selected as a reference value throughout the research in the laboratory.

2.2 Measuring method and results

Floats have been used to determine the depth averaged velocities in the harbor entrance. The floats used penetrated most of the water column. The clearance from the bottom was 0.5 cm. They were made of PVC pipes with a diameter of 15 mm and partially filled with sand.

After the floats had been placed in the harbor, their movements were recorded on video. Four times a second an image from the tape was digitized on a computer, and the positions of the floats were determined. From these positions the velocities of the floats could be computed (e.g. by central differencing in time). It is assumed that the velocity of a float equals the depth averaged flow velocity at its position.

The flow patterns in the course of time for a period of 500 s are shown in figures 2.3.a to k. It was verified that the flow patterns reproduced each period. Therefore each of these figures could be composed using several recordings. Figures 2.3.a to d show the flow patterns just after maximum current ($\frac{1}{4}T=125$ s) in the river, while figures 2.3.e to k show the flow patterns just before and after slack water ($\frac{1}{2}T$).

During maximum current in the river a single eddy exists in the harbor. Its center is approximately positioned in the center of the harbor. From these figures it can be concluded that the water motion is quasi-steady at this stage of the tide.

The figures 2.3.e and f show that, when the velocity in the river decreases to that in the eddy, the eddy increases in size and its center moves towards the river.

After slack water (250 s), when the flow direction in the river is reversed, the flow is guided from the river into the harbor by the rotation of the eddy and water is flowing out of the harbor at its downstream side, see fig. 2.3.g. When the velocity in the river increases a new eddy starts to develop at the upstream corner of the harbor entrance, and the old eddy is squeezed and breaks up into two parts. One part is transported with the flow in the river while the other part is pushed back into the harbor by the new eddy. This eddy is growing while moving towards the downstream side of the harbor (see fig. 2.3.h and i). The eddy increases further in size and after some time occupies the complete harbor (see fig. 2.3.j and k); this flow pattern is the reverse of that in figures 2.3.a to d.

The flow patterns for the periods 250 s and 1000 s are shown in figures 2.4.a to j and 2.5.a to j, respectively. Figures 2.4.a to d and 2.5.a to d show the flow patterns around maximum current (¾T) while figures 2.4.e to j and 2.5.e to j show the flow patterns just before and after slack water (T and ½T, respectively).

The flow patterns around maximum current in the river for the periods 250 s and 1000 s show a single eddy in the harbor. These patterns are similar to those shown before for the period of 500 s, except that the center of the eddy in the case with a period of 250 s is positioned besides the center of the harbor at first (see fig. 2.4.a and b) but then moves towards the center (see fig. 2.4.c and d). Apart from that, the flow for both periods appears quasi-steady during this stage of the tide. However, before slack water the flow velocities in the harbor are a little higher for a period of 250 s and a little smaller for a period of 1000 s in comparison with the velocities for a period of 500 s (see figures 2.3.e 2.4.e and 2.5.e). More time is available for the flow in the harbor to adapt itself to the decelerating flow in the river when the period is larger.

After slack water, the same phenomena, that is the development of a new eddy and the destruction of the old eddy, can be noticed as in the case of a period of 500 s. However, the figures also show (e.g. 2.3.h, 2.4.h and 2.5.h) that the development of the new eddy has progressed further for the larger period at equal phases. The differences between the periods of 250 s and 500 s are larger than those between the periods of 500 s and 1000 s.

To get a correct reproduction of the phenomena occurring in the harbor entrance with a semi-diurnal tidal period (see section 2.1), the new eddy has to reach its ultimate shape (occupation of the complete harbor and with its center approximately coinciding with the center of the harbor) before maximum current in the river. This is the case for the periods of 500 s and 1000 s, but only approximately so for the period of 250 s.

The last observation indicates that the requirements as to the scaled tidal period are slightly more severe than discussed on page 3, where it was indicated that a period of 250 s should suffice.

3. Mathematical models

3.1 Introduction

Prior to the experiments discussed in the preceding section, two kinds of numerical computations have been performed. The aim of these computations was to simulate the water movement and the transport of matter that would occur in the physical model. The two numerical models are depth averaged ones, and were developed by the Hydraulics Group (Department of Civil Engineering, Delft University of Technology). The first model, DUCHESS, solves the two-dimensional shallow water equations and the second, ESTRA, solves the depth averaged convection-diffusion equation. The velocity field computed by DUCHESS is used as input for ESTRA. For a more elaborate discussion of the models see Booij (1989[a]) and Sokolewicz & Booij (1988).

The harbor geometry in the numerical computations has the same dimensions as in the physical model. However, there are two differences: (1) the water depth equals 0.10 m instead of 0.11 m as used in the laboratory model, and (2) the amplitude of the discharge is 50 ℓ/s instead of 42 ℓ/s.

Eight runs have been made with DUCHESS in which the period, eddy viscosity and gridsize were varied to examine their influences. The selected values of these parameters are listed in table 3.1.

Table 3.1 Values of parameters in runs with DUCHESS.

Run	T0	T1	T2	T3	T4	T5	T6	T7
period [s]	500	500	500	500	250	375	750	500
eddy viscosity [m^2/s]	5E-4	5E-3	1E-3	u_*h [1]	5E-4	5E-4	5E-4	5E-4
gridsize [m]	0.10	0.10	0.10	0.10	0.10	0.10	0.10	0.05

---

[1] A u_*h formulation is used for this run. See section 3.2 for further details.

Run T0 has been used as a reference run in this study.

The schematization of the model is shown in fig. 3.1. The open boundaries are represented as velocity boundaries and are weakly reflecting. At the closed boundaries the velocity normal to the boundary equals zero. Partial slip was applied for the tangential velocities to obtain the correct magnitude of the shear stress at the wall. The coefficient of Chézy was kept constant at 50 $m^{\frac{1}{2}}/s$. (For comparison, the Chézy-coefficient determined from steady-flow measurements in the physical model was 51.1 $m^{\frac{1}{2}}/s$.)

The influences of the eddy viscosity, period, and gridsize on the flow pattern in the harbor are discussed in the sections 3.2, 3.3, and 3.4, respectively. The results of the computations with ESTRA are discussed in section 3.5.

3.2 Influence of the eddy viscosity

The influence of the eddy viscosity can be examined from the runs T0, T1, T2, and T3. A constant eddy viscosity of 5.0E-4 m^2/s has been used as a reference value. This value results from calculations by Booij (1989[b]) with a mathematical model using a k-ϵ formulation to model the turbulence. In these calculations a steady flow (of the same magnitude as in this research) in a similar harbor has been examined.

A constant eddy viscosity has also been used in runs T1 (5.0E-3 m^2/s) and T2 (1.0E-3 m^2/s). In the fourth run, T3, the eddy viscosity has been modelled via a $u_x h$ formulation. In the numerical model this can be done using the formulation: $\nu_t = C|q|+D$, where C and D are constants and q=uh with u the depth averaged velocity and h the water depth. The constant C is derived from formulations given by Lean & Weare (1979) and Rodi (1980). Lean and Weare give for the average eddy viscosity in the shear layer at the transition from river to harbor $\nu_t = 0.0017 U_0 x$, where U_0 is the velocity along the center axis of the shear layer and x the axial distance from the origin of the shear layer. According to Rodi the depth averaged eddy viscosity for turbulence generated at the bed is $\nu_t = 0.1 u_x h$, where u_x is the shear velocity. The eddy viscosity in the shear layer has approximately the same magnitude, when averaged over the shear layer, as that for bed generated turbulence. Therefore C was fixed at 7.0E-3 (with $u_x \approx 0.07u$). To prevent the eddy viscosity from becoming zero, the constant D was given a value of 1.0E-5 m^2/s.

The flow patterns for the four runs at 175 s, 200 s, 225 s, 250 s (slack water), 275 s, 300 s, 325 s, and 350 s are shown in figures 3.2.a to 3.2.h.

The flow patterns in run T1 differ clearly from the flow patterns in runs T0, T2, and T3. The flow velocities in the harbor are much smaller, which is caused by the high eddy viscosity that is used in this run. Also the development of the new eddy after slack water and the movement of its center differ in run T1.

It may be concluded from these runs that the influence of the eddy viscosity on the flow patterns in the harbor is: (1) the higher the eddy viscosity, the lower the velocities in the eddy, (2) the length of the path travelled by the center of the eddy is smaller when the eddy viscosity is

higher (longest path for the u_*h formulation), (3) the increase in size of the eddy just before slack water is larger for smaller eddy viscosities.

3.3 Influence of the period

The runs T0, T4, T5, and T6 have been used to study the influence of the period on the flow patterns in the harbor entrance. In all four runs the eddy viscosity and gridsize have been kept the same, 5.0E-4 m^2/s and 0.10 m, respectively. The periods examined are 250 s (run T4), 375 s (run T5), 500 s (run T0), and 750 s (run T6). The flow patterns are plotted in figures 3.3.a to 3.3.h at times 0.35*T, 0.40*T, 0.45*T, 0.50*T, 0.55*T, 0.60*T, 0.65*T, and 0.70*T (where T is the period).

There is little difference between the runs around maximum current in the river. Differences arise after slack water during the development of the new eddy. Figures 3.3.f to 3.3.h show that the smaller the period, the slower the process of the development of the new eddy at equal phases. The phase difference between the growth of this eddy and the accelerating flow in the river after slack water increases as the period decreases. The same occurred in the physical model (see section 2.2).

3.4 Influence of the gridsize

Runs T0 and T7 show the influence of the gridsize on the calculated flow
patterns in the harbor entrance. The gridsize in run T0 is 0.10 m and in
run T7 0.05 m. The eddy viscosity and period are kept constant, $5.0E-4$ m^2/s
and 500 s, respectively. The flow patterns are plotted in figures 3.4.a to
3.4.h for the times given in section 3.2.

Around maximum current in the river there is little difference between the
two runs. After slack water the process of the development of the new eddy
lags more behind the increase in water velocity in the river for the
coarser grid. When comparing the flow patterns of run T6 (see previous
section) and run T7, the flow patterns seem to be quite similar.

The conclusion from these figures must be that the gridsize of 0.10 m was
too coarse to predict the time scales of the phenomena arising after slack
water.

3.5 Calculations with the ESTRA model

The numerical model ESTRA solves the depth averaged convection-diffusion equation using the flow field computed by DUCHESS as input.

The exchange between a harbor and a river of a well-mixed solute was simulated with ESTRA using run T7. At maximum current in the river, the harbor is uniformly filled with a solute with a concentration of 50 mg/ℓ, and the changes in concentration in the harbor and the river are computed (the flow fields from ¼T and after have been used). Two different formulations to model the dispersion have been considered, namely a constant, isotropic dispersion coefficient and a formulation with a variable, anisotropic dispersion coefficient according to Elder.

On the basis of Reynolds' analogy the constant dispersion coefficient should have a value of 5.0E-4 m^2/s. However, using this value the cell Péclet number locally became larger than two. Instability of the computation resulted, because the advection terms are discretisized by central differences. Therefore a minimum value of 5.0E-3 m^2/s had to be used. This value was applied in the streamwise direction as well as the transverse direction (isotropic dispersion). The results of the computation with this value at times 375 s, 400 s, 425 s, 450 s, 475 s, 0 s (slack water), 5 s, 35 s and 60 s are shown in figures 3.5.a to 3.5.i.

At the downstream side of the harbor, new water from the river enters the harbor and flows along the walls further into the harbor (see fig. 3.5.b). The highest concentrations are found besides the center of the harbor. The figures also show that the diffusion of the solute in the harbor and in the shear layer is quite fast. During and just after slack water the model predicts too large values for the concentrations at the downstream corner of the harbor entrance (see figures 3.5.f and 3.5.g). Here the flow near the wall converges, the solute is being collected and the maximum concentration increases as time elapses, which is impossible. However when the flow velocity in the river increases, this cloud of solute is washed away with the river flow. New water enters the harbor again and the highest concentrations occur at the back of the harbor (see figures 3.5.h and 3.5.i).

The expression for the streamwise dispersion coefficient given by Elder

(1959) is $D_t \approx 6u_* h$. The transverse dispersion coefficient is taken an order of magnitude smaller, $D_t = 0.5u_* h$. Thus the dispersion is anisotropic for this formulation. The cell Péclet number in this computation will be approximately:

$$Pe_{\Delta x} = \frac{u\Delta x}{D_t} = \frac{u\Delta x}{6u_* h} = \frac{16u\Delta x}{6uh} = 1.33$$

where the gridsize $\Delta x = 0.05$ m and the water depth $h = 0.10$ m. This value is less than 2, and hence the computation is stable.

The results of the computation are shown in figures 3.6.a to 3.6.j.

With the variable, anisotropic dispersion model, it is found that new water enters the harbor from the river at the downstream corner of the harbor entrance and flows along the walls further into the harbor, just as in the computation with the constant isotropic dispersion coefficient. In comparison with the former calculations, the diffusion of the solute is much slower, especially in the transverse direction, and, until slack water, the highest concentrations occur in the center of the harbor. As a result, the exchange between harbor and river is also less. The exchanged solute stays also nearer to the wall in the river.

The properties of the eddy can be recognized from the figures. Fig. 3.6.e shows that the eddy begins to move into the direction of the river, as a result of which more solute is being exchanged between harbor and river.

The problem of too large concentrations during slack water in the computation with constant dispersion coefficient does not occur in this computation (compare figures 3.5.f and g with 3.6.f and g). Around slack water a high convective transport of solute from harbor to river develops. After slack water the new eddy transports new water into the harbor, which pushes the remaining part of the old eddy containing the solute back into the harbor (see fig. 3.6.h). When the new eddy increases in size, the new water mixes with the water containing the solute (see fig. 3.6.j) and in contrast with the start of the computation, the lowest concentrations now are found in the center of the harbor and the highest concentrations near the walls.

4. Comparison of the results of physical and the mathematical models

A comparison between the results of the physical model and the mathematical model can be made because both the measurements in the physical model and the computations with the DUCHESS model yield depth averaged velocities. The results of run T7 with the fine grid have been compared to the results of the measurements in the physical model which had a period of 500 s.

The results of the physical model and the mathematical model cannot be compared directly, because the amplitudes of the velocity in the river are different. This causes a difference in magnitude of the velocities in the harbor. The flow velocity in the eddy is proportional to the velocity in the river (e.g. Booij (1986); Dursthoff (1970)), hence normalizing the measured and computed velocities with the amplitude of the velocity in the river should give comparable velocities in the harbor. In the physical model the amplitude of the velocity in the river is 0.38 m/s and in the mathematical model 0.50 m/s. The velocities of the randomly positioned floats have been transformed to velocities on a regular grid (the grid used in run T7) through linear interpolation. The various flow patterns are shown in figures 4.1.a to j. Observed velocities in grid points that had to be calculated through extrapolation are not shown.

All figures show much the same flow patterns in physical and mathematical models. The sizes of the different eddies and the positions of their centers are quite similar. However, the mathematical model slightly overpredicts the velocities in the eddy after maximum current in the river until slack water. When the new eddy arises after slack water the velocities in the eddy are underpredicted by the mathematical model. The small eddies observed in the back corners of the harbor cannot be simulated by the mathematical model, because the grid is too coarse.

To examine the differences in the computed and measured velocities, normalized velocity profiles of the velocity v, in y-direction, along a transect in x-direction through the center of the eddy (the position of which changes in the course of time) are shown in figure 4.2. Before slack water (t=250 s) the computed velocities are larger near the sidewalls of the harbor. The predicted velocities increase almost linearly from the center of the eddy to the sidewalls, whereas the measured velocities tend to reach an almost constant value near the walls. A possibility to decrease the computed velocities near the harbor sidewalls may be to reduce the

amount of (partial) slip applied.

The differences between the distributions are more distinct just after slack water, especially at 275 s. This is mainly caused by the incorrect position of the center of the eddy in the mathematical model. If the computed velocity distribution is shifted somewhat to the right, it will fit the measured velocity distribution better. However, the velocities are still underpredicted. At 300 s the velocity distribution is correct, but the magnitude is slightly underpredicted.

5. Conclusions

The research that has been discussed in this report concerned the first part of an on-going study — using both physical and mathematical models — on the siltation of tidal harbors. The study is mainly focussed on the water motion in the harbor entrance, which causes the siltation. As yet, too little is known about this complicated time-dependent water motion.

In this report a simple geometry of the tidal river and the harbor was considered as a first step. Depth averaged flow patterns were measured and calculated. The phenomena which occurred in the harbor entrance around and after slack water may be important for the exchange of matter between harbor and river. Large parcels of water from the river are exchanged with water from the harbor. This convective exchange is much larger than the exchange around maximum current in the river, when there is only a turbulent transport through the shear layer at the transition between harbor and river. The mathematical model ESTRA, which has been used to study the exchange of a well-mixed solute, also predicted this behavior.

The progress of the phenomena after slack water (e.g. the development of the new eddy) depends on the period of the oscillatory flow in the river. The phase difference between the development of the eddy and the accelerating flow in the river increases as the period decreases. This is shown by both physical and mathematical models.

Taking into account the fact that the numerical calculations were made before the experiments had been performed, and consequently tuning of the various parameters in the mathematical model was not possible, the similarities between the results of the physical and mathematical models are quite satisfactory. The flow patterns in the course of time are predicted correctly by the mathematical model, and the calculated water velocities in the harbor are close to the measured values.

Future research comprises the measurement of flow patterns and dispersion of heated water in harbor entrances of various geometries.

References

Booij, N. (1989[a]), "USER MANUAL FOR THE PROGRAM DUCHESS Delft University Computer program for 2-dimensional Horizontal Estuary and Sea Surges.", Department of Civil Engineering, Delft University of Technology.

Booij, R. (1986), "Metingen van uitwisselingen tussen rivier en haven.", report no. 9-86 (three parts), Department of Civil Engineering, Delft University of Technology.

Booij, R. (1989[b]), "Depth averaged k-ϵ model in ODYSSEE.", report no.1-89, Department of Civil Engineering, Delft University of Technology. (in preparation)

Elder, J.W. (1959), "The Dispersion of Marked Fluid in Turbulent Shear Flow", Journal of Fluid mechanics, Vol.5, No. 4, pp. 544-560.

Dursthoff, W. (1970), "Über den quantitativen Wasseraustausch zwischen Fluss und Hafen.", Mitteilungen des Franzius-Instituts für Grund- und Wasserbau der Technischen Universität Hannover, heft 34, pp. 194-368.

Langendoen, E.J. (1988), "Waterbeweging en massatransport in havenmonden – een literatuuronderzoek.", report no. 13-88, Department of Civil Engineering, Delft University of Technology.

Lean, G.H. & Weare, T.J. (1979), "Modelling two-dimensional circulating flow.", J.Hydr.Div., ASCE, 105, HY1, pp. 17-26.

Rodi, W. (1980), "Turbulence models and their application in hydraulics.", Monograph, International Association for Hydraulic Research, Delft, The Netherlands.

Sokolewicz, M.J. & Booij, N. (1988), "USER GUIDE FOR THE PROGRAM ESTRA Delft University Computer program for 2-dimensional Horizontal Transport of Matter due to Estuary and Sea Surges.", Department of Civil Engineering, Delft University of Technology.

Notation

B	width of the harbor
B_m	width of the harbor entrance
b	constant depending on the harbor geometry
C	constant
D	constant
D_t	dispersion coefficient
h	water depth
L_e	length of the eddy
$Pe_{\Delta x}$	cell Péclet number
q	discharge per unit width
T	tidal period
T_e	time scale of the development of the eddy
t	time
U_0	velocity along the center axis of the shear layer
U_r	velocity in the river
u, v	two components of the depth averaged velocity in x and y-direction
u_*	shear velocity
x, y	cartesian co-ordinates
Δx	gridsize
ν_t	eddy viscosity

FIGURES

Figure 2.1

L=1.0 m

B=1.0 m

x,u

y,v
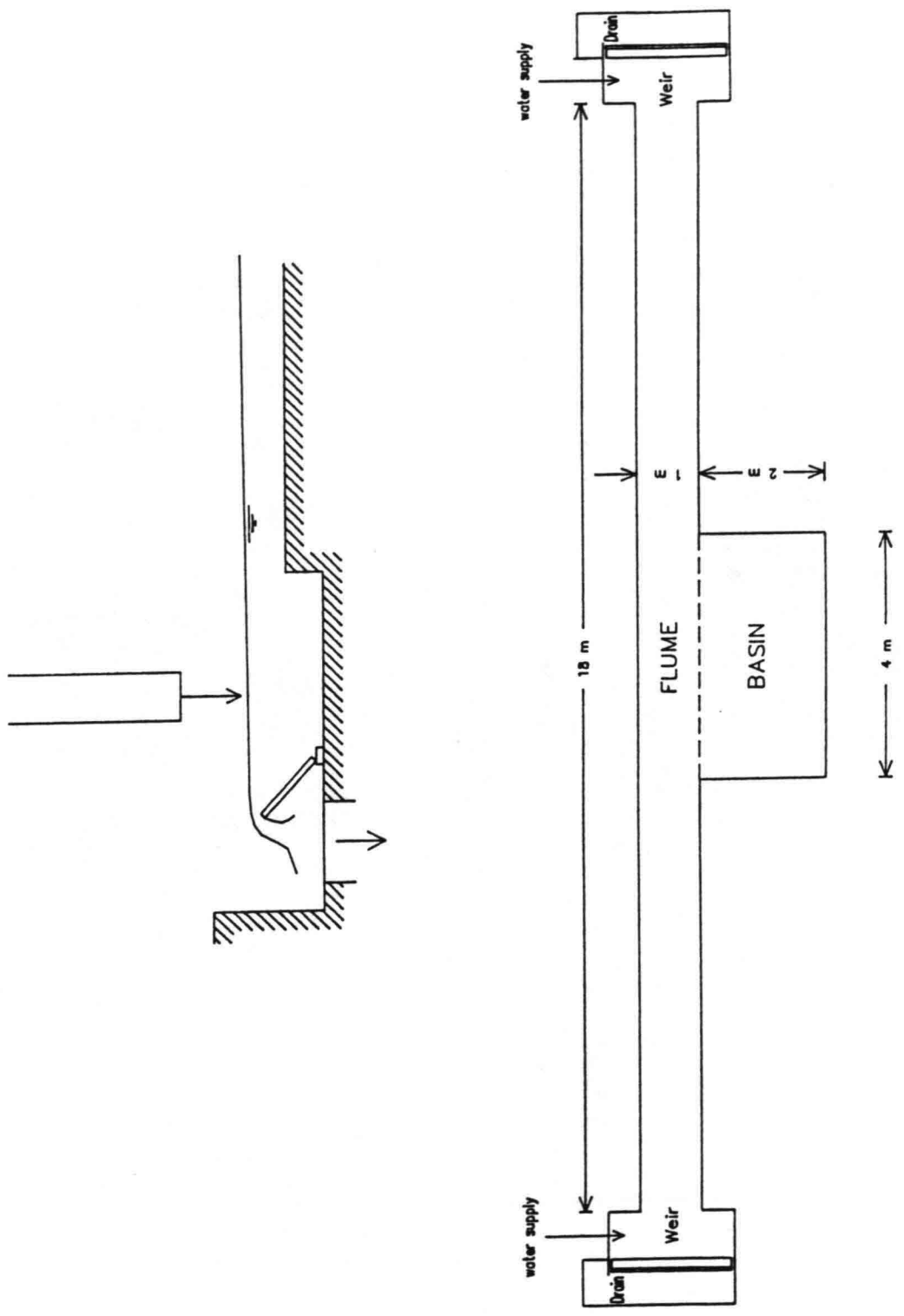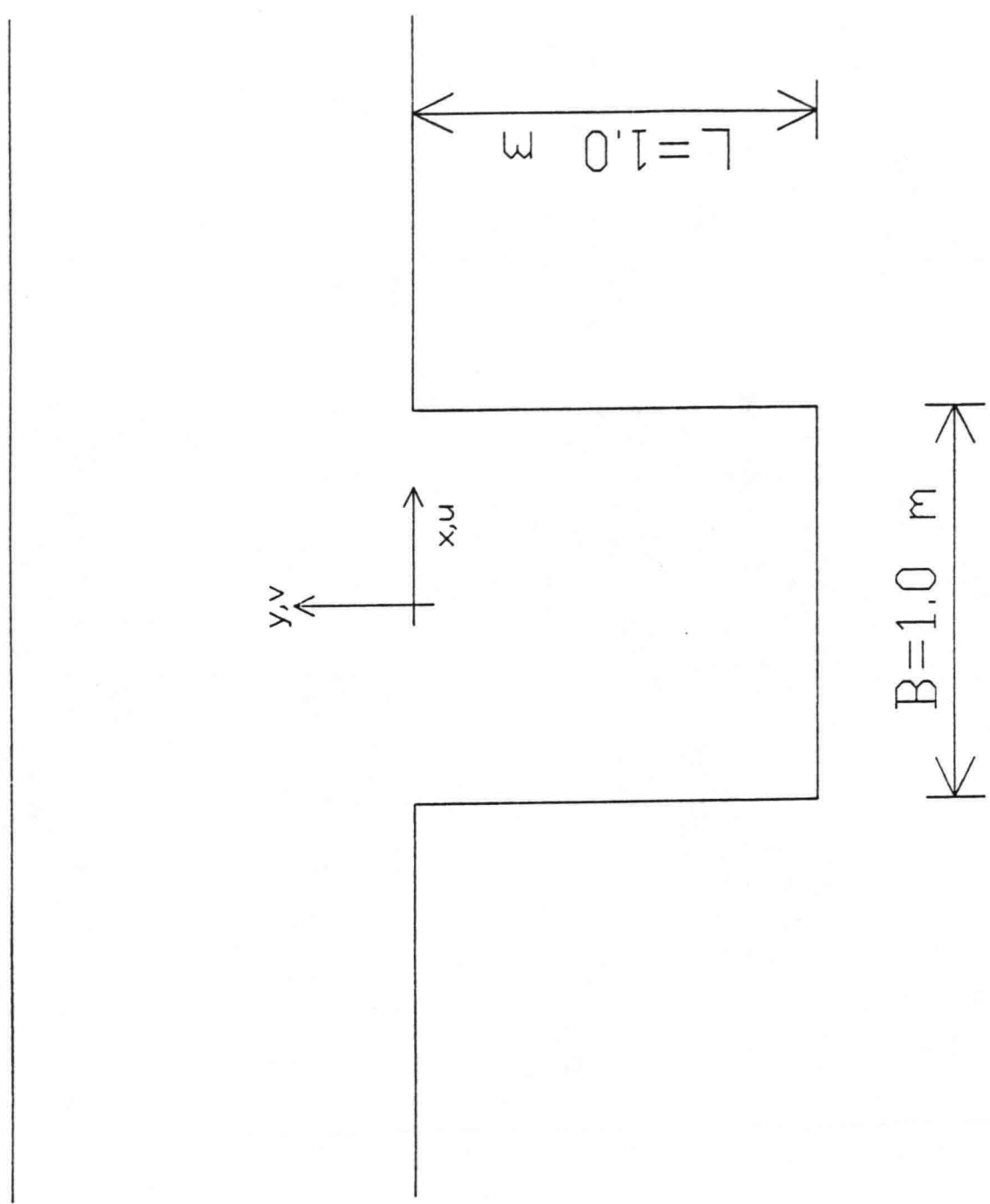
Figure 2.2
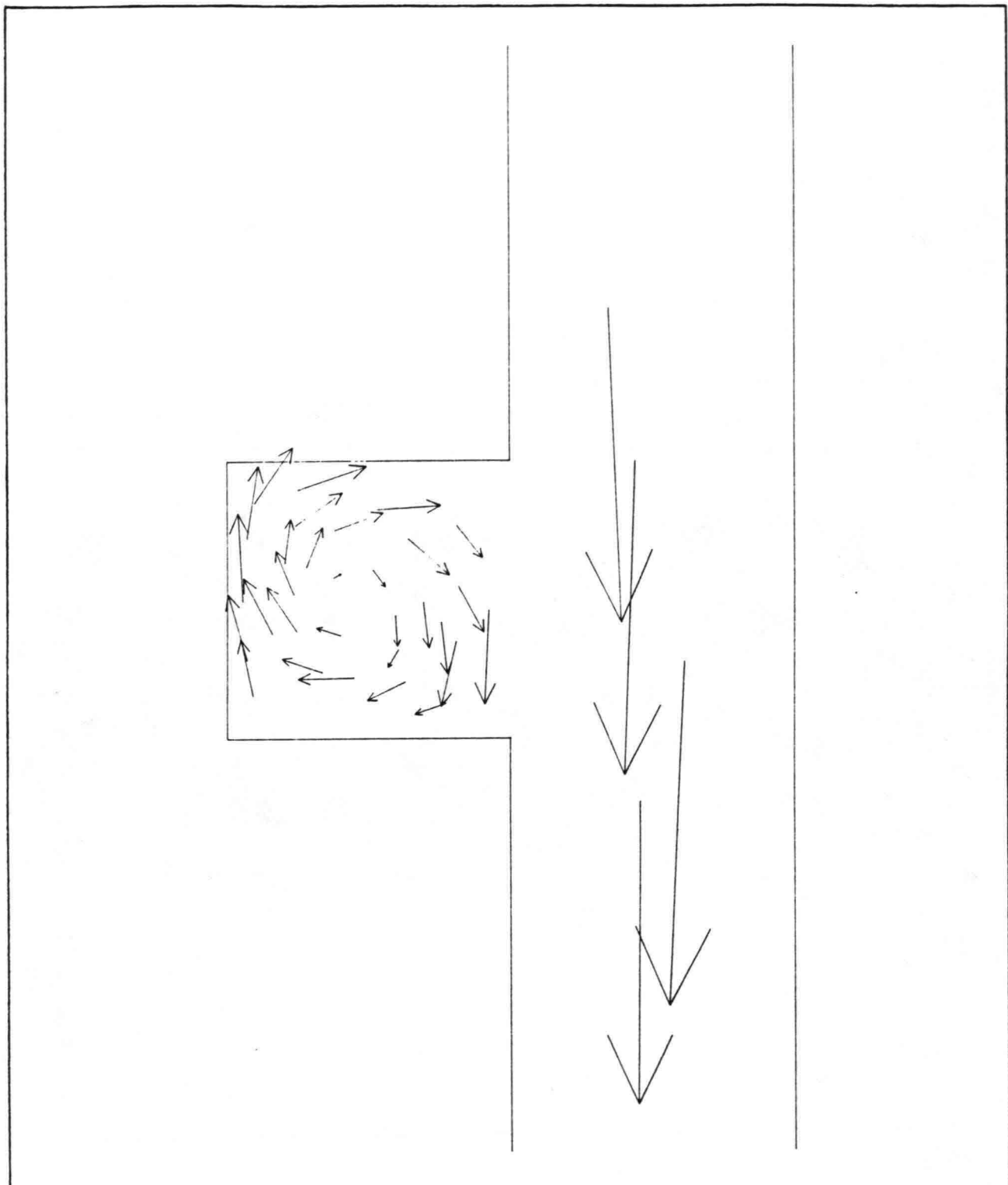
Depth averaged flow pattern

T = 500 s, h = 0.11 m

TIME = 135.0 s

⊢——⊣ = 0.15 m

⊢——→ = 0.05 m/s

Delft University of Technology

Fig. 2.3.a
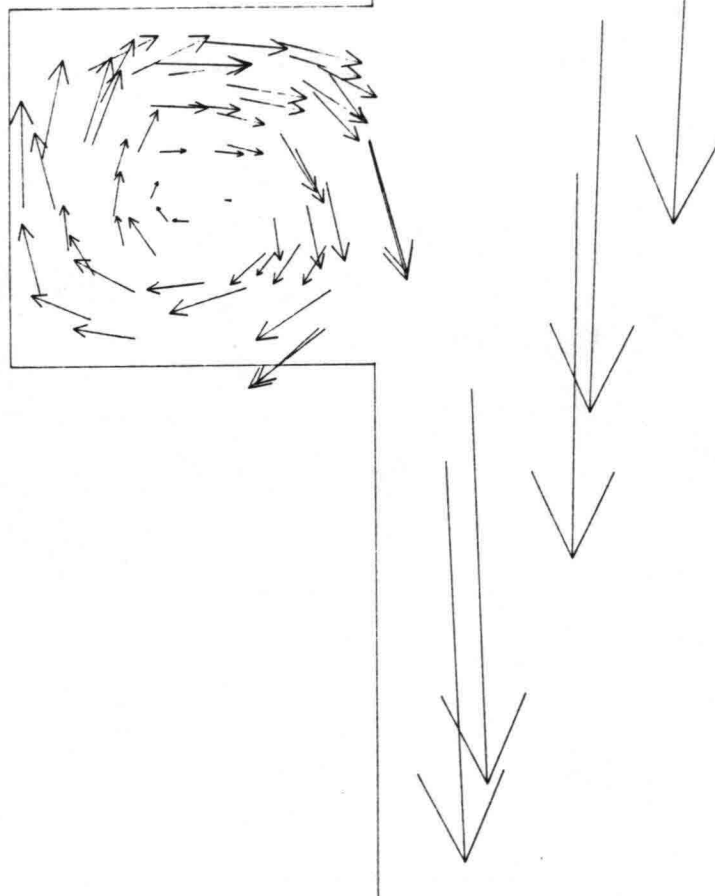
Depth averaged flow pattern

T = 500 s, h = 0.11 m

TIME = 150.0 s

⊢——⊣ = 0.15 m

⊢——▶ = 0.05 m/s

Delft University of Technology

Fig. 2.3.b
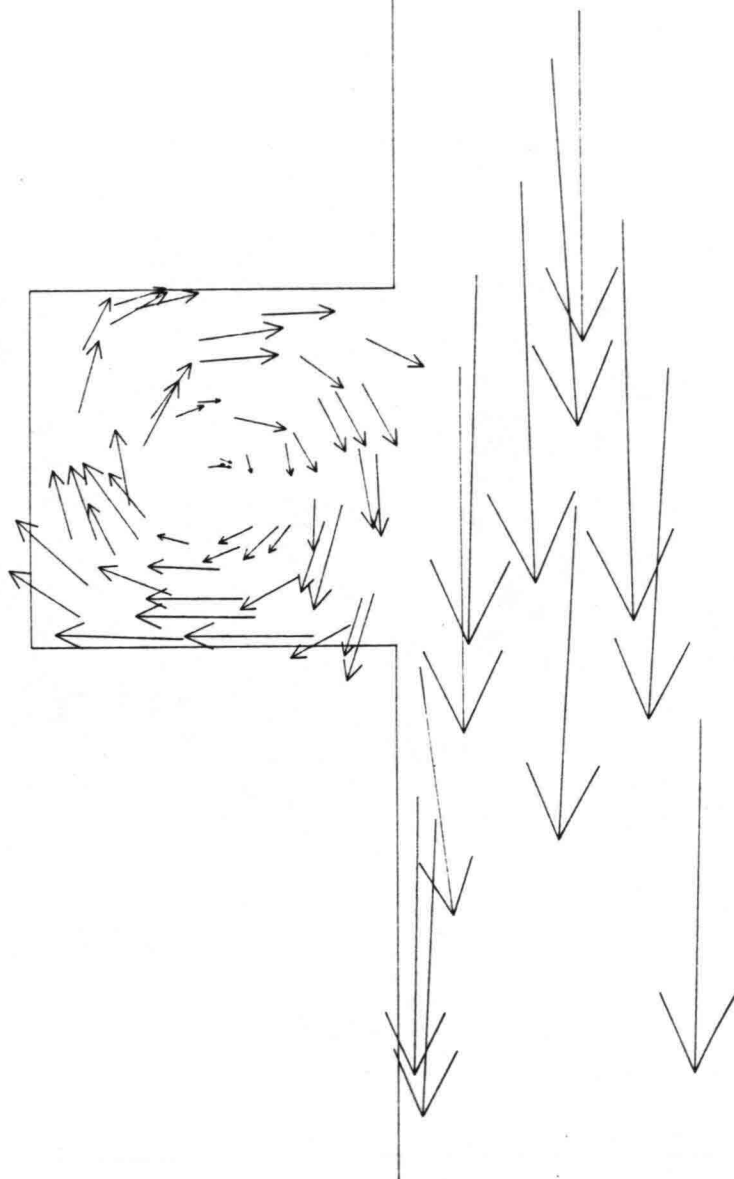
Depth averaged flow pattern

T = 500 s, h = 0.11 m

TIME = 160.0 s

├───┤ = 0.15 m

├───→ = 0.05 m/s

Delft University of Technology

Fig. 2.3.c
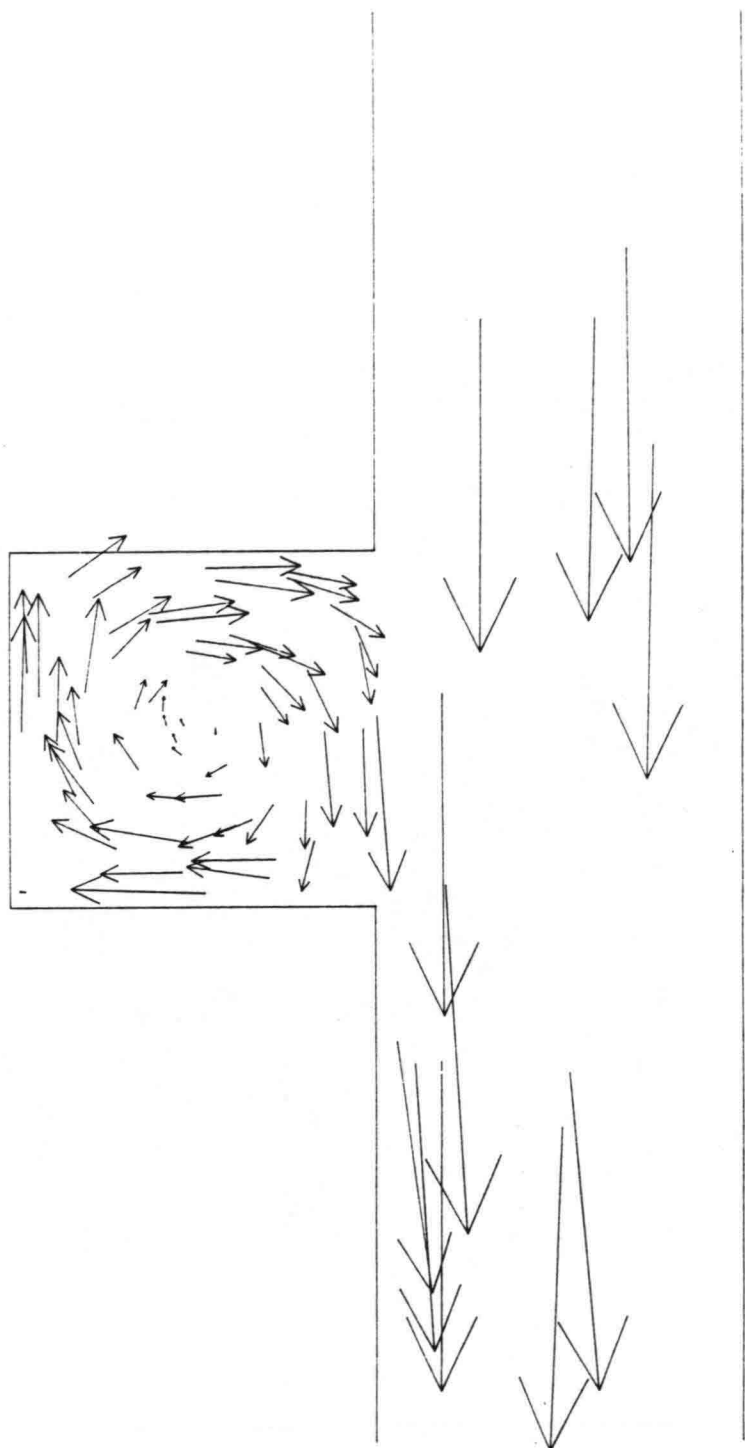
Depth averaged flow pattern

T = 500 s, h = 0.11 m

TIME = 175.0 s

⊢——⊣ = 0.15 m

⊢——→ = 0.05 m/s

Delft University of Technology

Fig. 2.3.d
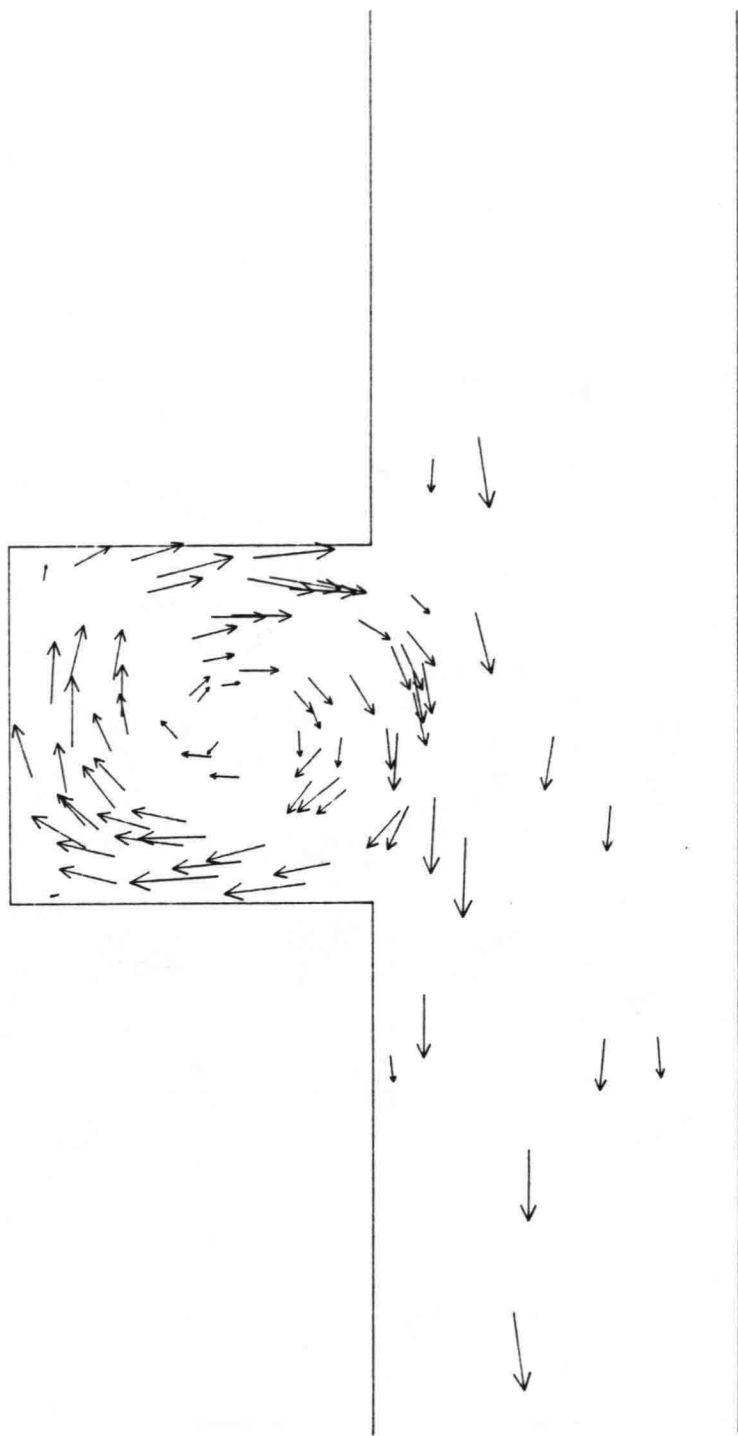
Depth averaged flow pattern

T = 500 s, h = 0.11 m

TIME = 240.0 s

⊢——⊣ = 0.15 m

⊢——→ = 0.05 m/s

Delft.University of Technology

Fig. 2.3.e
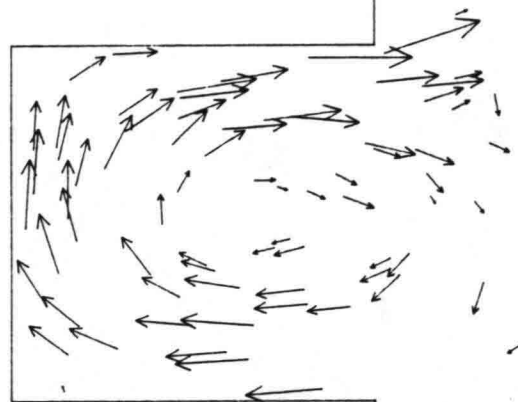
Depth averaged flow pattern

T = 500 s, h = 0.11 m

TIME = 250.0 s
├──┤ = 0.15 m
├──→ = 0.05 m/s

Delft University of Technology

Fig. 2.3.f
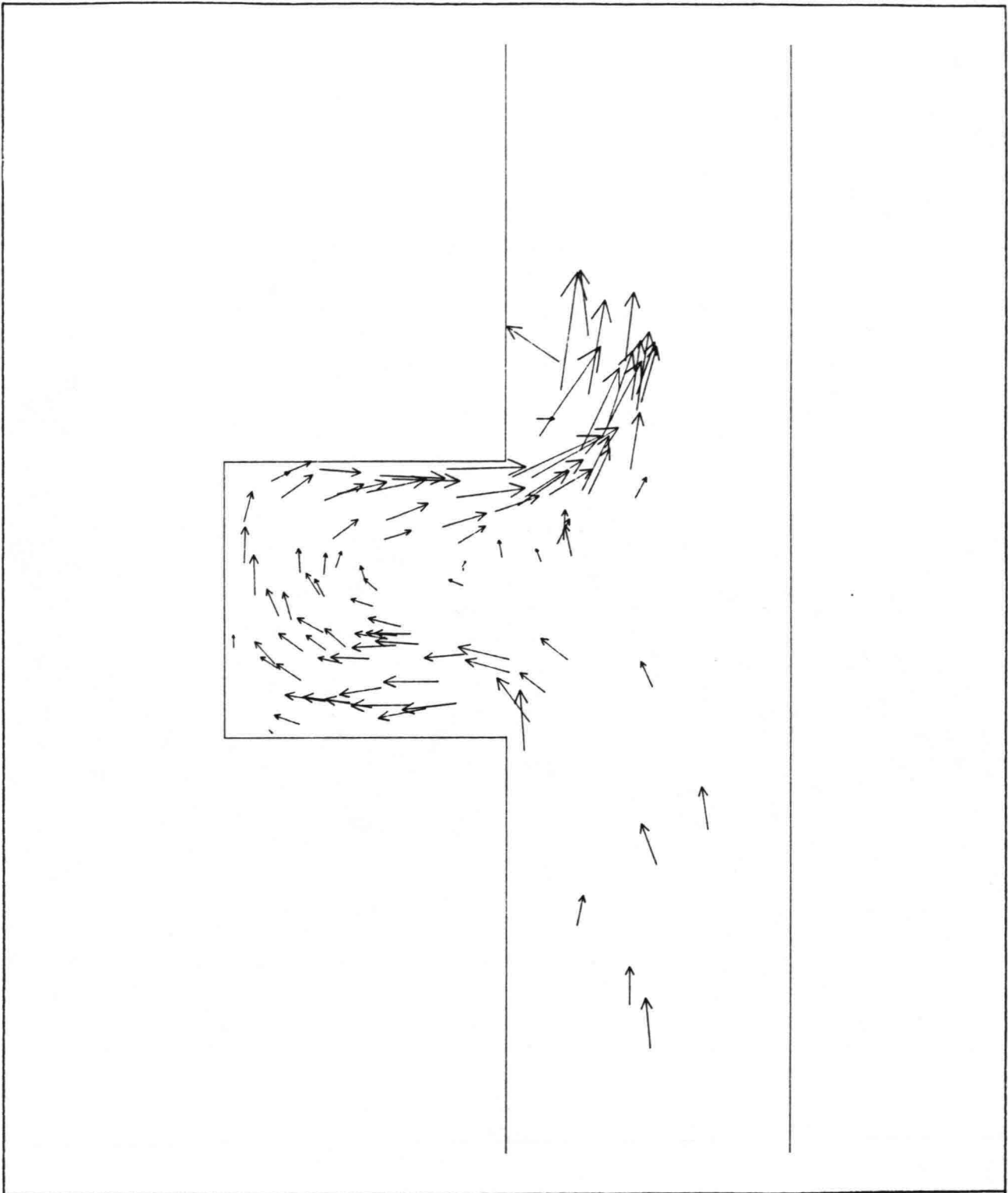
Depth averaged flow pattern	TIME = 260.0 s
T = 500 s, h = 0.11 m	⊢⊣ = 0.15 m
	⊢⟶ = 0.05 m/s
Delft University of Technology	Fig. 2.3.g
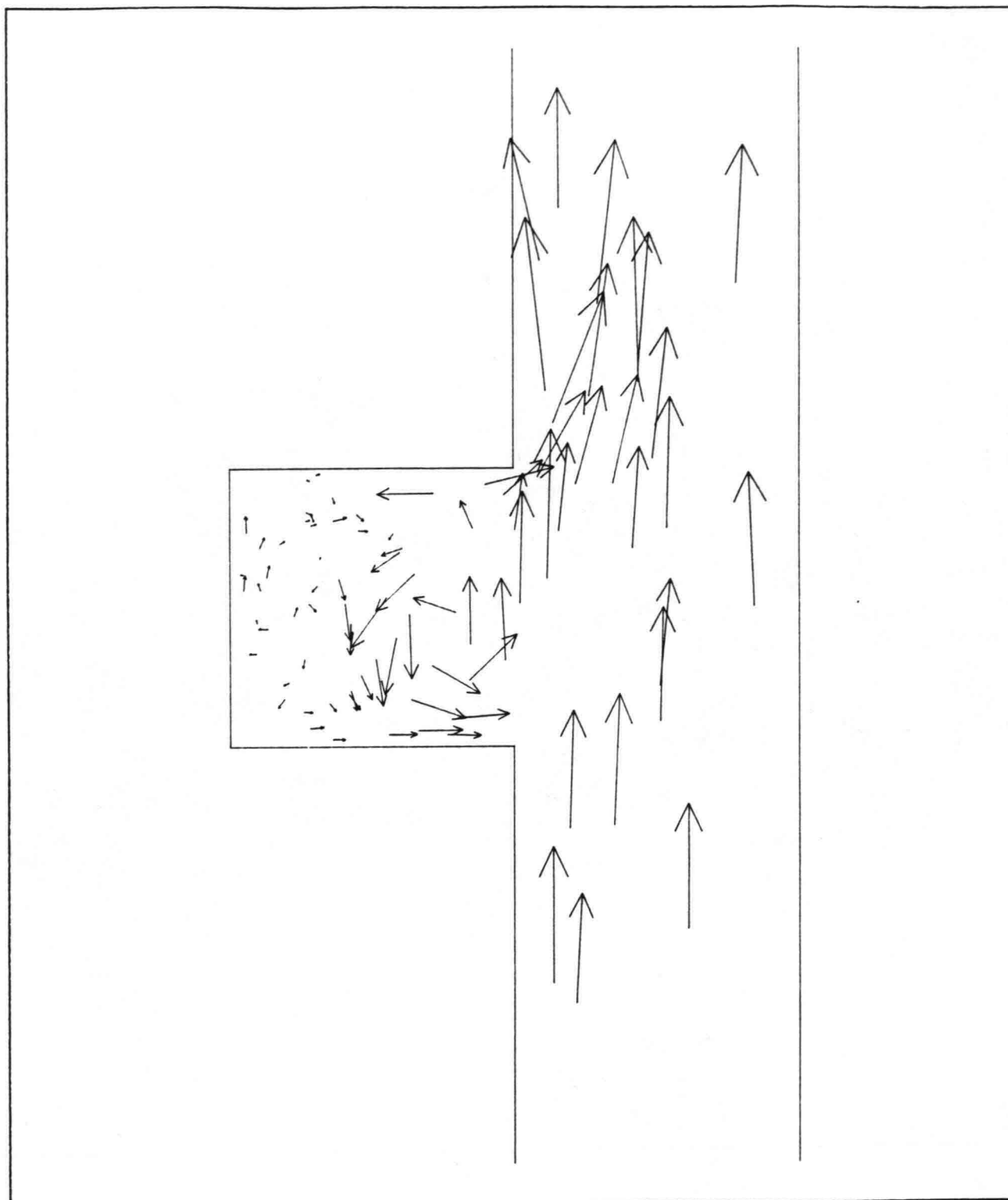
Depth averaged flow pattern

T = 500 s, h = 0.11 m

TIME = 280.0 s

⊢——⊣ = 0.15 m

⊢——→ = 0.05 m/s

Delft University of Technology

Fig. 2.3.h
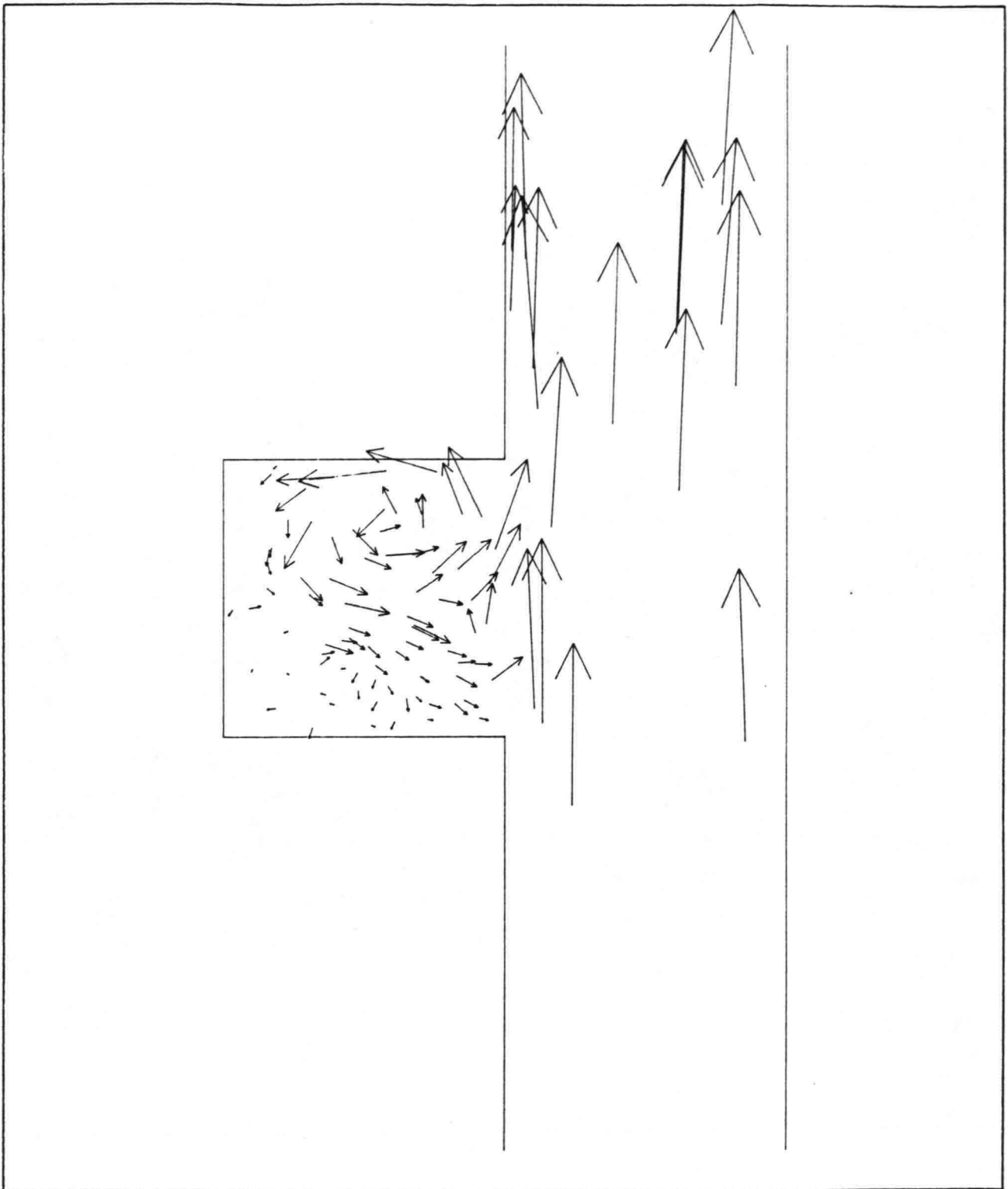
Depth averaged flow pattern

T = 500 s, h = 0.11 m

TIME = 300.0 s

⊢—⊣ = 0.15 m

⊢—→ = 0.05 m/s

Delft University of Technology

Fig. 2.3.i
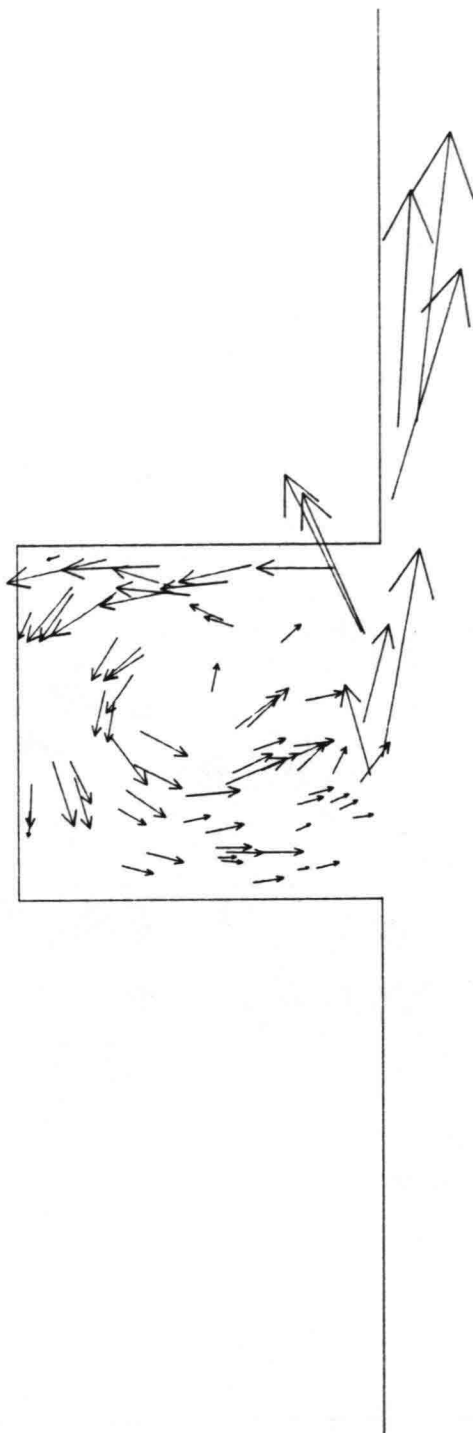
Depth averaged flow pattern

T = 500 s, h = 0.11 m

TIME = 325.0 s

⊢——⊣ = 0.15 m

⊢——→ = 0.05 m/s

Delft University of Technology

Fig. 2.3.j
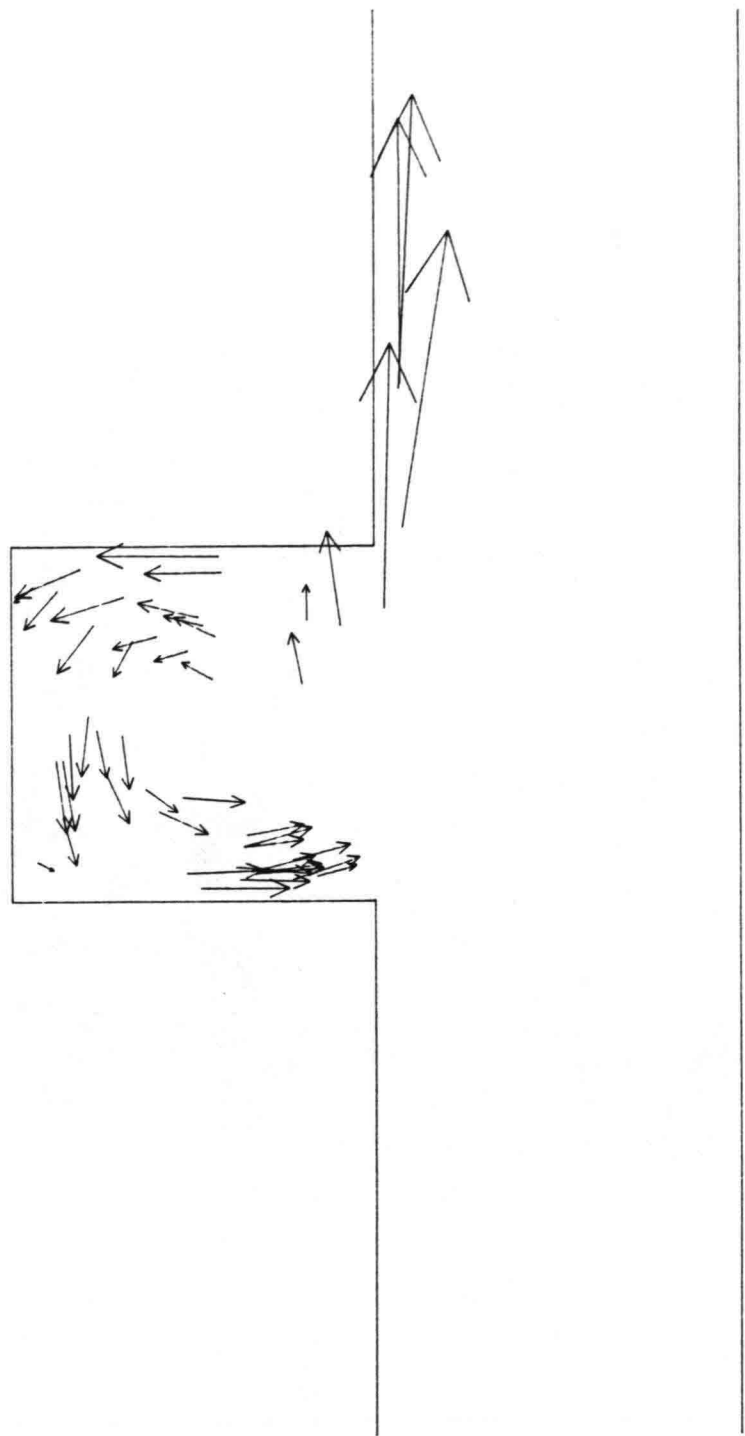
Depth averaged flow pattern

T = 500 s, h = 0.11 m

TIME = 350.0 s

⊢——⊣ = 0.15 m

⊢——→ = 0.05 m/s

Delft University of Technology

Fig. 2.3.k
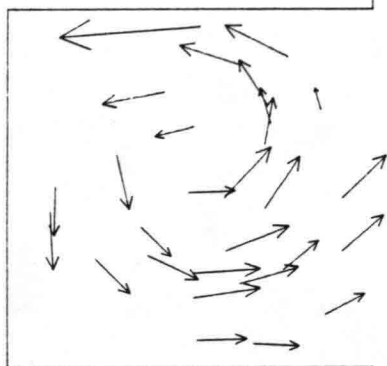
Depth averaged flow pattern

T = 250 s, h = 0.11 m

TIME = 195.0 s

⊢——⊣ = 0.15 m

⊢——→ = 0.05 m/s

Delft University of Technology

Fig. 2.4.a
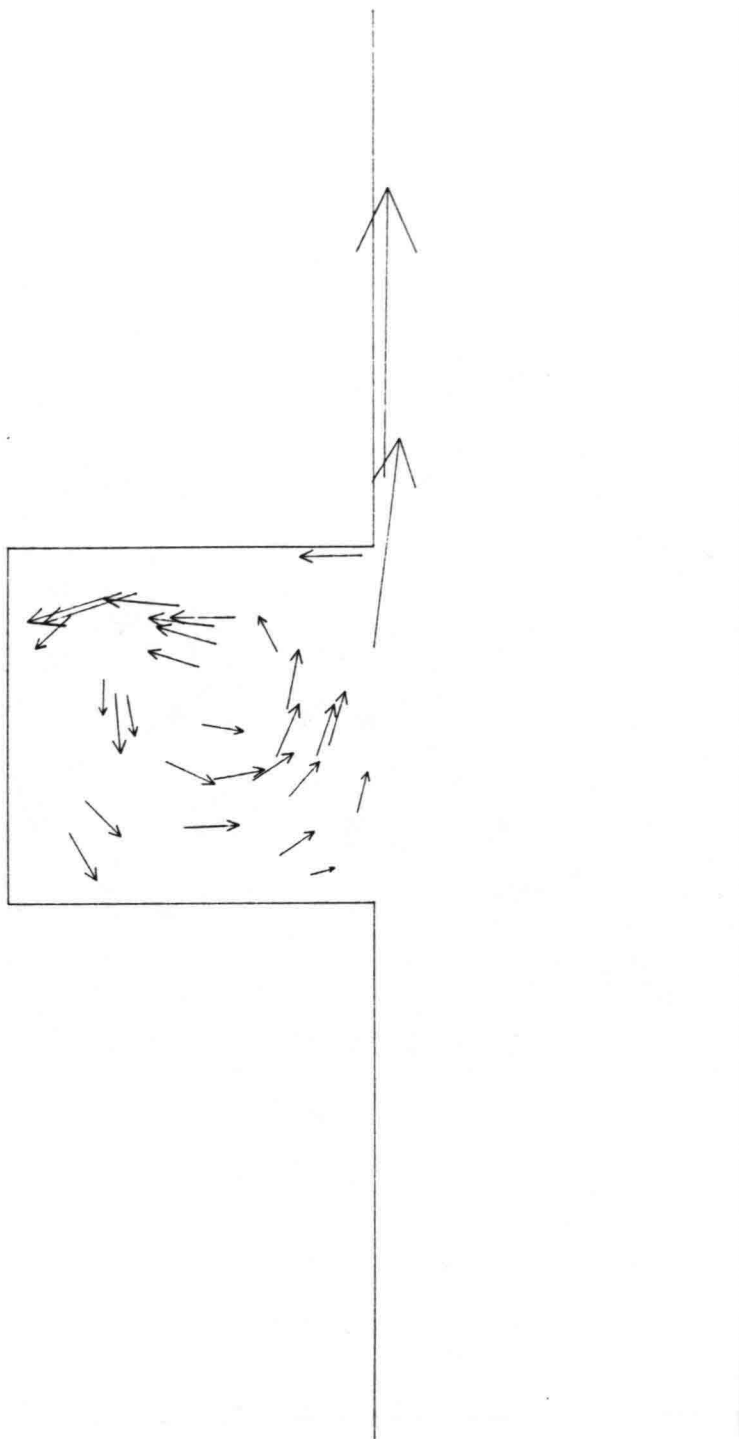
Depth averaged flow pattern

T = 250 s, h = 0.11 m

TIME = 200.0 s

├──┤ = 0.15 m

├──→ = 0.05 m/s

Delft University of Technology

Fig. 2.4.b

Depth averaged flow pattern

T = 250 s, h = 0.11 m

TIME = 205.0 s

⊢——⊣ = 0.15 m

⊢——→ = 0.05 m/s

Delft University of Technology
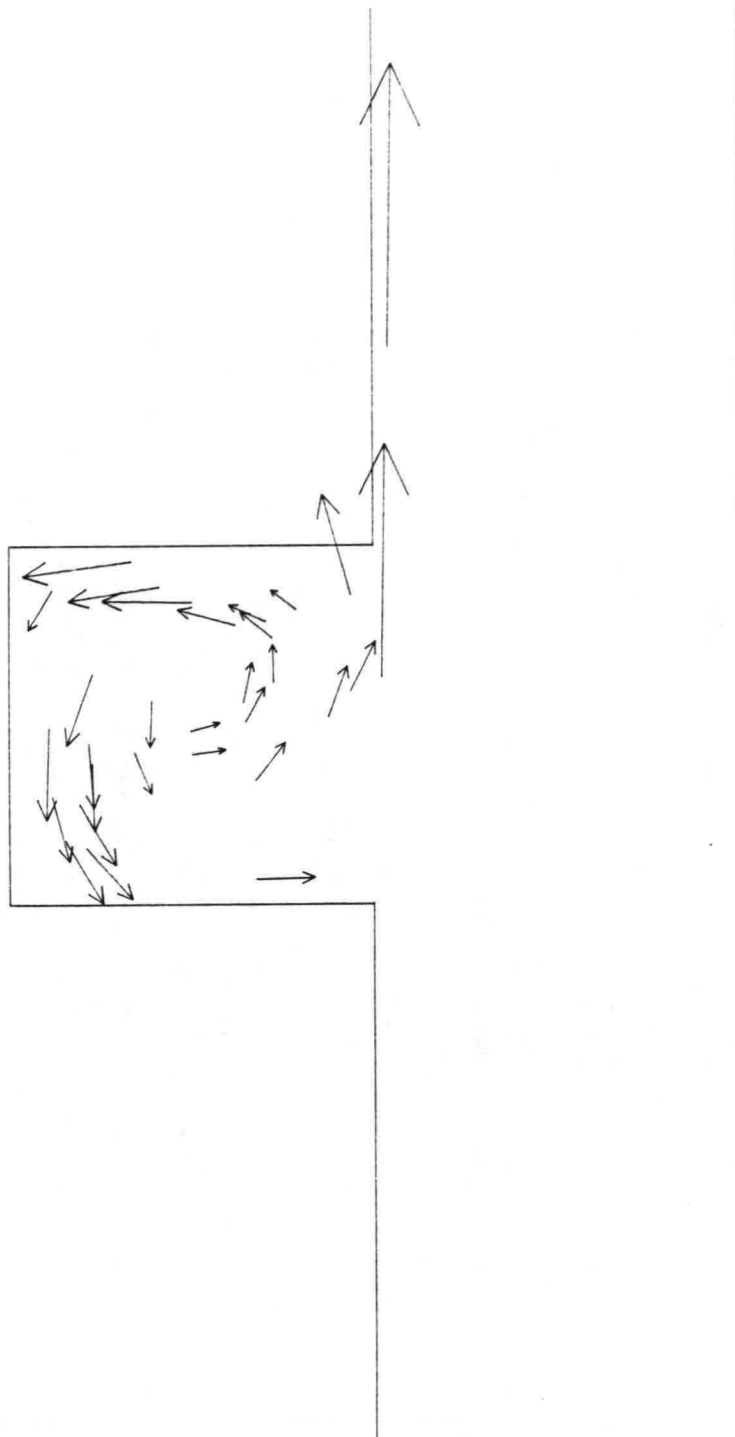
Fig. 2.4.c

Depth averaged flow pattern

T = 250 s, h = 0.11 m

TIME = 210.0 s

├──┤ = 0.15 m

├──→ = 0.05 m/s

Delft University of Technology

Fig. 2.4.d
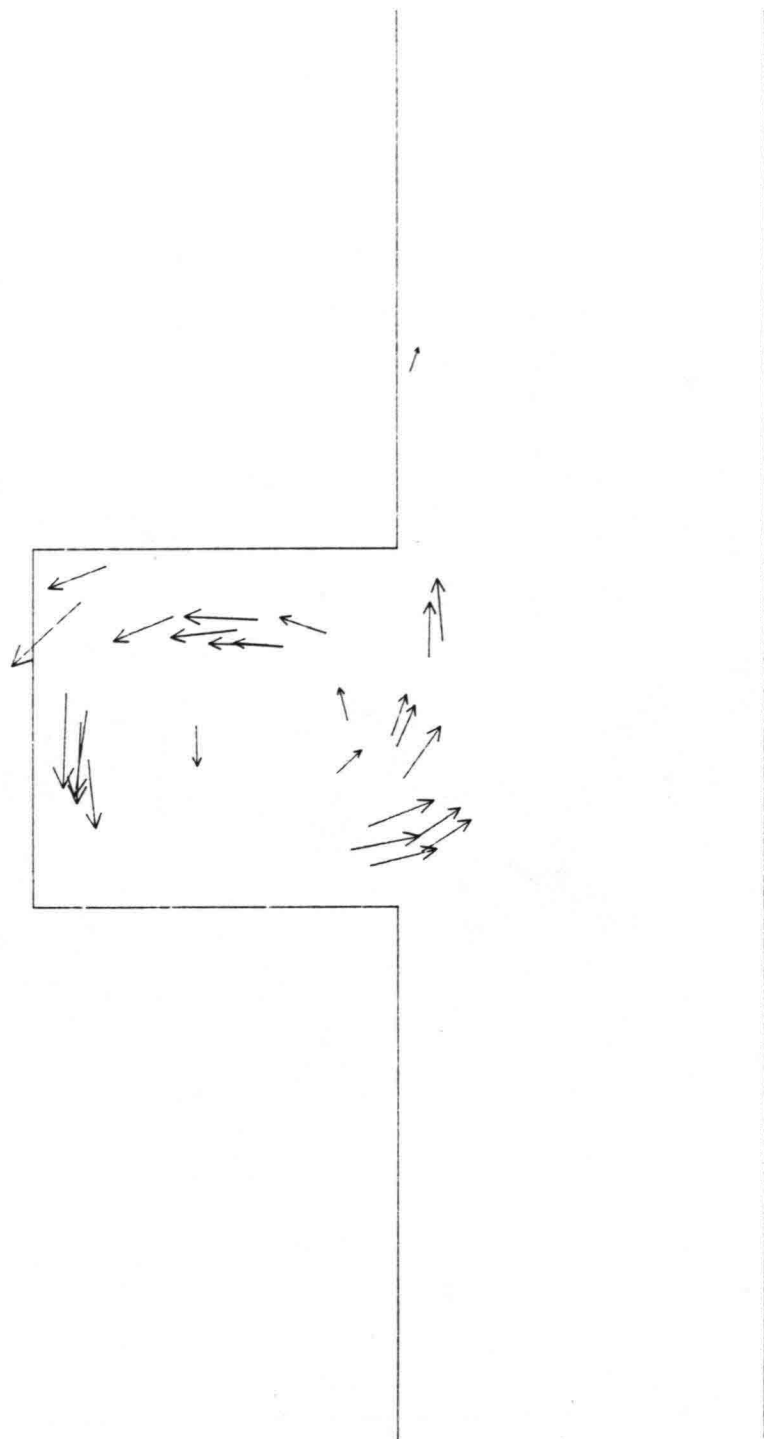
Depth averaged flow pattern

T = 250 s, h = 0.11 m

TIME = 245.0 s

⊢——⊣ = 0.15 m

⊢——→ = 0.05 m/s

Delft University of Technology

Fig. 2.4.e
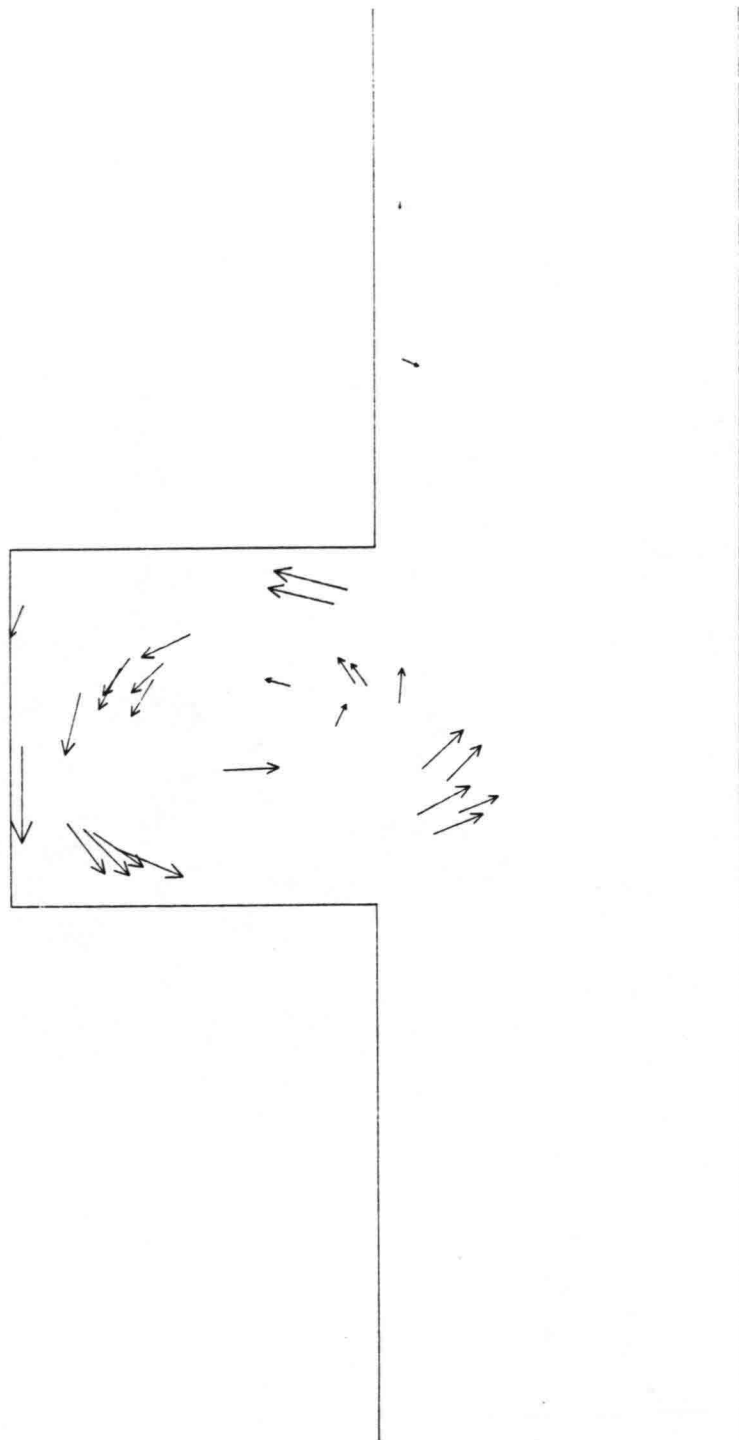
Depth averaged flow pattern

T = 250 s, h = 0.11 m

TIME = 0.0 s

⊢——⊣ = 0.15 m

⊢——→ = 0.05 m/s

Delft University of Technology

Fig. 2.4.f
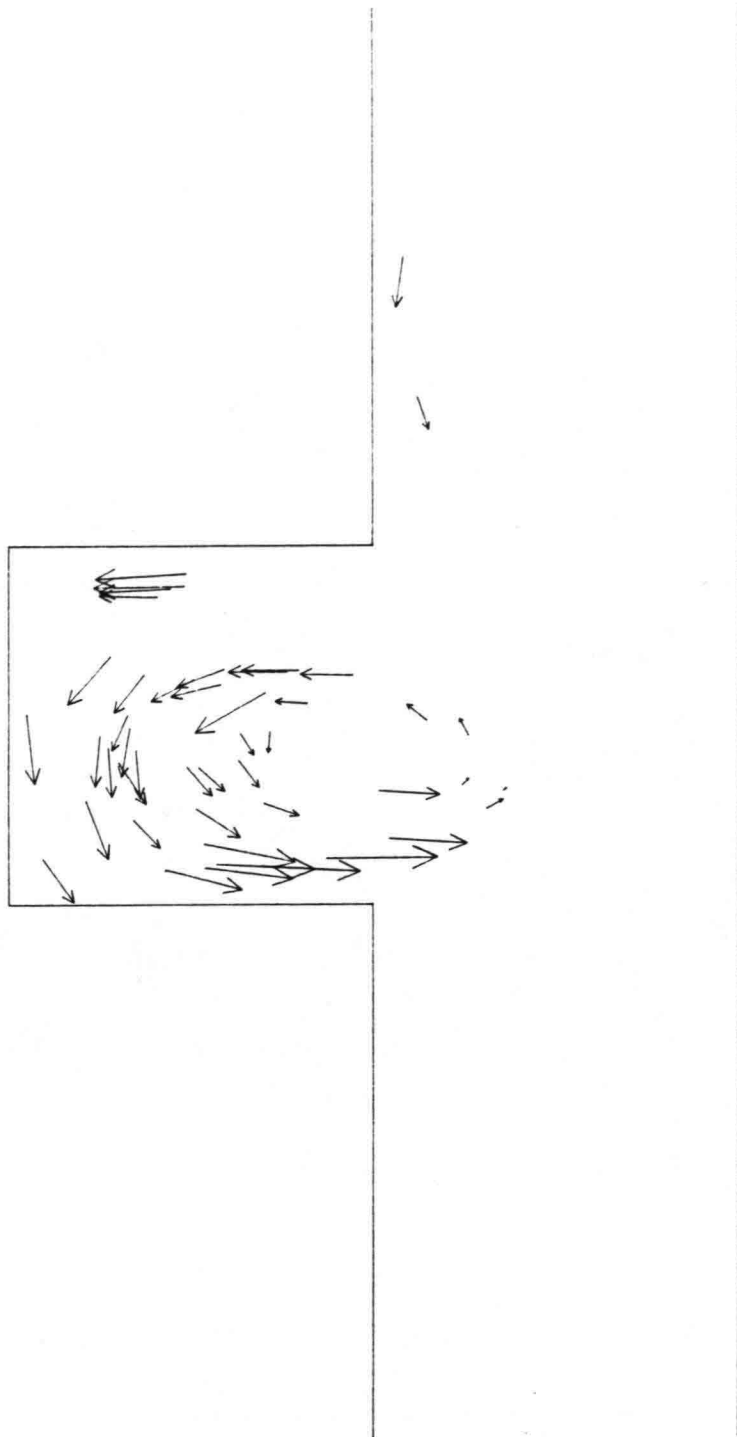
Depth averaged flow pattern

T = 250 s, h = 0.11 m

TIME =   5.0 s

├────┤ = 0.15 m

├────→ = 0.05 m/s

Delft University of Technology

Fig. 2.4.g
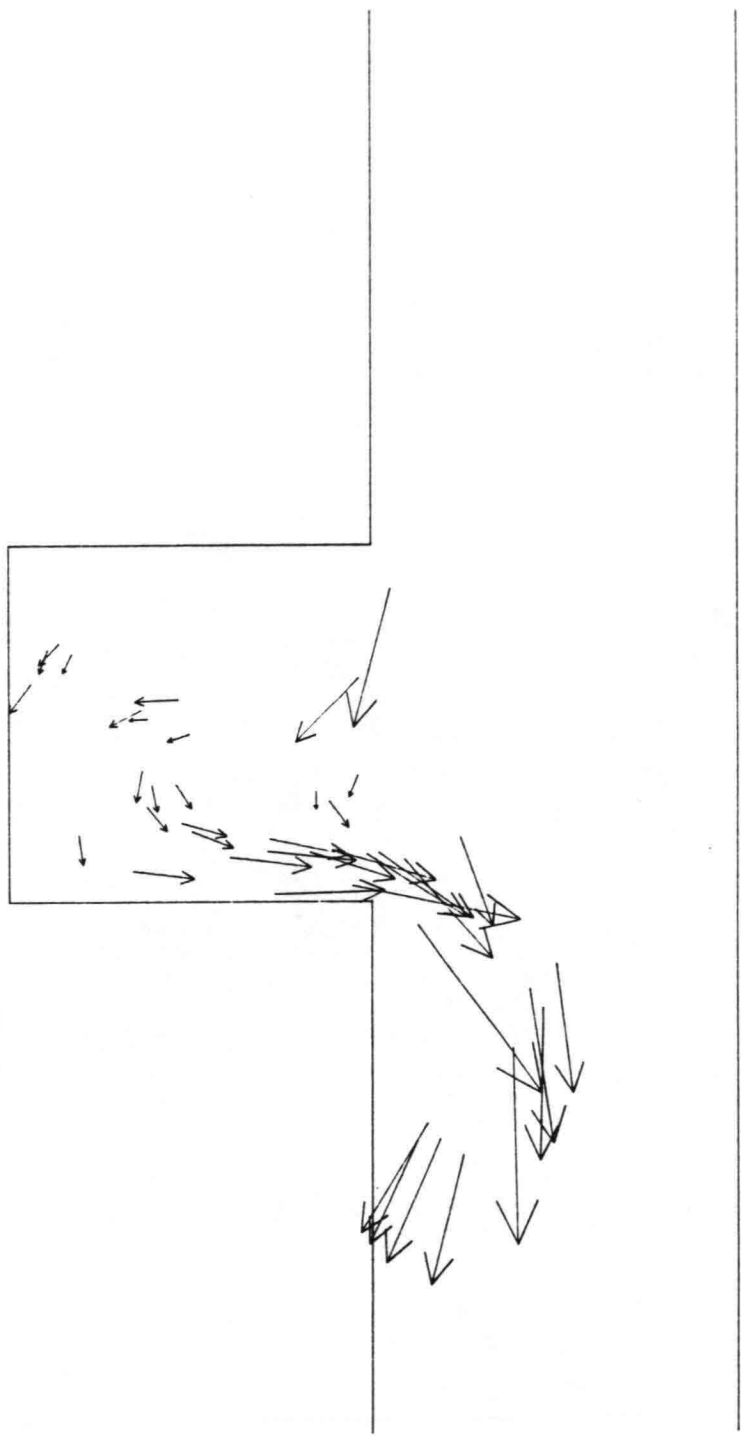
Depth averaged flow pattern

T = 250 s, h = 0.11 m

TIME = 15.0 s

⊢——⊣ = 0.15 m

⊢——→ = 0.05 m/s

Delft University of Technology

Fig. 2.4.h
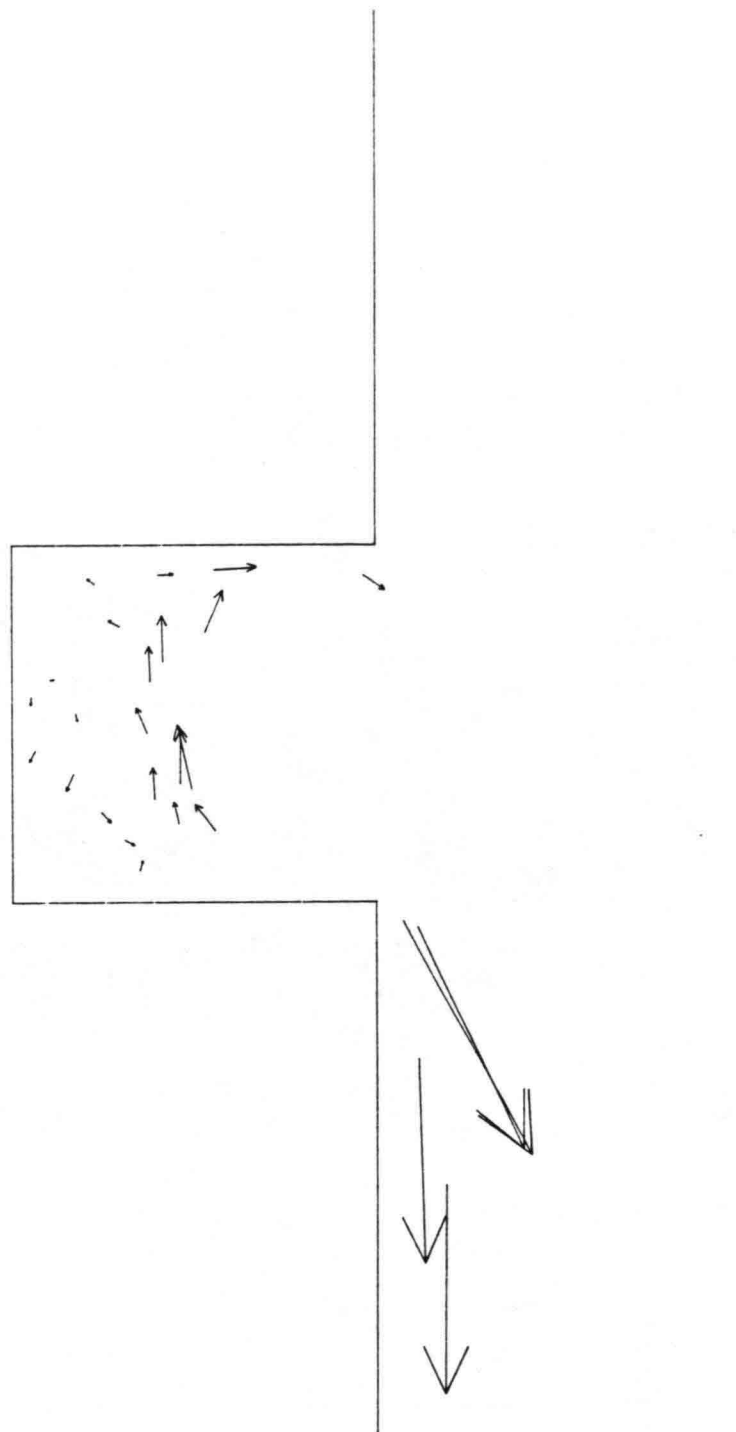
Depth averaged flow pattern

T = 250 s, h = 0.11 m

TIME = 25.0 s

⊢––⊣ = 0.15 m

⊢––→ = 0.05 m/s

Delft University of Technology

Fig. 2.4.i
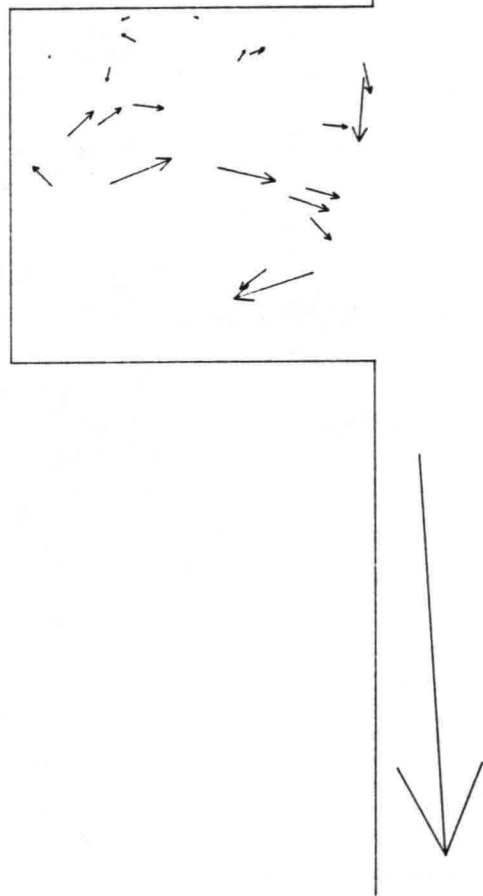
Depth averaged flow pattern

T = 250 s, h = 0.11 m

TIME = 45.0 s

⊢——⊣ = 0.15 m

⊢——→ = 0.05 m/s

Delft University of Technology

Fig. 2.4.j
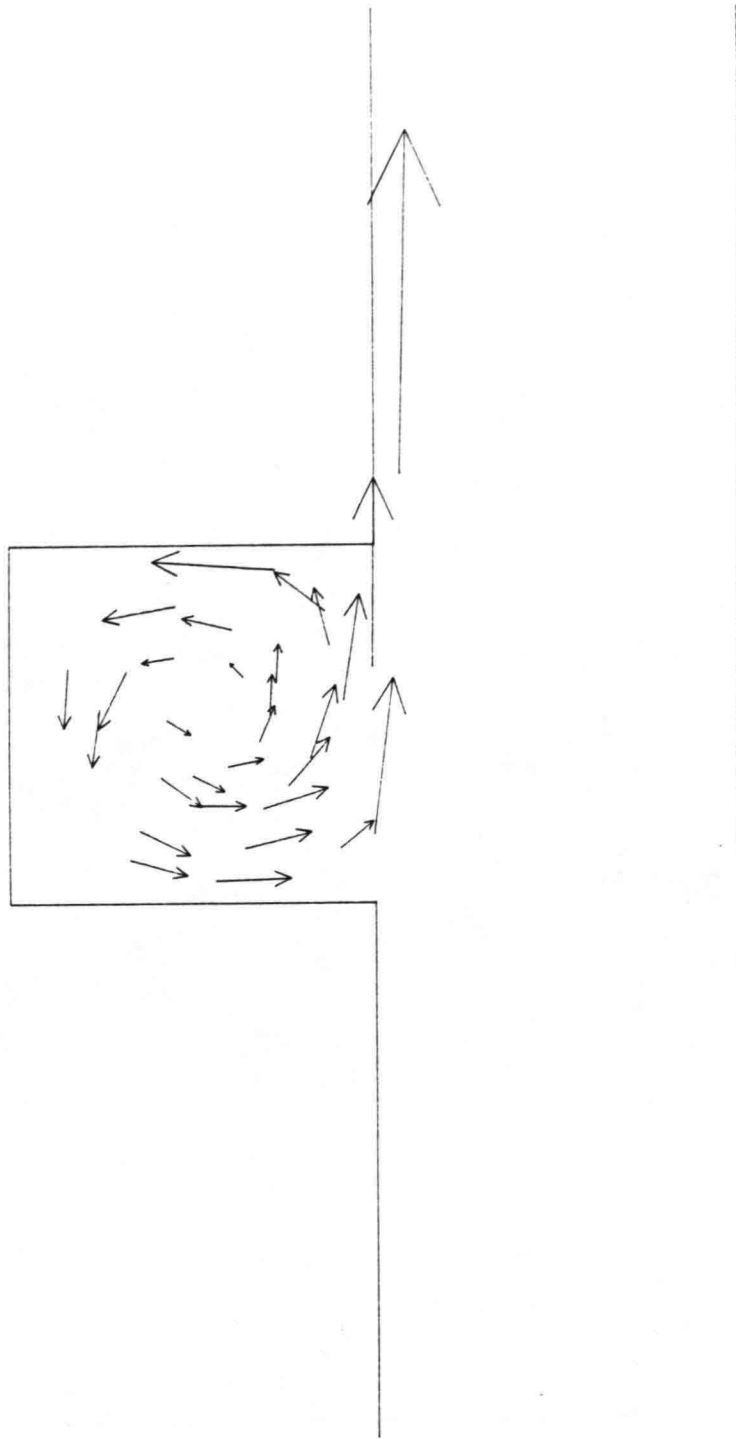
Depth averaged flow pattern

T = 1000 s, h = 0.11 m

TIME = 760.0 s

⊢——⊣ = 0.15 m

⊢——→ = 0.05 m/s

Delft University of Technology

Fig. 2.5.a
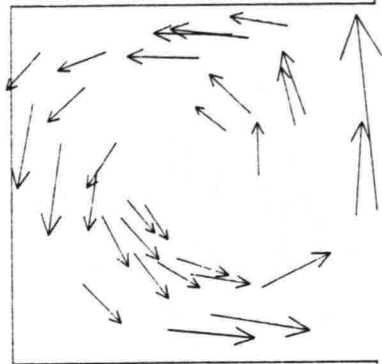
Depth averaged flow pattern

T = 1000 s, h = 0.11 m

TIME = 780.0 s

$\vdash\dashv$ = 0.15 m

$\longmapsto$ = 0.05 m/s

Delft University of Technology

Fig. 2.5.b
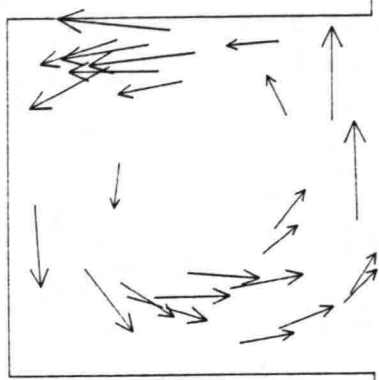
Depth averaged flow pattern

T = 1000 s, h = 0.11 m

TIME = 800.0 s

⊢—⊣ = 0.15 m

⊢—→ = 0.05 m/s

Delft University of Technology

Fig. 2.5.c
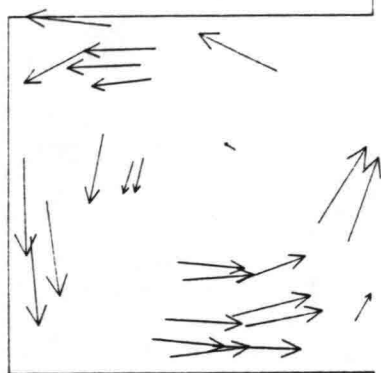
Depth averaged flow pattern

T = 1000 s, h = 0.11 m

TIME = 820.0 s

├──┤ = 0.15 m

├──→ = 0.05 m/s

Delft University of Technology

Fig. 2.5.d
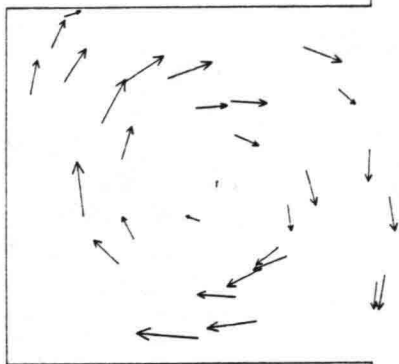
Depth averaged flow pattern

T = 1000 s, h = 0.11 m

TIME = 480.0 s

⊢——⊣ = 0.15 m

⊢——→ = 0.05 m/s

Delft University of Technology

Fig. 2.5.e
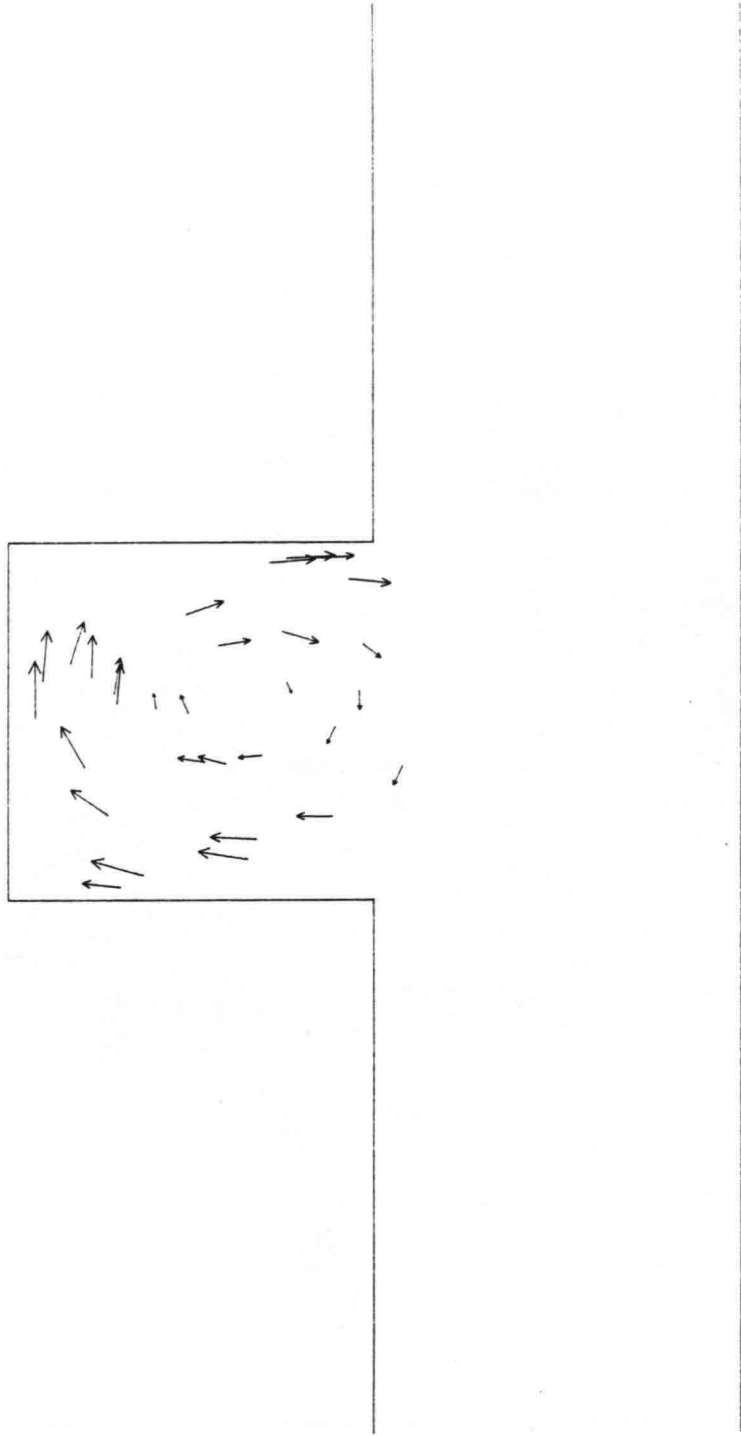
Depth averaged flow pattern	TIME = 500.0 s
T = 1000 s, h = 0.11 m	⊢——⊣ = 0.15 m
	⊢——→ = 0.05 m/s
Delft University of Technology	Fig. 2.5.f
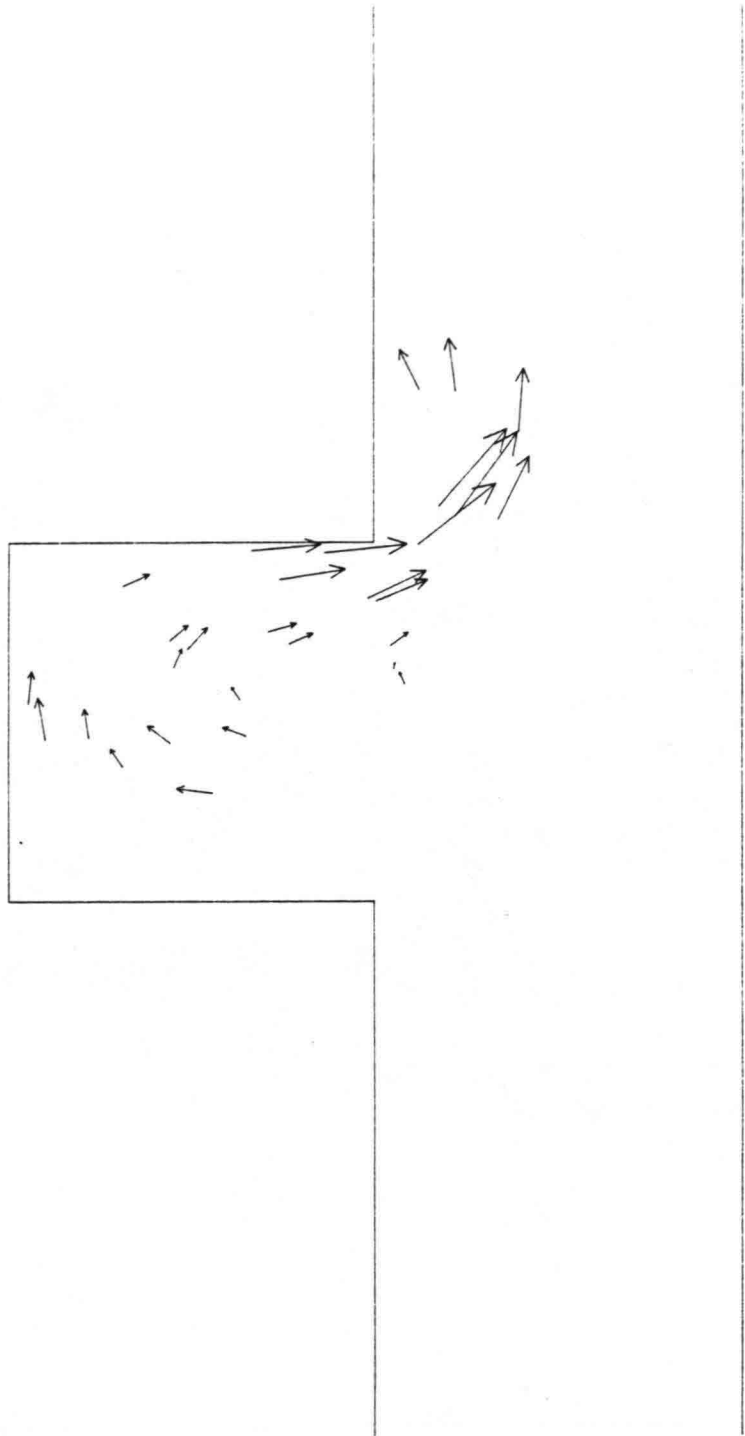
Depth averaged flow pattern

T = 1000 s, h = 0.11 m

TIME = 520.0 s
⊢——⊣ = 0.15 m
⊢——→ = 0.05 m/s

Delft University of Technology

Fig. 2.5.g
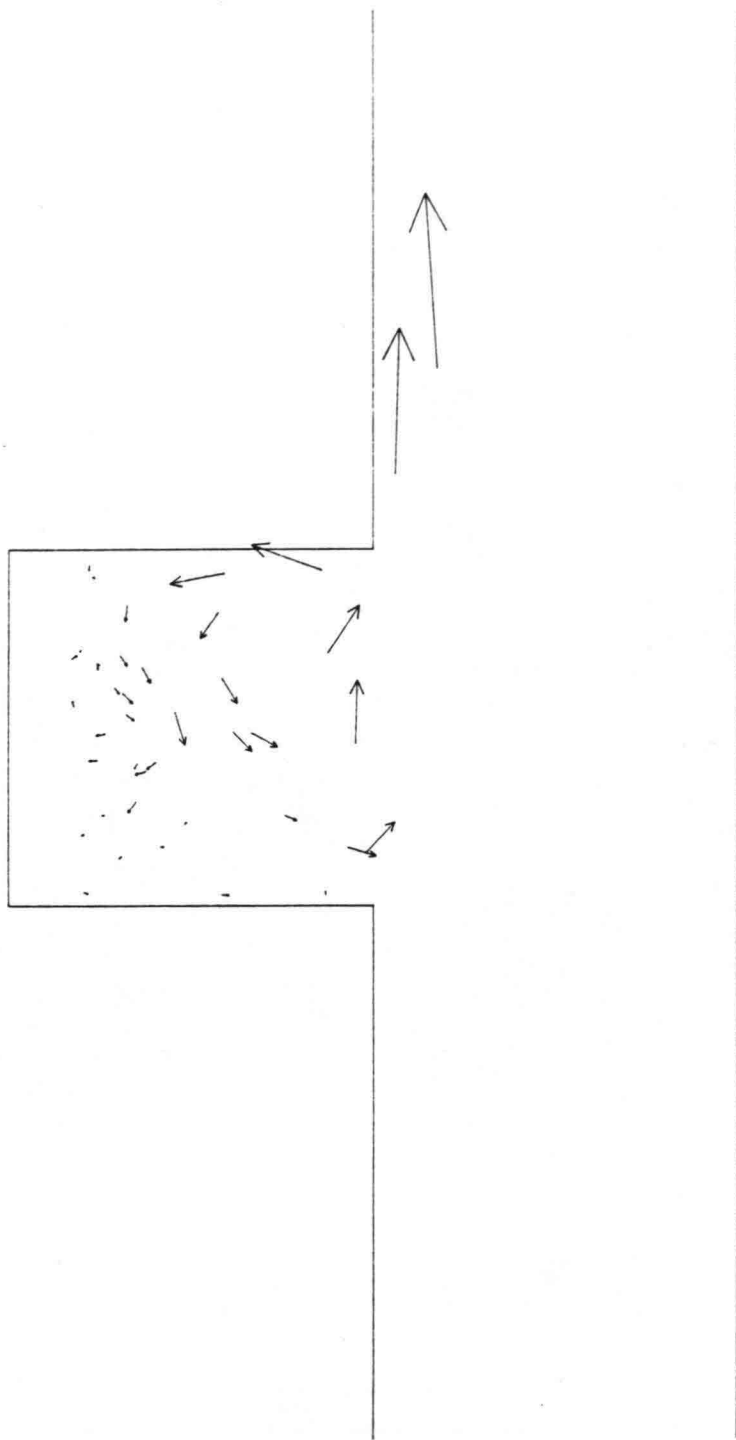
Depth averaged flow pattern

T = 1000 s, h = 0.11 m

TIME = 560.0 s

⊢——⊣ = 0.15 m

⊢——→ = 0.05 m/s

Delft University of Technology

Fig. 2.5.h
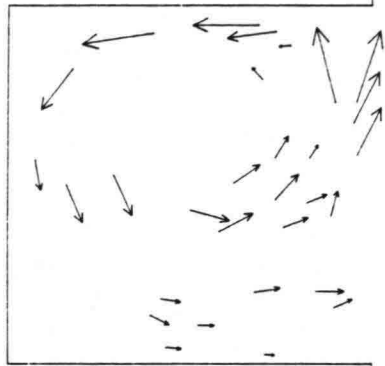
Depth averaged flow pattern

T = 1000 s, h = 0.11 m

TIME = 600.0 s

⊢——⊣ = 0.15 m

⊢——→ = 0.05 m/s

Delft University of Technology

Fig. 2.5.i
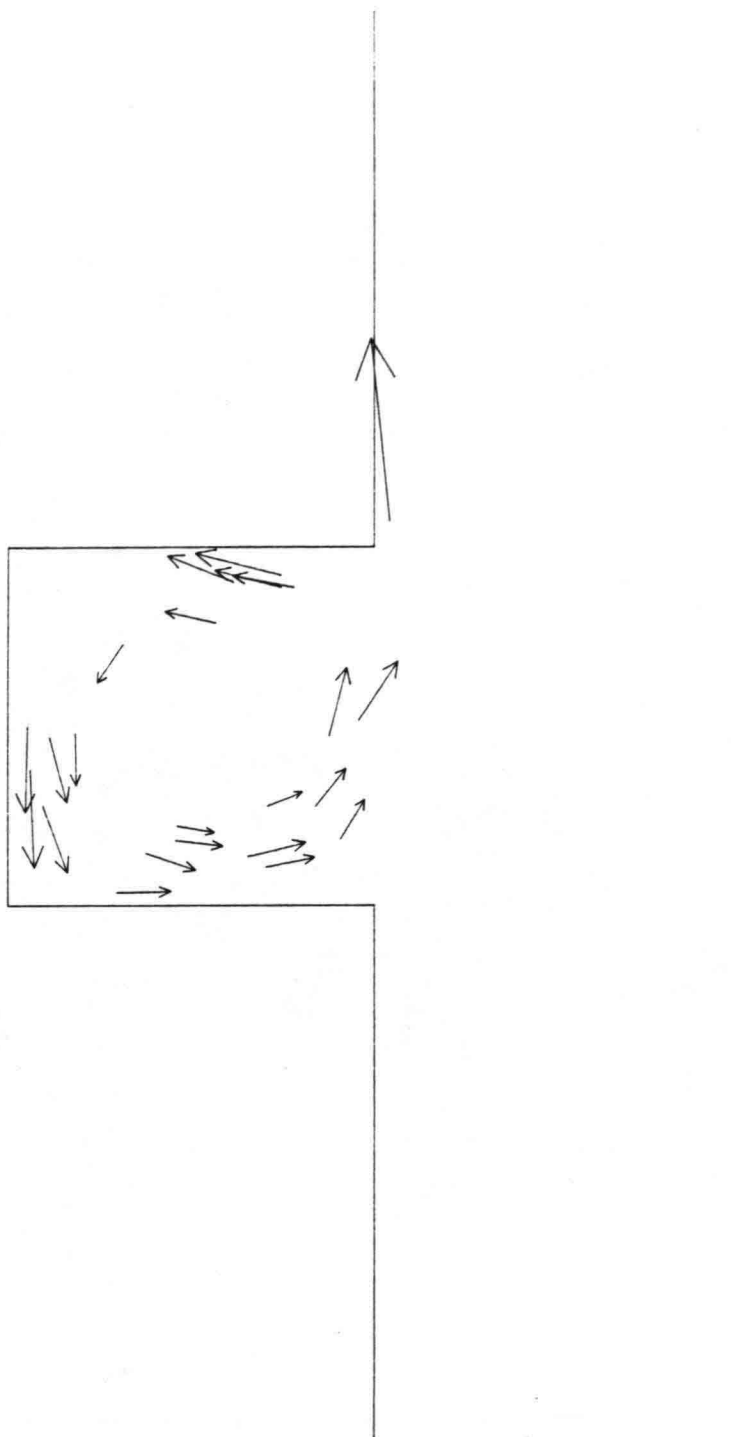
Depth averaged flow pattern

T = 1000 s, h = 0.11 m

TIME = 650.0 s
├──┤ = 0.15 m
├──→ = 0.05 m/s

Delft University of Technology

Fig. 2.5.j
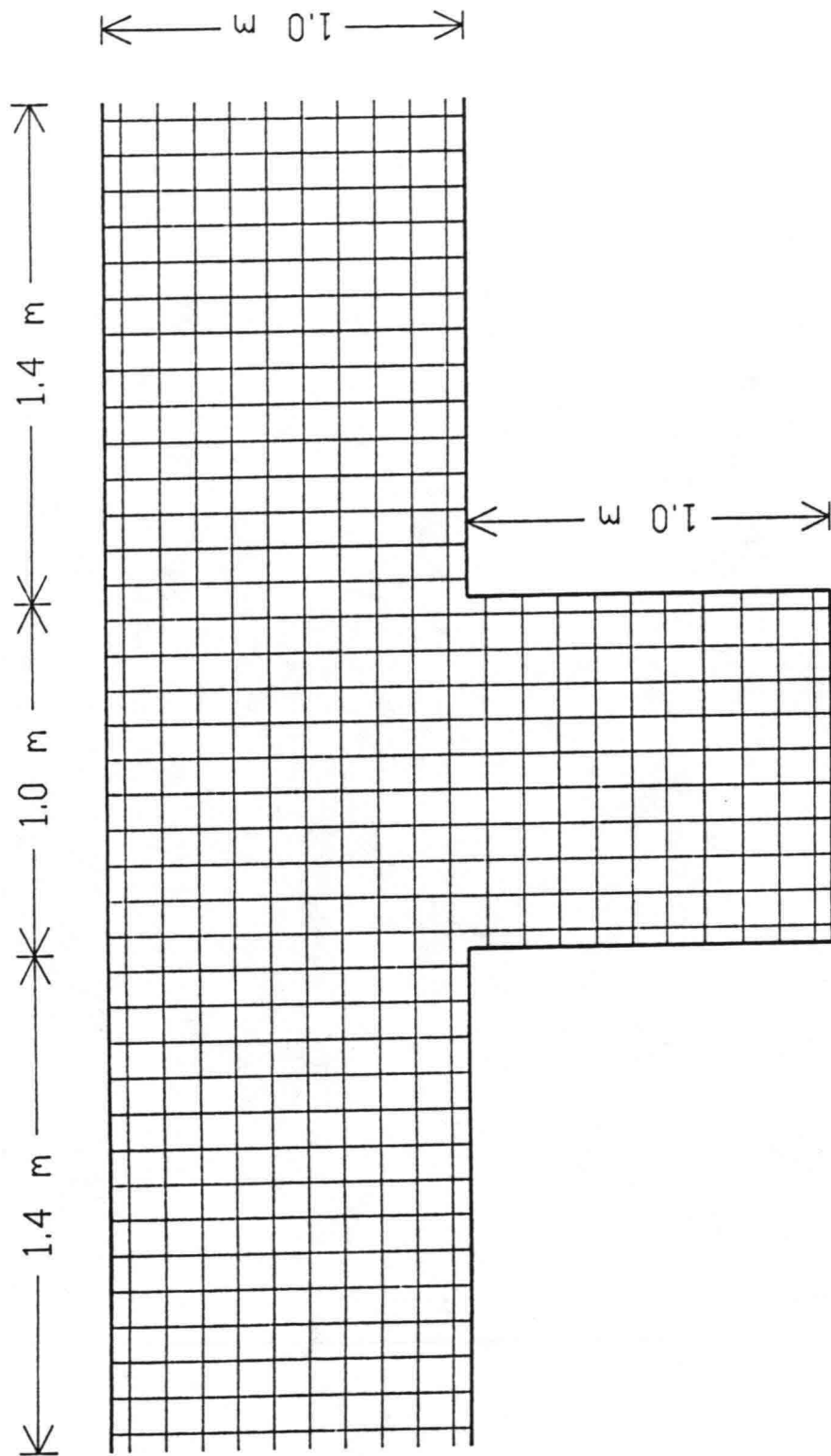
Figure 3.1
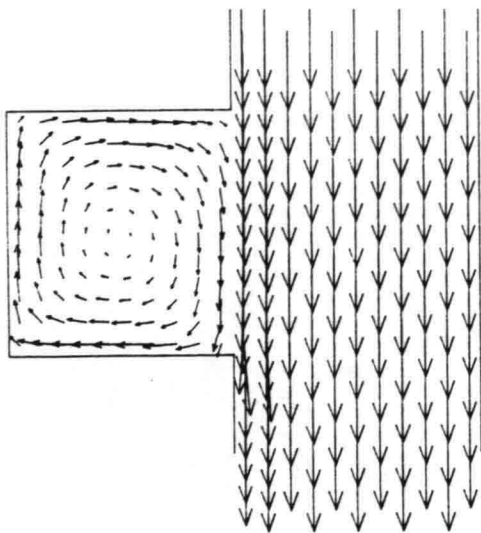
I) Run T0
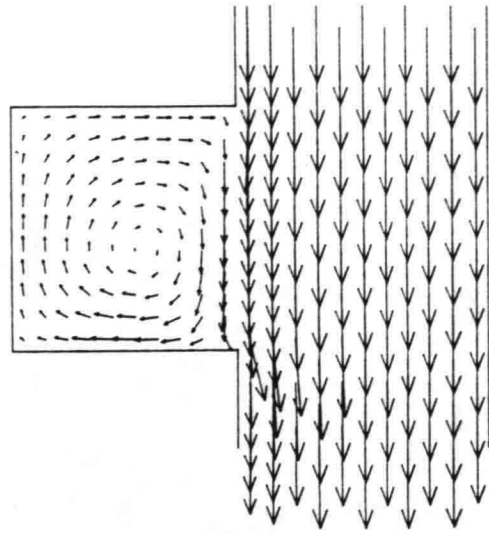
II) Run T1
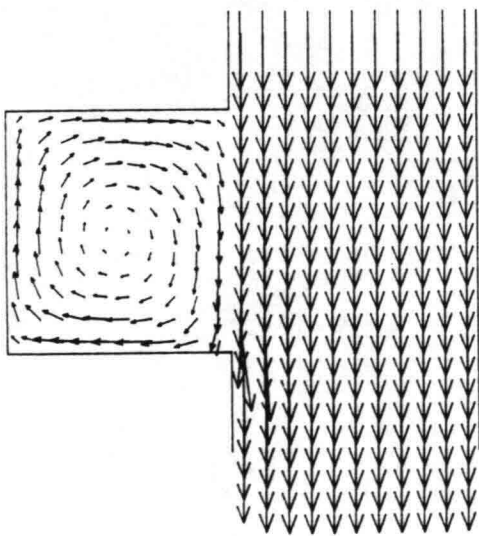
III) Run T2
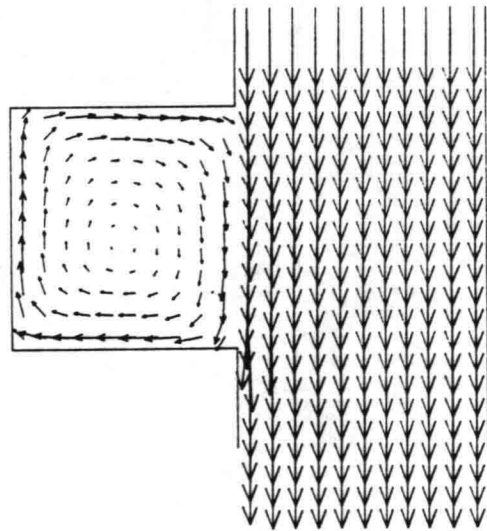
IV) Run T3

Influence of eddy viscosity on flow pattern.	TIME = 175.0 s ⊢——⊣ = 0.24 m ⊢——→ = 0.27 m/s
Delft University of Technology	Fig. 3.2.a
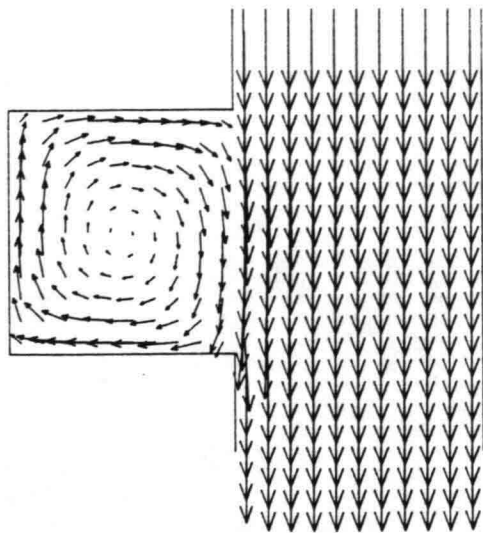
I) Run T0   II) Run T1
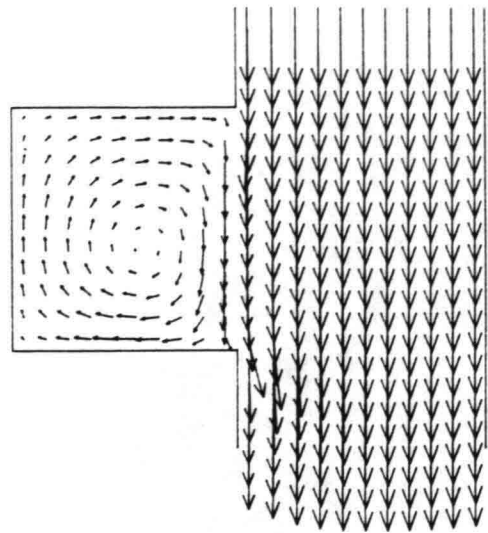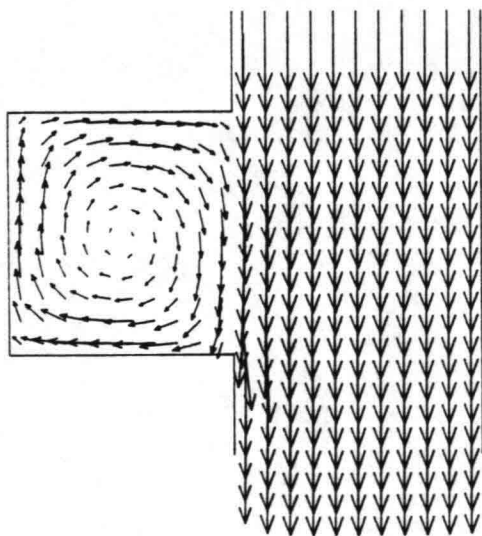
III) Run T2   IV) Run T3
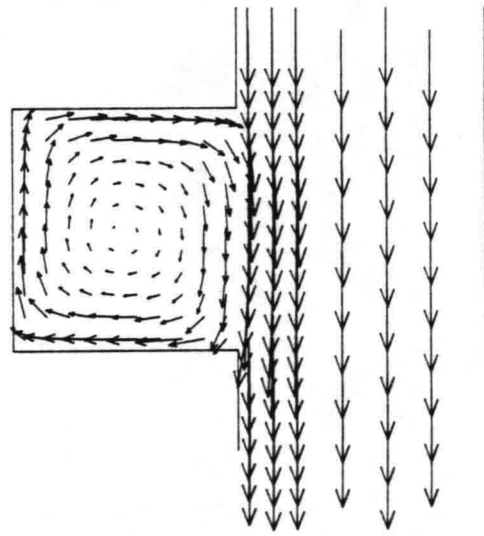
Influence of eddy viscosity on flow pattern.	TIME = 200.0 s ⊢—⊣ = 0.24 m ⊢——➤ = 0.20 m/s
Delft University of Technology	Fig. 3.2.b
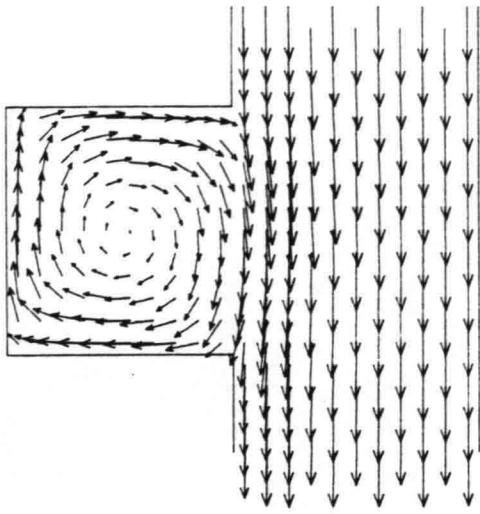
I) Run T0   II) Run T1
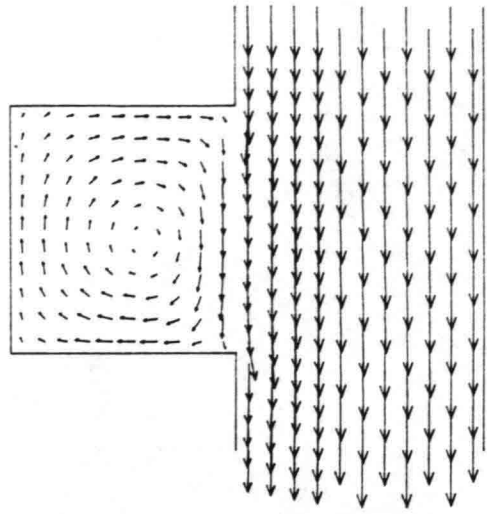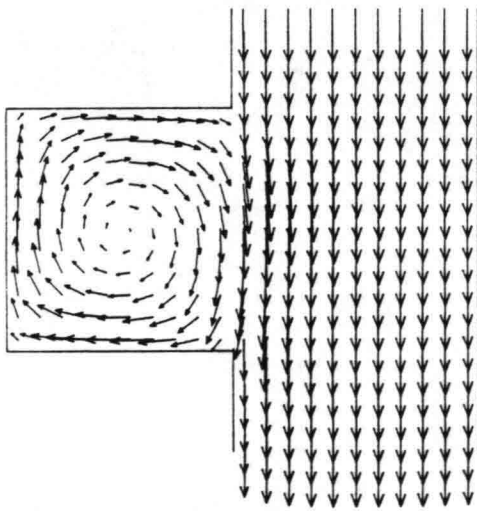
III) Run T2   IV) Run T3
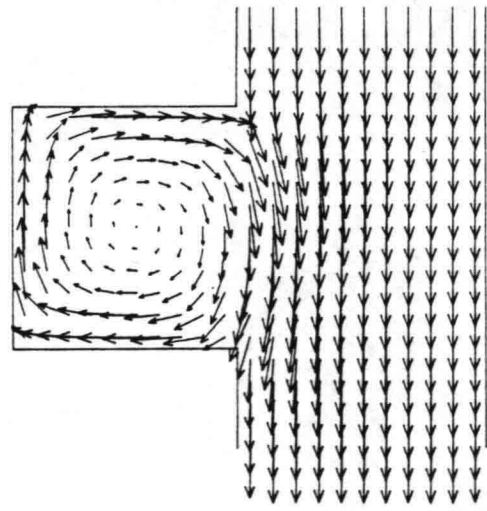
Influence of eddy viscosity on flow pattern.	TIME = 225.0 s ⊢──⊣ = 0.24 m ⊢──⟶ = 0.16 m/s
Delft University of Technology	Fig. 3.2.c
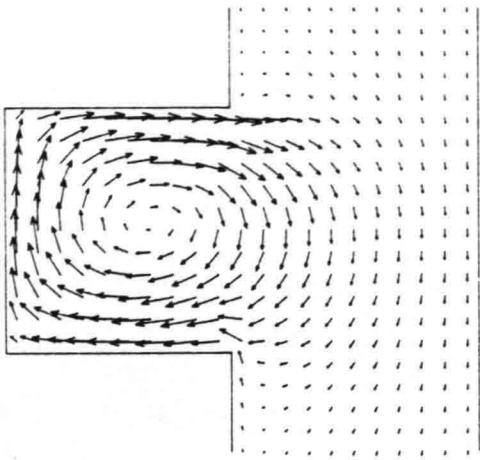
I) Run T0   II) Run T1
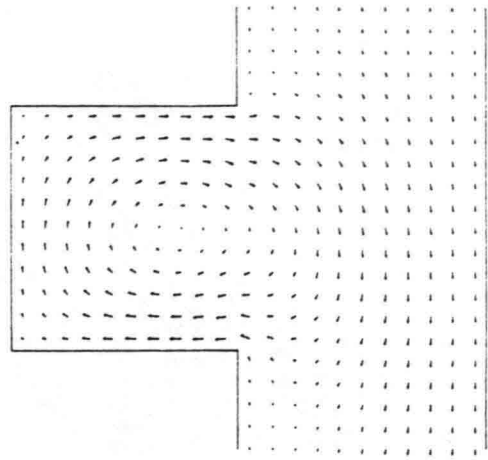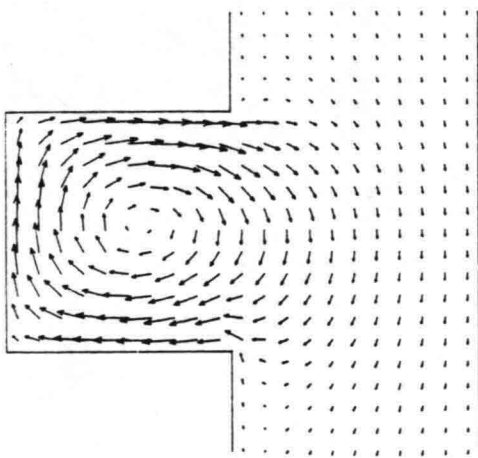
III) Run T2   IV) Run T3
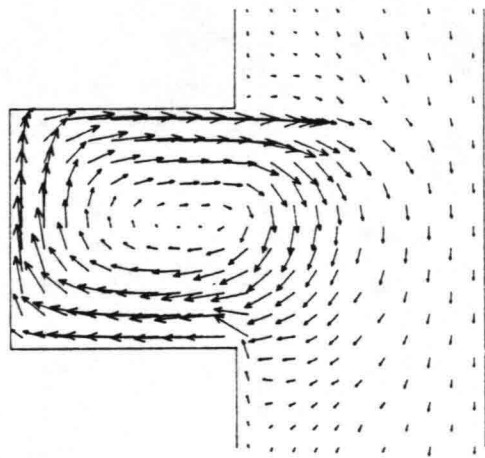
Influence of eddy viscosity on flow pattern.	TIME = 250.0 s ⊢——⊣ = 0.24 m ⊢——➔ = 0.13 m/s
Delft University of Technology	Fig. 3.2.d
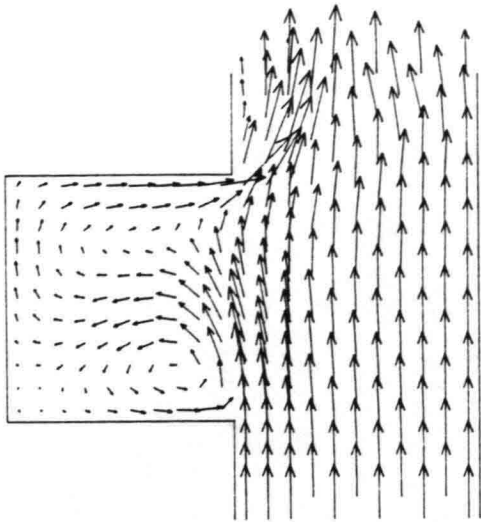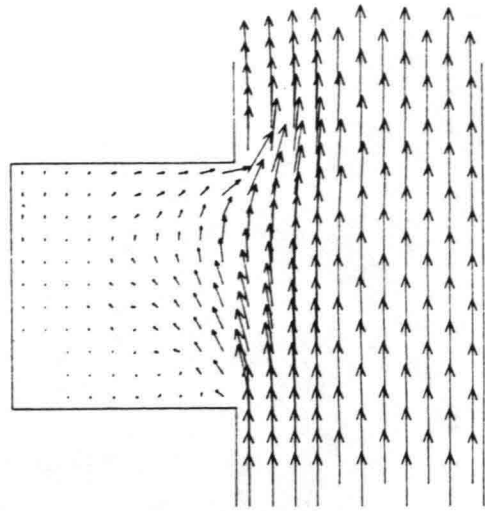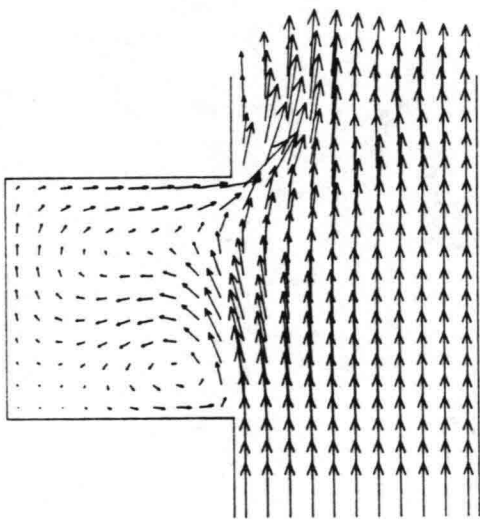
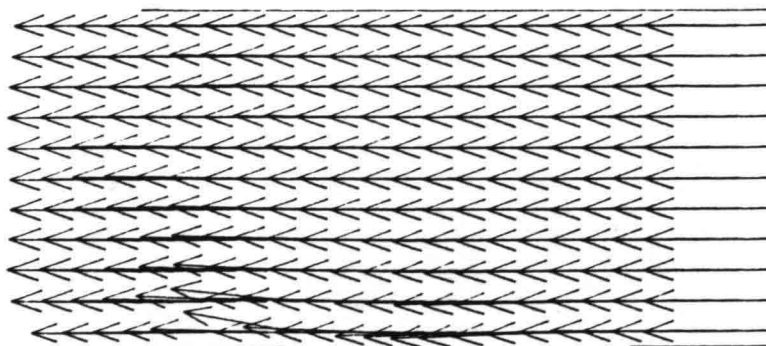I) Run T0   II) Run T1
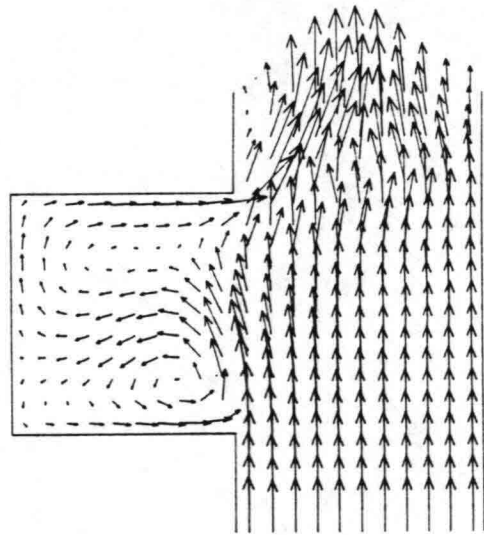
III) Run T2   IV) Run T3

Influence of eddy viscosity on flow pattern.

TIME = 275.0 s

├──┤ = 0.24 m

├──→ = 0.15 m/s

Delft University of Technology   Fig. 3.2.e
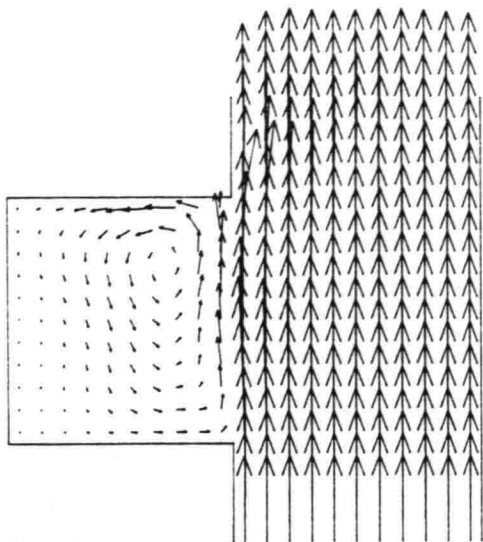
I) Run T0   II) Run T1
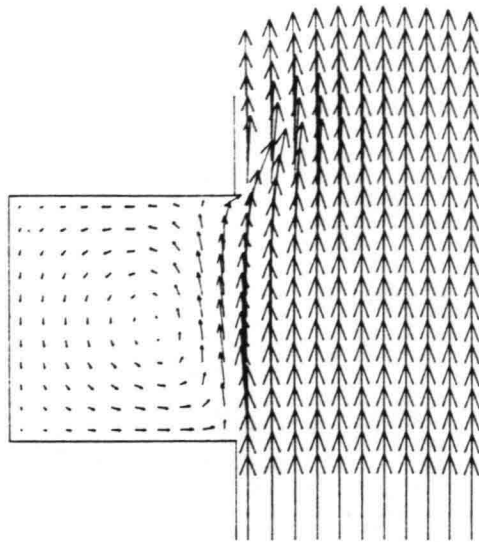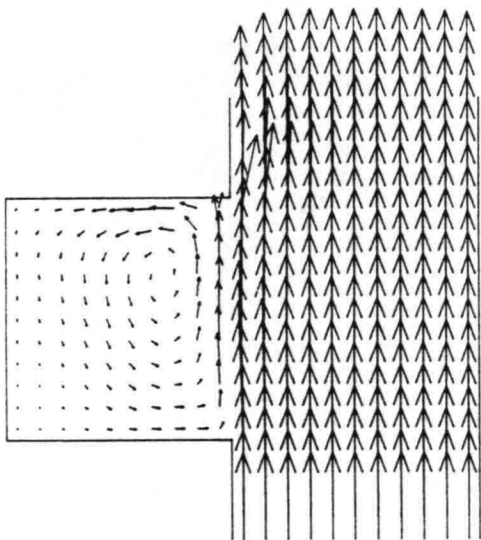
III) Run T2   IV) Run T3
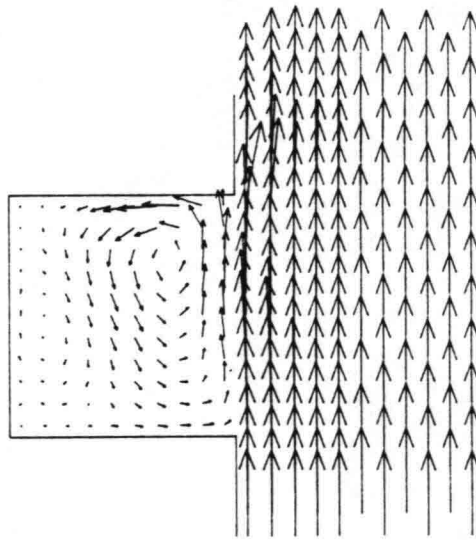
Influence of eddy viscosity on flow pattern.

TIME = 300.0 s
⊢——⊣ = 0.24 m
⊢——→ = 0.18 m/s

Delft University of Technology   Fig. 3.2.f
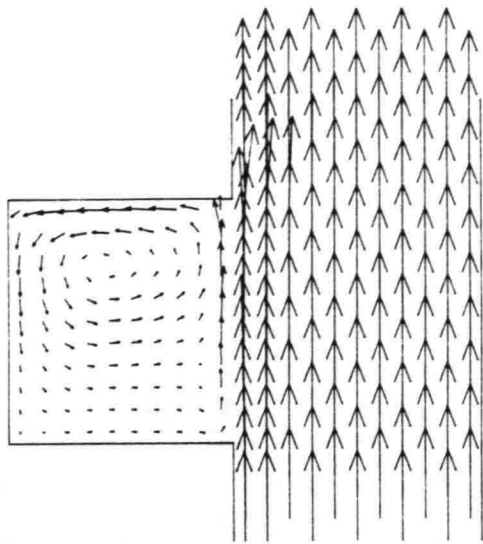
I) Run T0
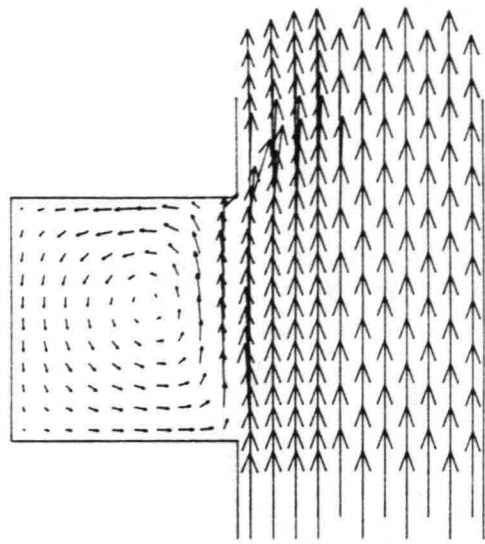
II) Run T1
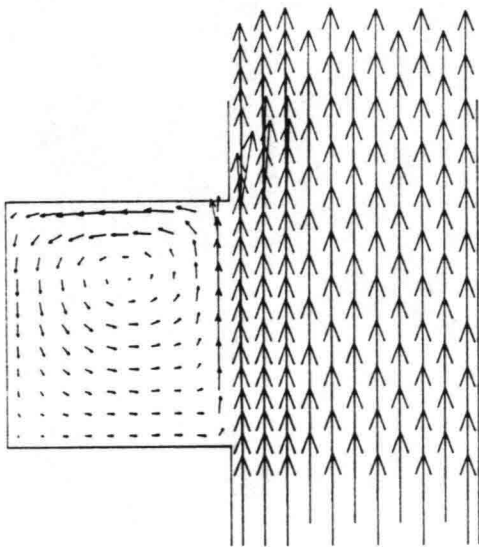
III) Run T2
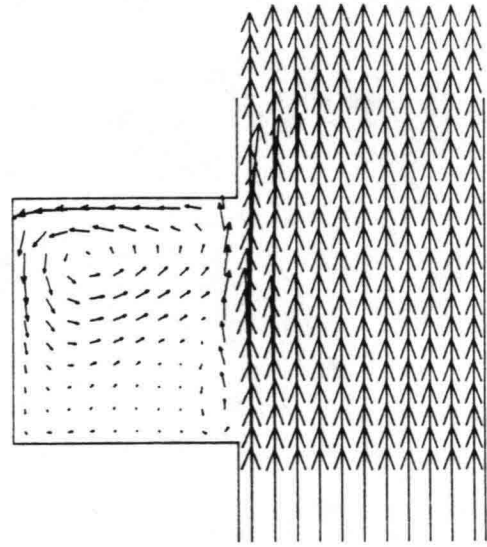
IV) Run T3

Influence of eddy viscosity on flow pattern.	TIME = 325.0 s ⊢───┤ = 0.24 m ⊢───▶ = 0.23 m/s
Delft University of Technology	Fig. 3.2.g
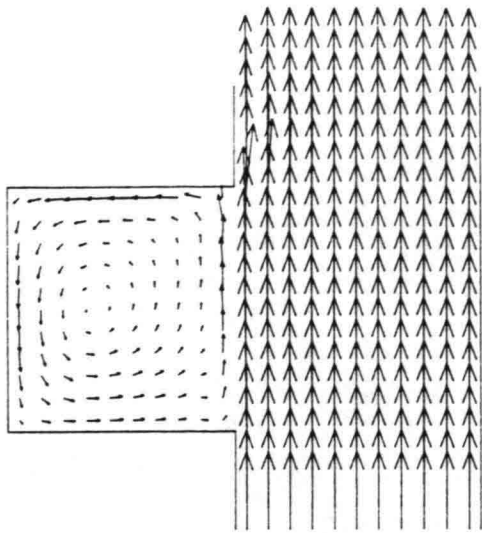
I) Run T0   II) Run T1
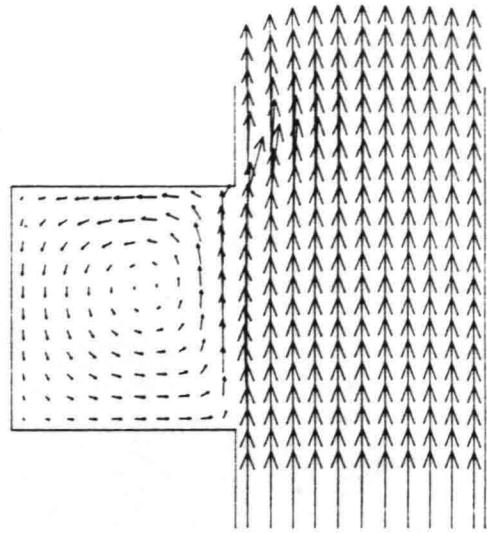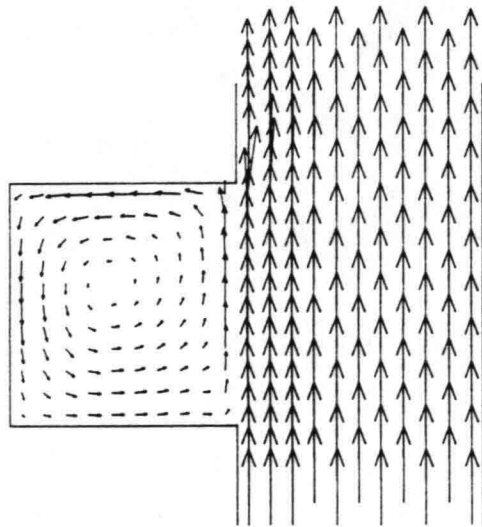
III) Run T2   IV) Run T3
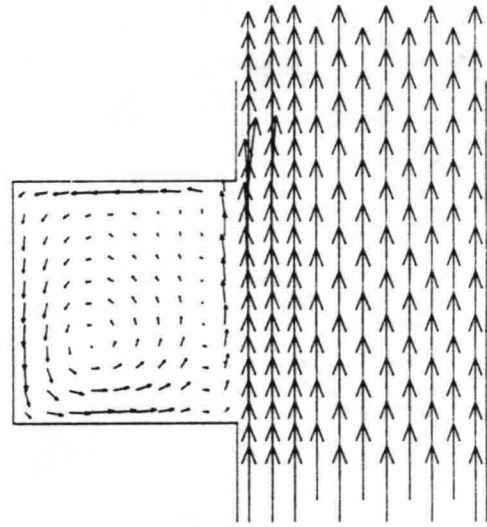
Influence of eddy viscosity on flow pattern.

TIME = 350.0 s
⊢⊣ = 0.24 m
⊢→ = 0.32 m/s

Delft University of Technology   Fig. 3.2.h
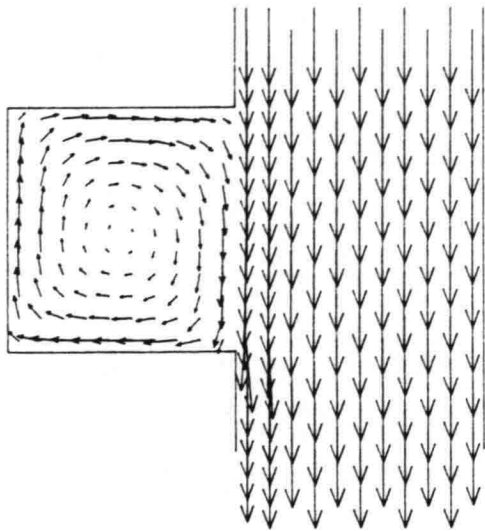
I) Run T0
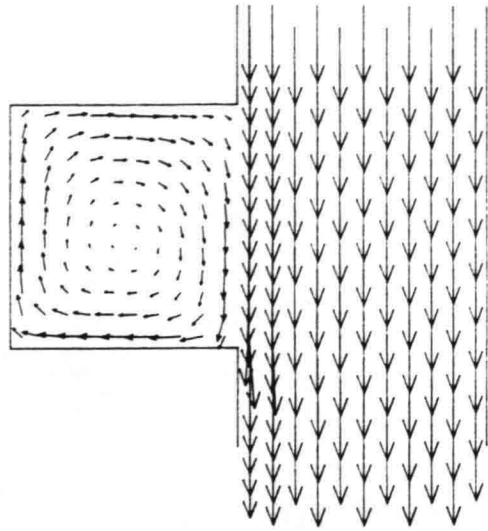
II) Run T4,
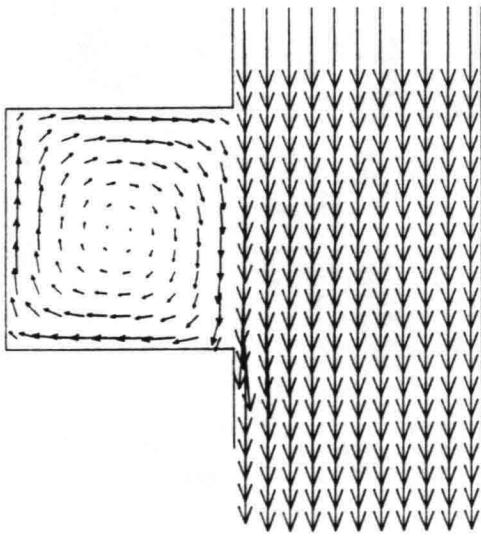
III) Run T5
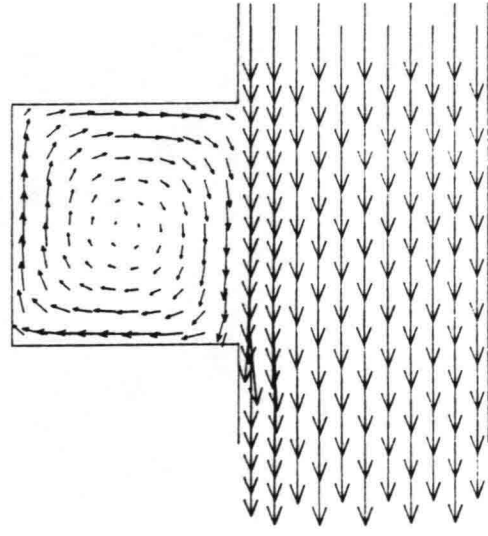
IV) Run T6

Influence of period on flow pattern.	TIME = 0.35*T ⊢——⊣ = 0.24 m ⊢——→ = 0.27 m/s
Delft University of Technology	Fig. 3.3.a
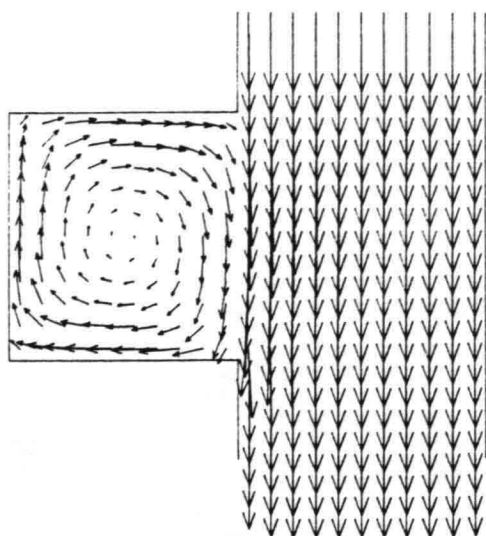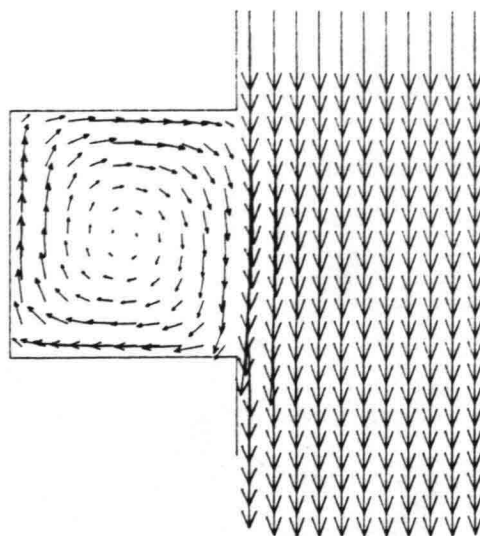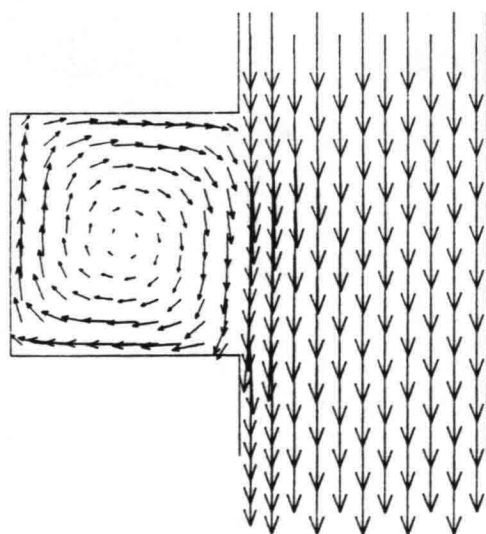
I) Run T0   II) Run T4
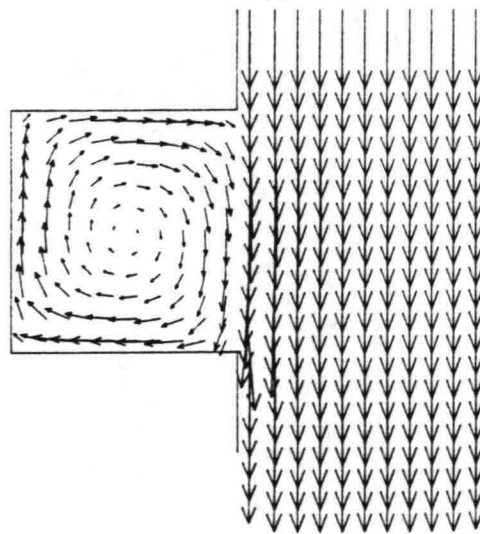
III) Run T5   IV) Run T6

Influence of period on flow pattern.

TIME = 0.40*T

⊢—⊣ = 0.24 m

⊢—→ = 0.20 m/s

Delft University of Technology

Fig. 3.3.b
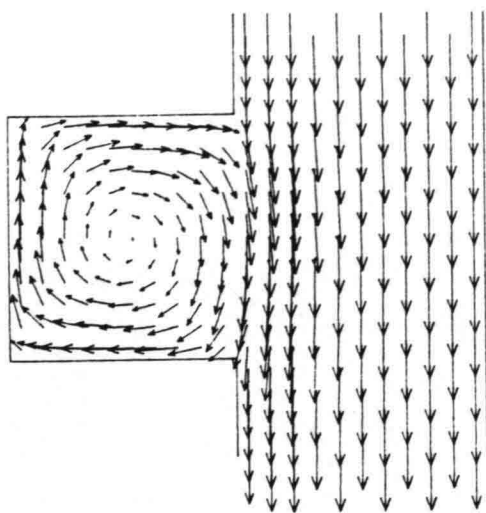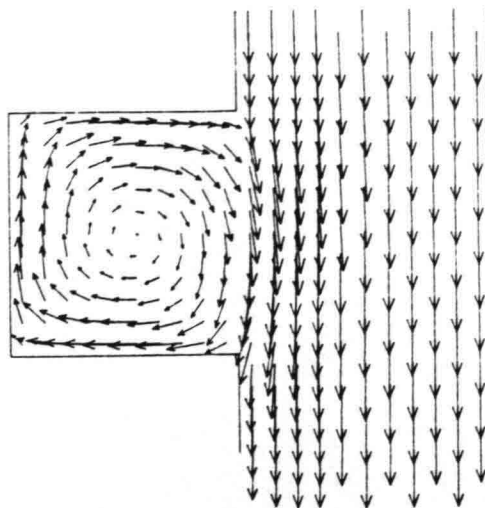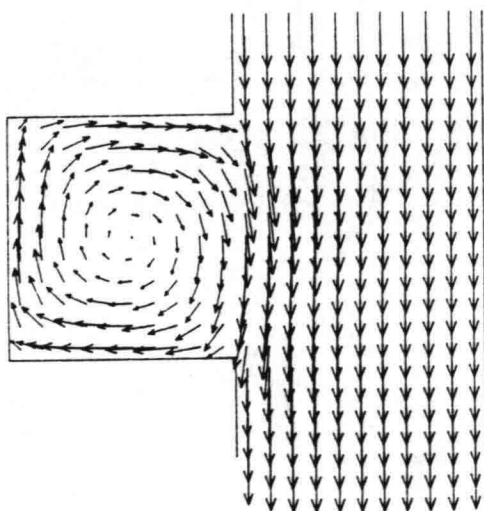
I) Run T0   II) Run T4
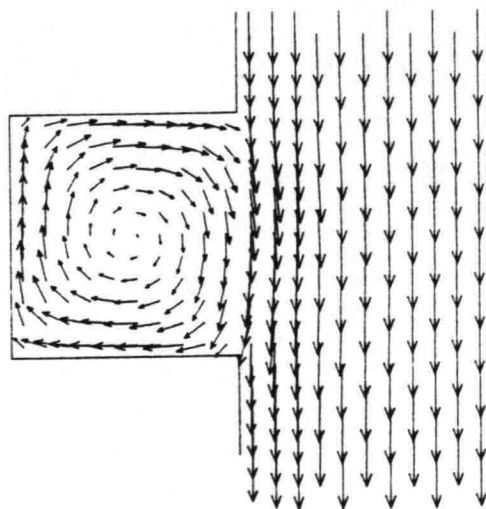
III) Run T5   IV) Run T6

Influence of period on flow pattern.	TIME = 0.45*T
	⊢——⊣ = 0.24 m
	⊢——→ = 0.16 m/s
Delft University of Technology	Fig. 3.3.c
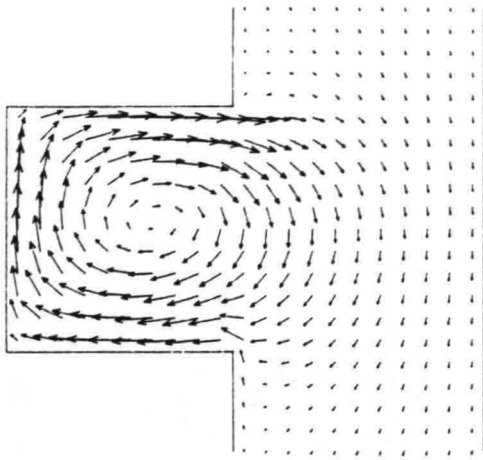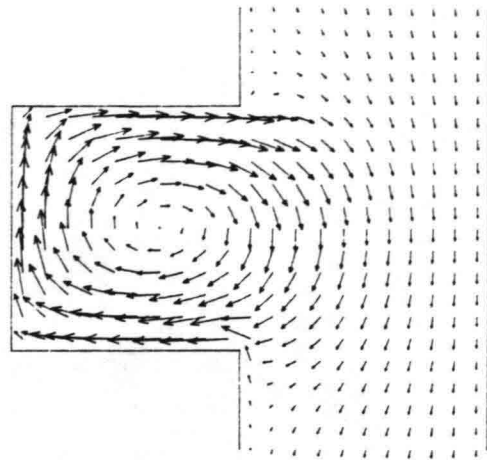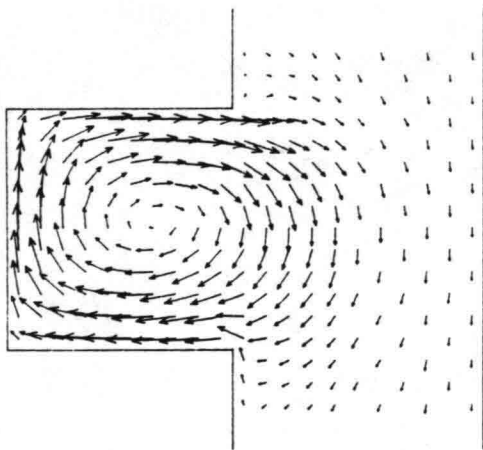
I) Run T0 II) Run T4
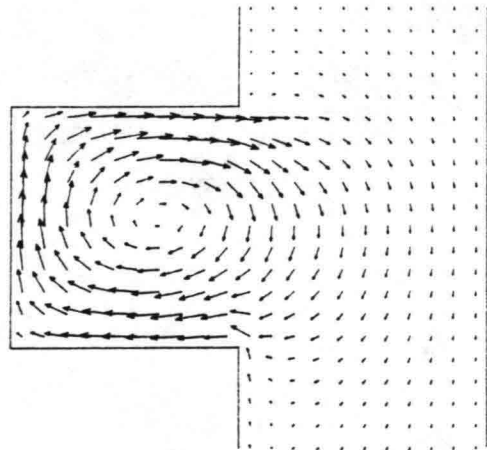
III) Run T5 IV) Run T6

Influence of period on flow pattern.	TIME = 0.50*T ⊢——⊣ = 0.24 m ⊢——→ = 0.13 m/s
Delft University of Technology	Fig. 3.3.d
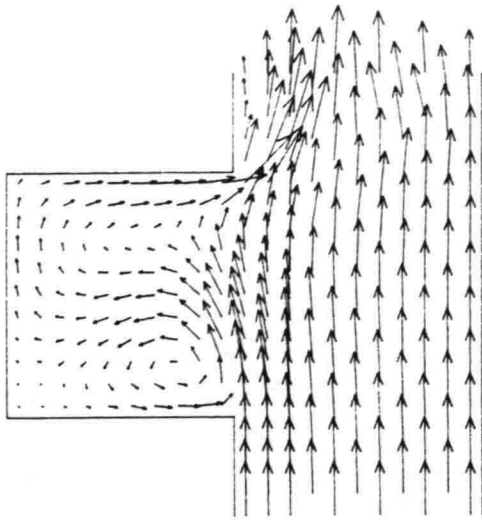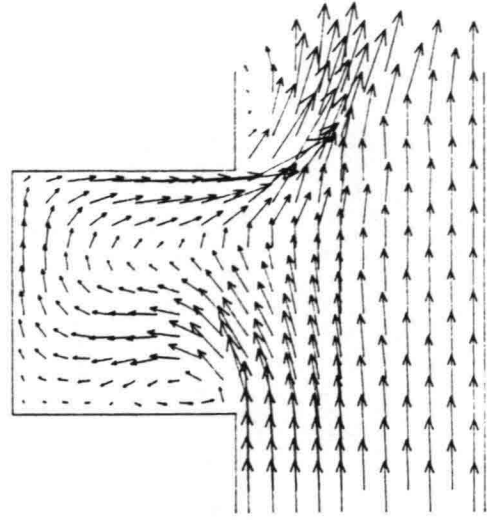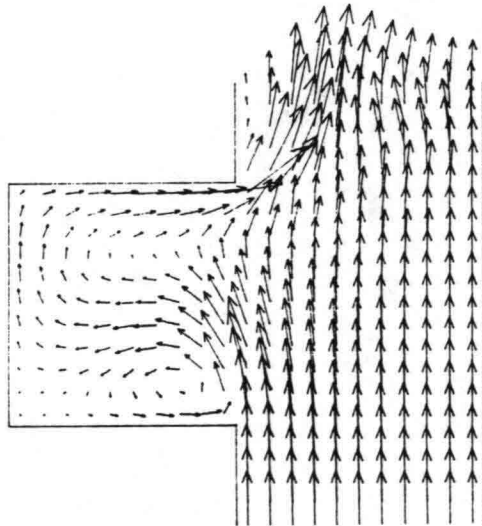
I) Run T0
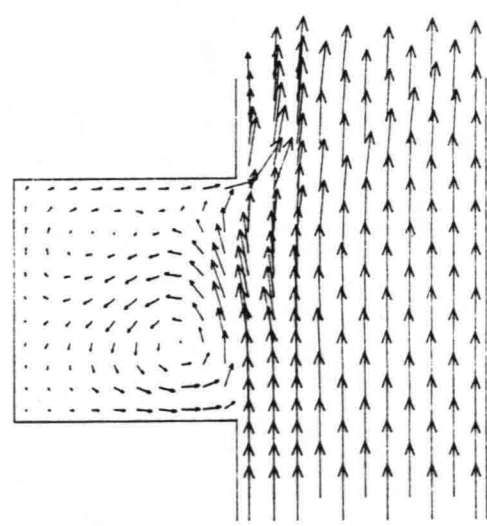
II) Run T4

III) Run T5

IV) Run T6

Influence of period on flow pattern.	TIME = 0.55*T ⊢——⊣ = 0.24 m ⊢——▶ = 0.15 m/s
Delft University of Technology	Fig. 3.3.e
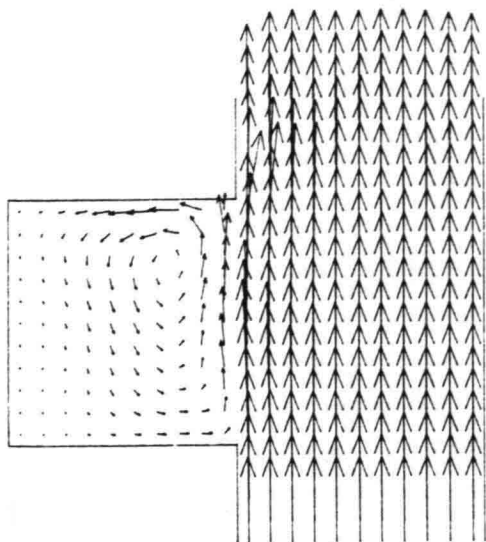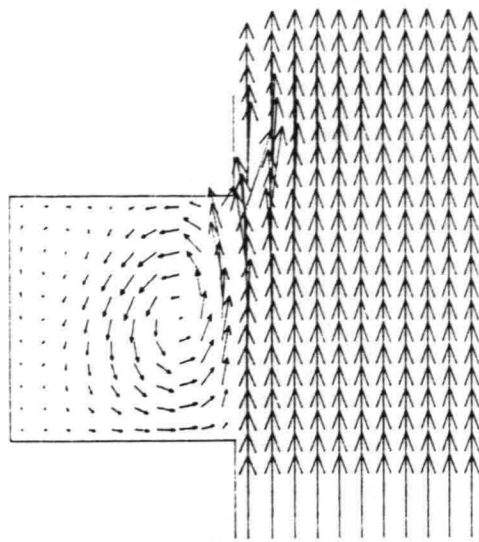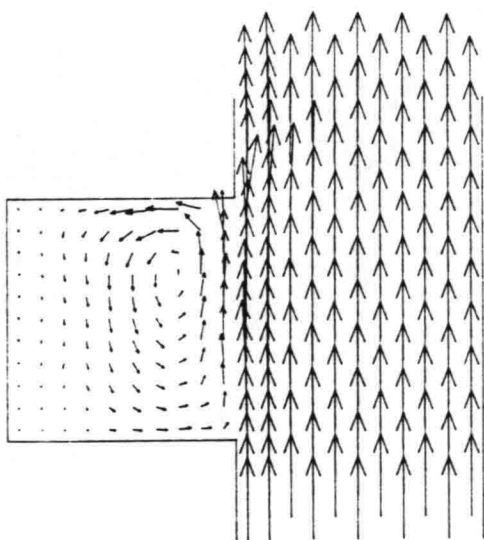
I) Run T0
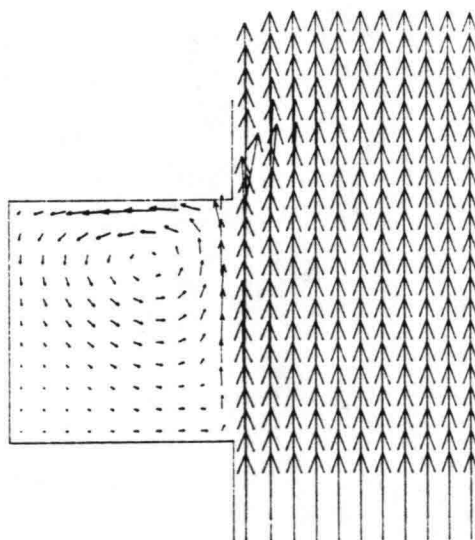
II) Run T4

III) Run T5

IV) Run T6

Influence of period on flow pattern.	TIME = 0.60*T ⊢——⊣ = 0.24 m ⊢——→ = 0.18 m/s
Delft University of Technology	Fig. 3.3.f
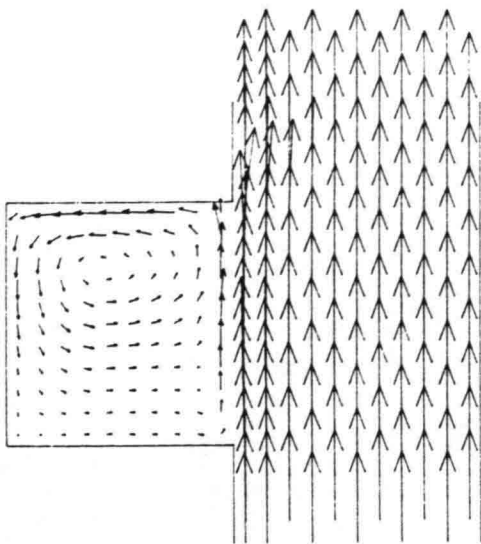
I) Run T0
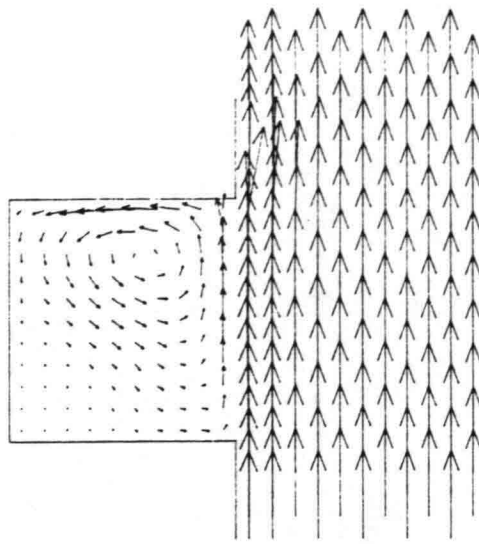
II) Run T4
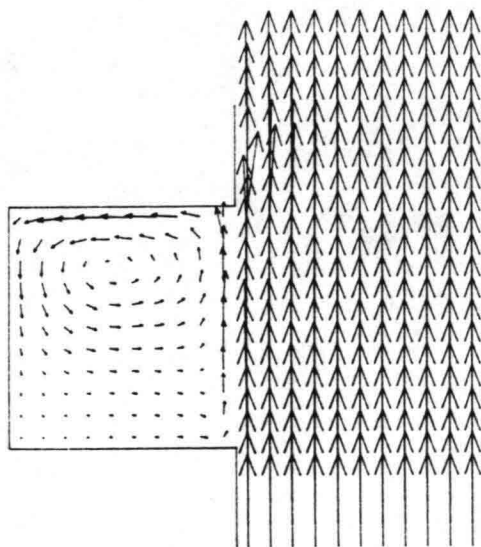
III) Run T5
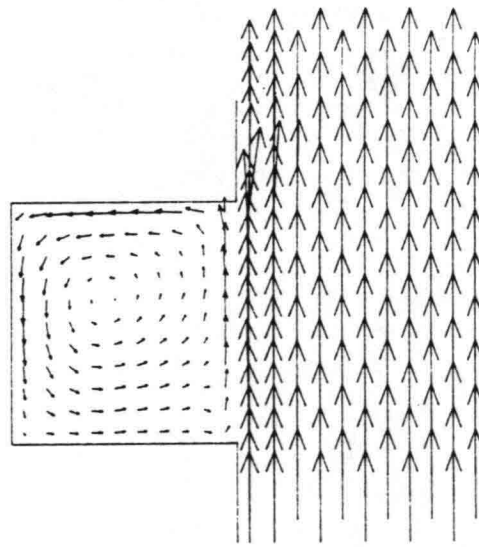
IV) Run T6

Influence of period on flow
pattern.

TIME = 0.65*T
⊢——⊣ = 0.24 m
⊢——→ = 0.23 m/s

Delft University of Technology
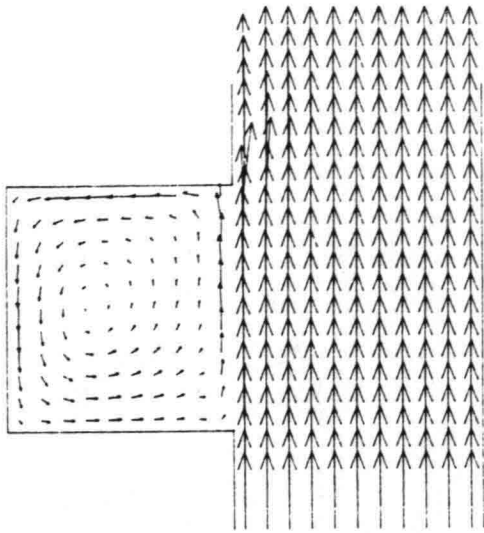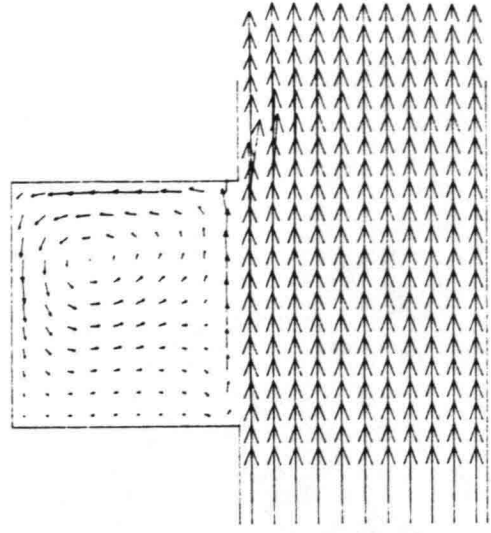
Fig. 3.3.g
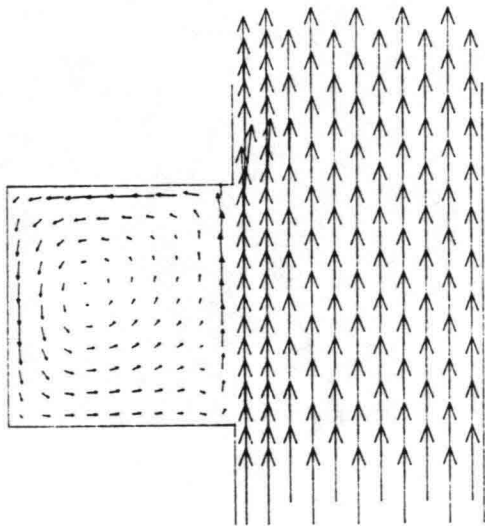
I) Run T0   II) Run T4

III) Run T5   IV) Run T6
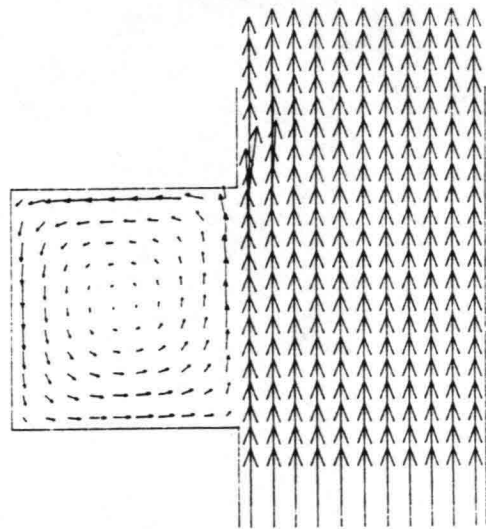
Influence of period on flow pattern.	TIME = 0.70*T ⊢—⊣ = 0.24 m ⊢—→ = 0.32 m/s
Delft University of Technology	Fig. 3.3.h

I) Run T0
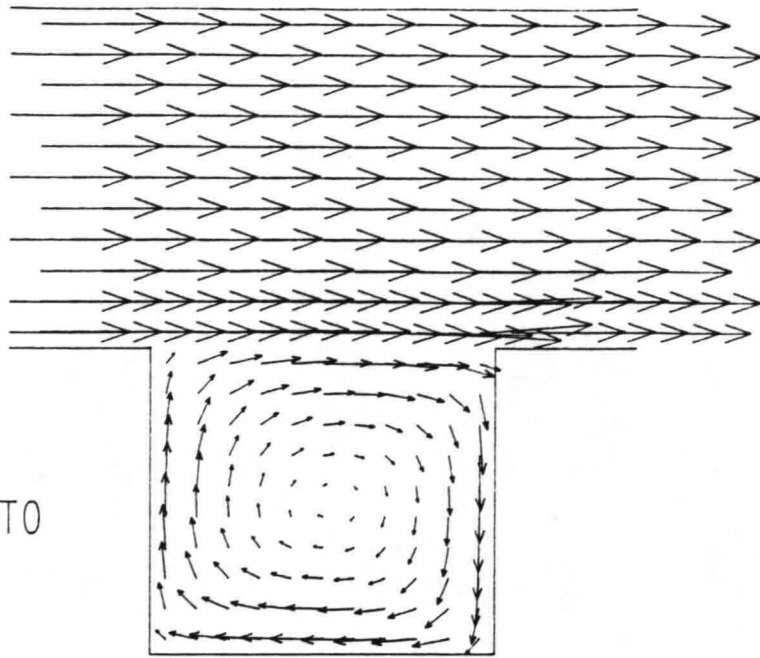
II) Run T7
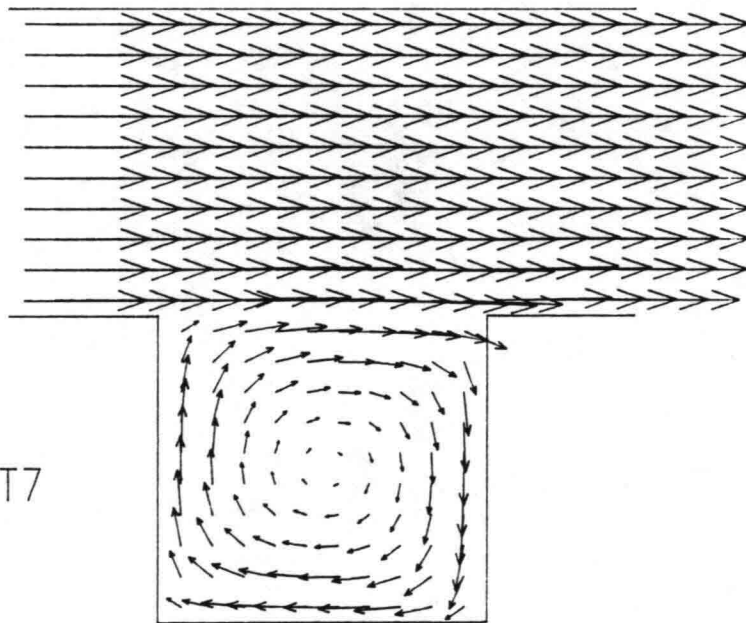
Influence of gridsize on flow pattern.	TIME = 175.0 s ⊢——⊣ = 0.17 m ⊢——→ = 0.18 m/s
Delft University of Technology	Fig. 3.4.a

I) Run T0
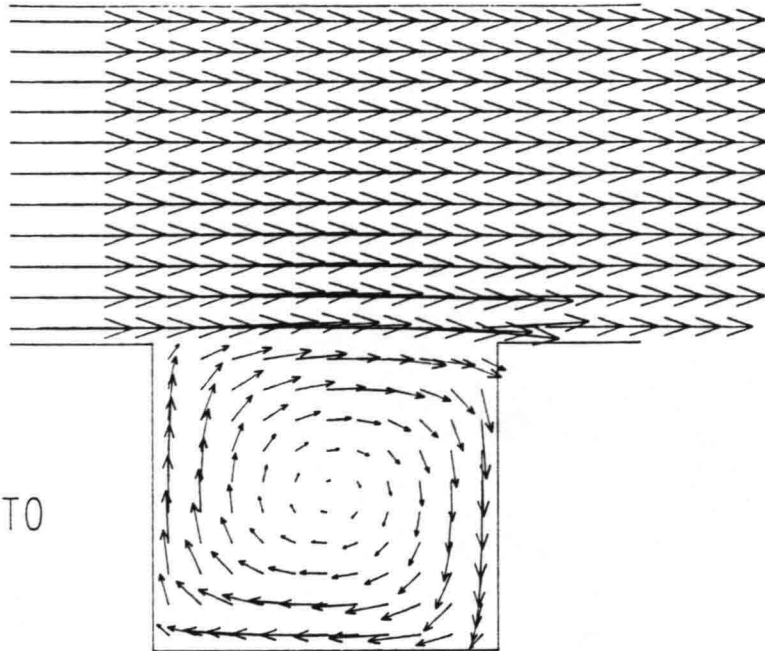
II) Run T7
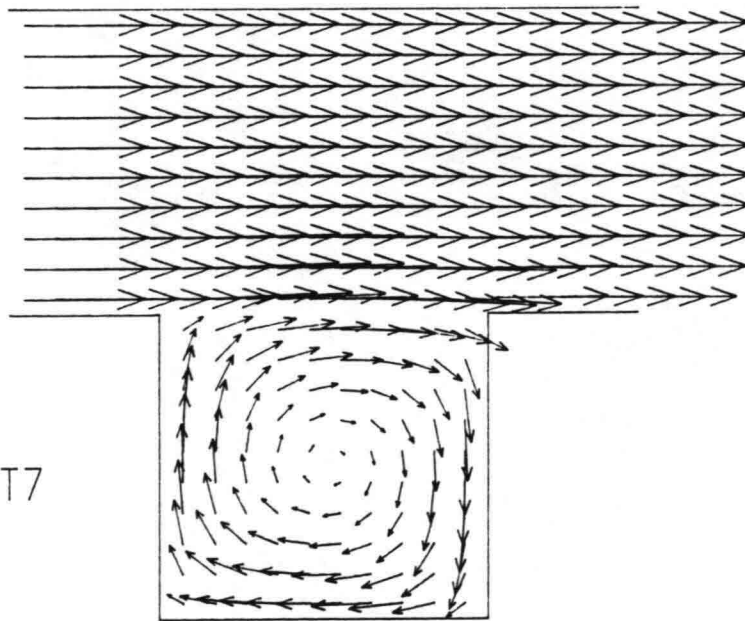
Influence of gridsize on flow pattern.

TIME = 200.0 s
⊢——⊣ = 0.17 m
⊢——→ = 0.13 m/s

Delft University of Technology

Fig. 3.4.b

I) Run T0
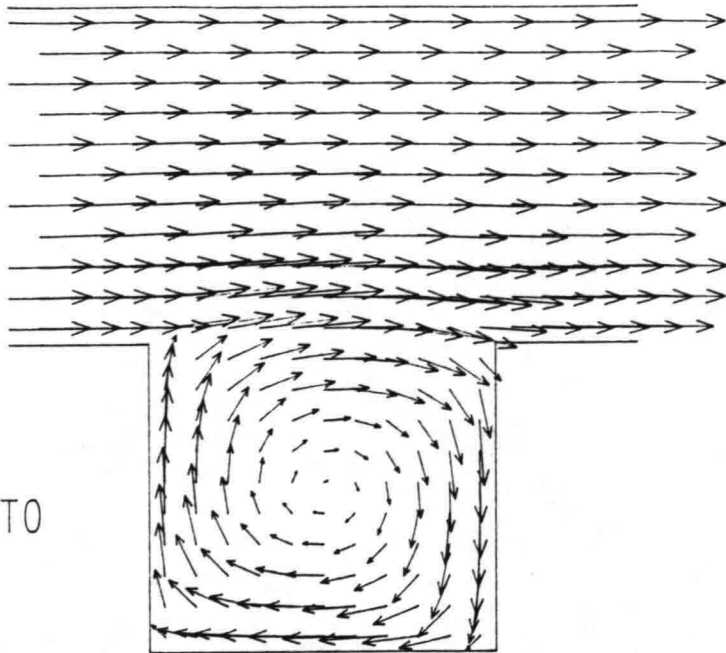
II) Run T7
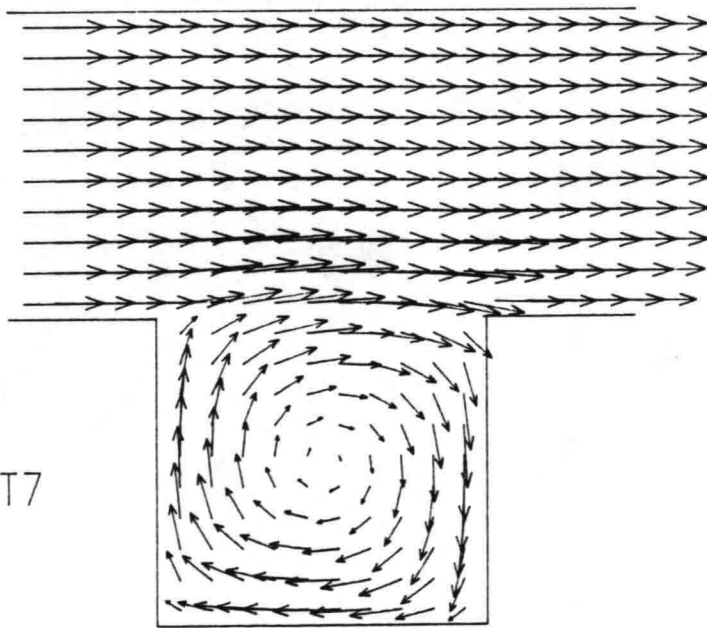
Influence of gridsize on flow pattern.	TIME = 225.0 s ├──┤ = 0.17 m ├──→ = 0.11 m/s
Delft University of Technology	Fig. 3.4.c

I) Run T0
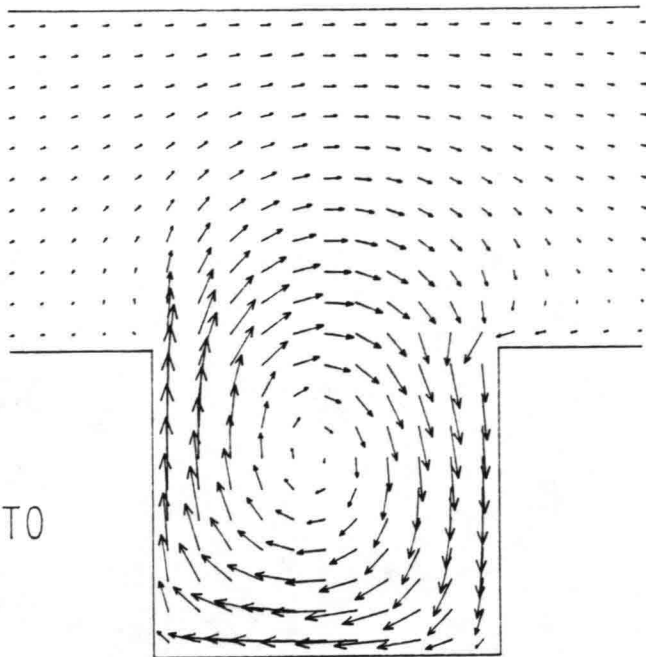
II) Run T7
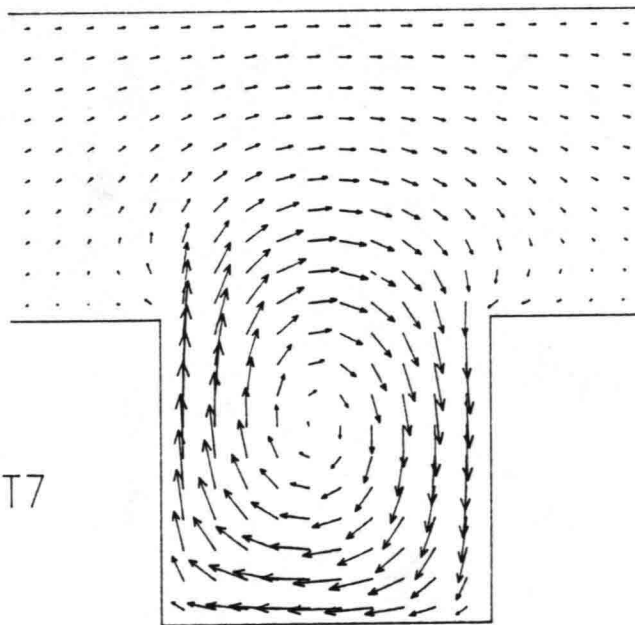
Influence of gridsize on flow pattern.	TIME = 250.0 s ├──┤ = 0.17 m ├──▶ = 0.09 m/s
Delft University of Technology	Fig. 3.4.d
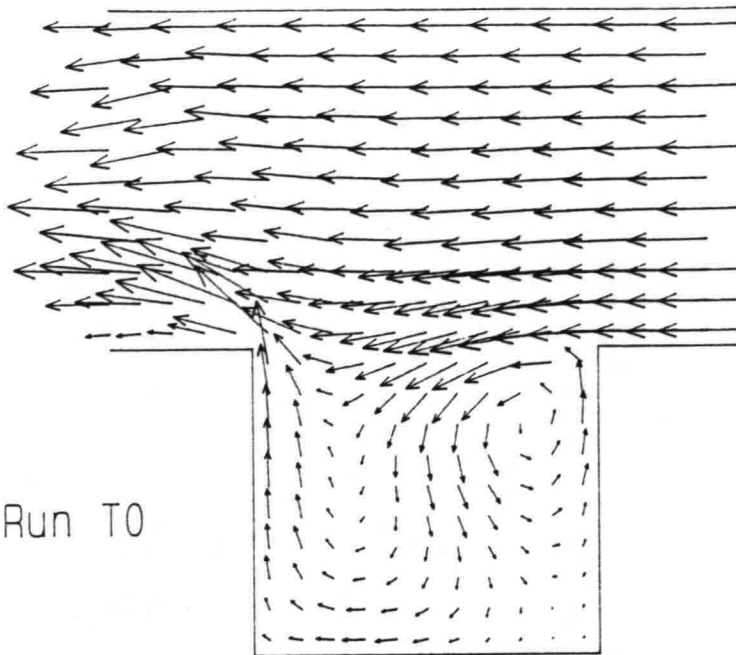
I) Run T0
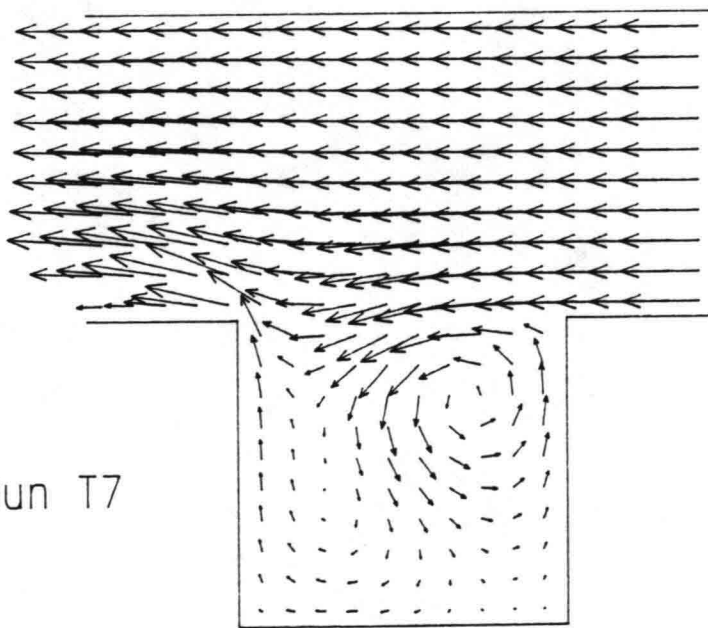
II) Run T7

Influence of gridsize on flow pattern.	TIME = 275.0 s ⊢——⊣ = 0.17 m ⊢——→ = 0.10 m/s
Delft University of Technology	Fig. 3.4.e

I) Run T0
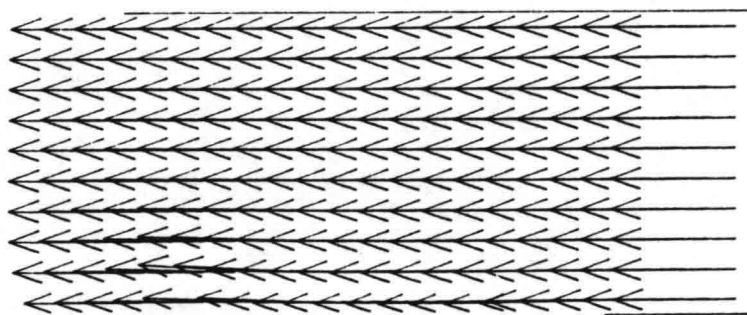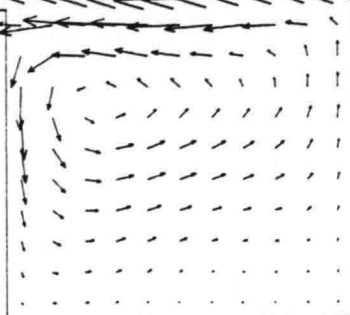
II) Run T7
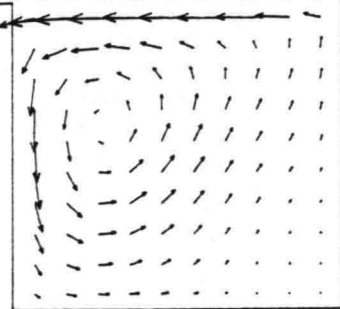
Influence of gridsize on flow pattern.

TIME = 300.0 s
⊢——⊣ = 0.17 m
⊢——➤ = 0.12 m/s

Delft University of Technology

Fig. 3.4.f
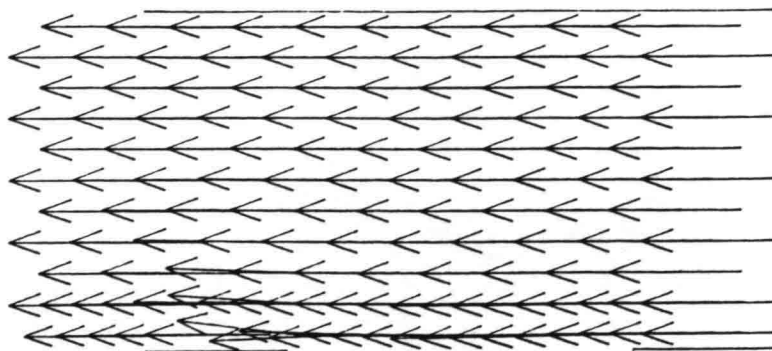
I) Run T0
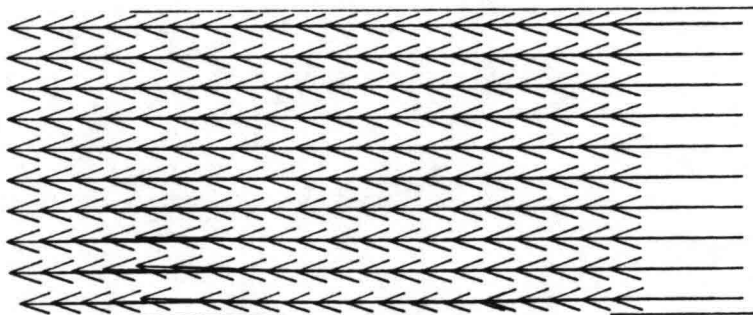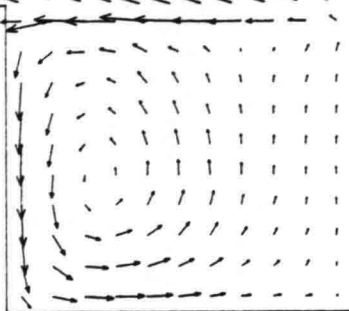
II) Run T7
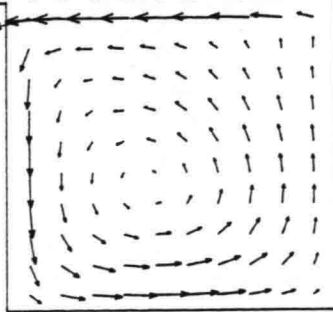
Influence of gridsize on flow pattern.	TIME = 325.0 s ⊢——⊣ = 0.17 m ⊢——→ = 0.16 m/s
Delft University of Technology	Fig. 3.4.g

I) Run T0

II) Run T7
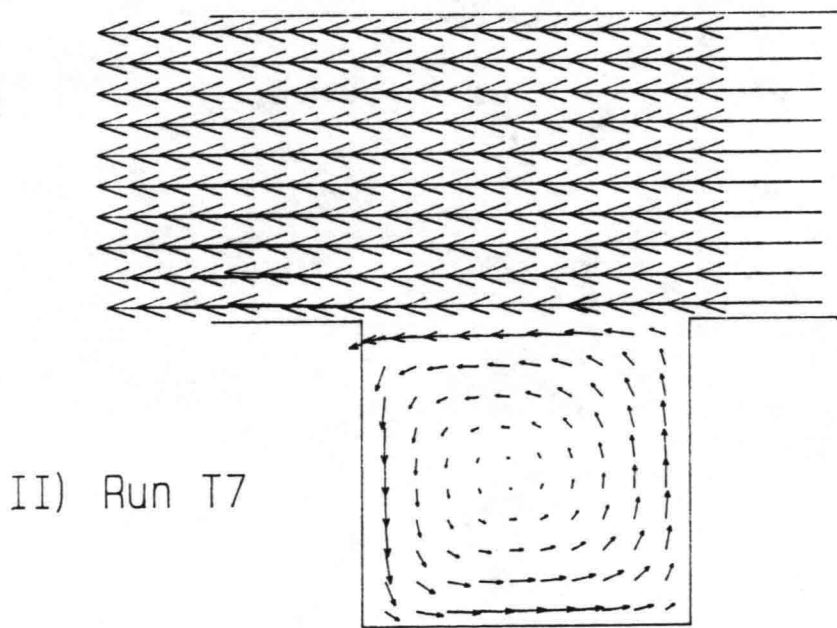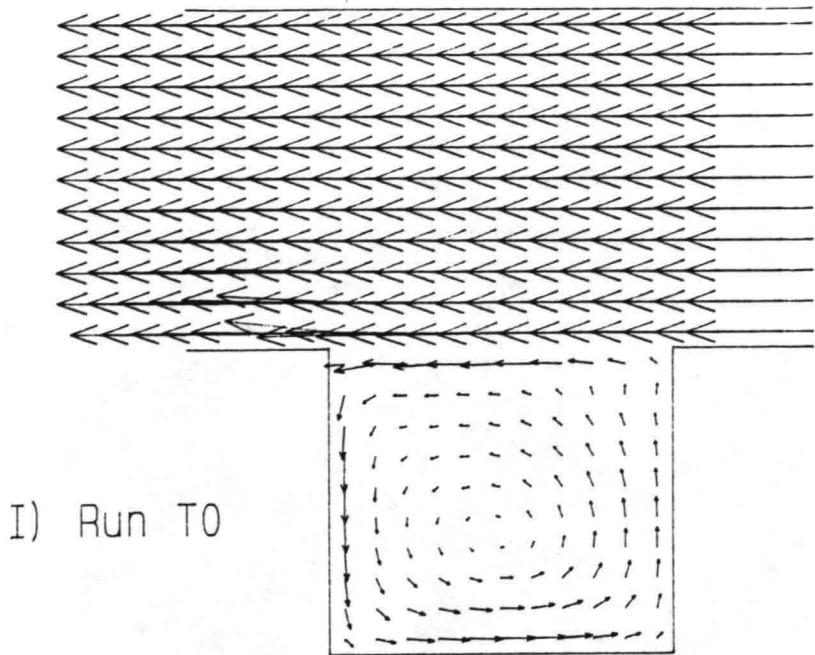
Influence of gridsize on flow pattern.

TIME = 350.0 s
⊢——⊣ = 0.17 m
⊢——→ = 0.20 m/s

Delft University of Technology

Fig. 3.4.h
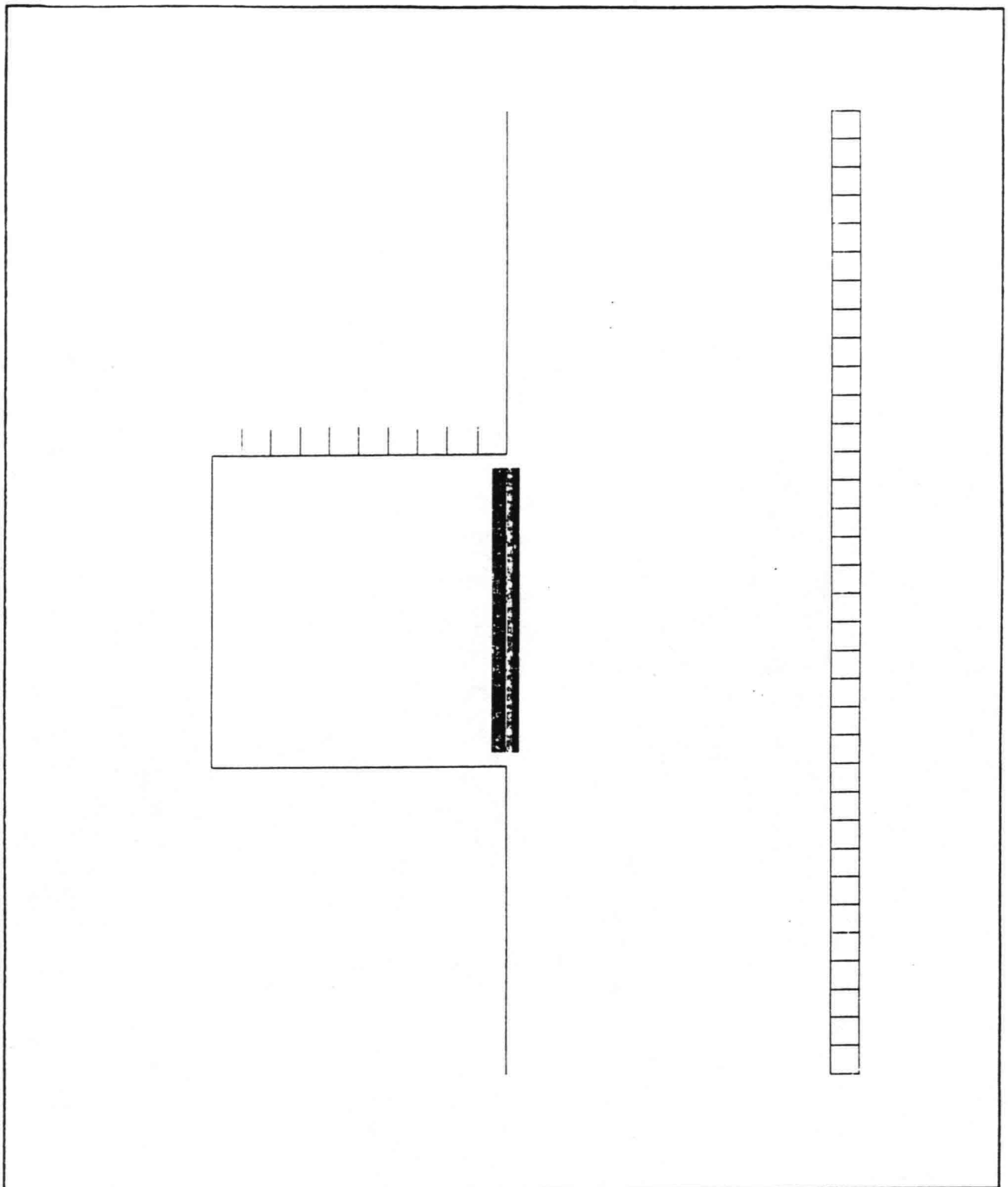
Isolines of the concentration (mg/l) constant dispersion coefficient	TIME = 375.0 s $\longmapsto$ = 0.14 m $\triangle$ = 2.5 mg/l
Delft University of Technology	Fig. 3.5.a
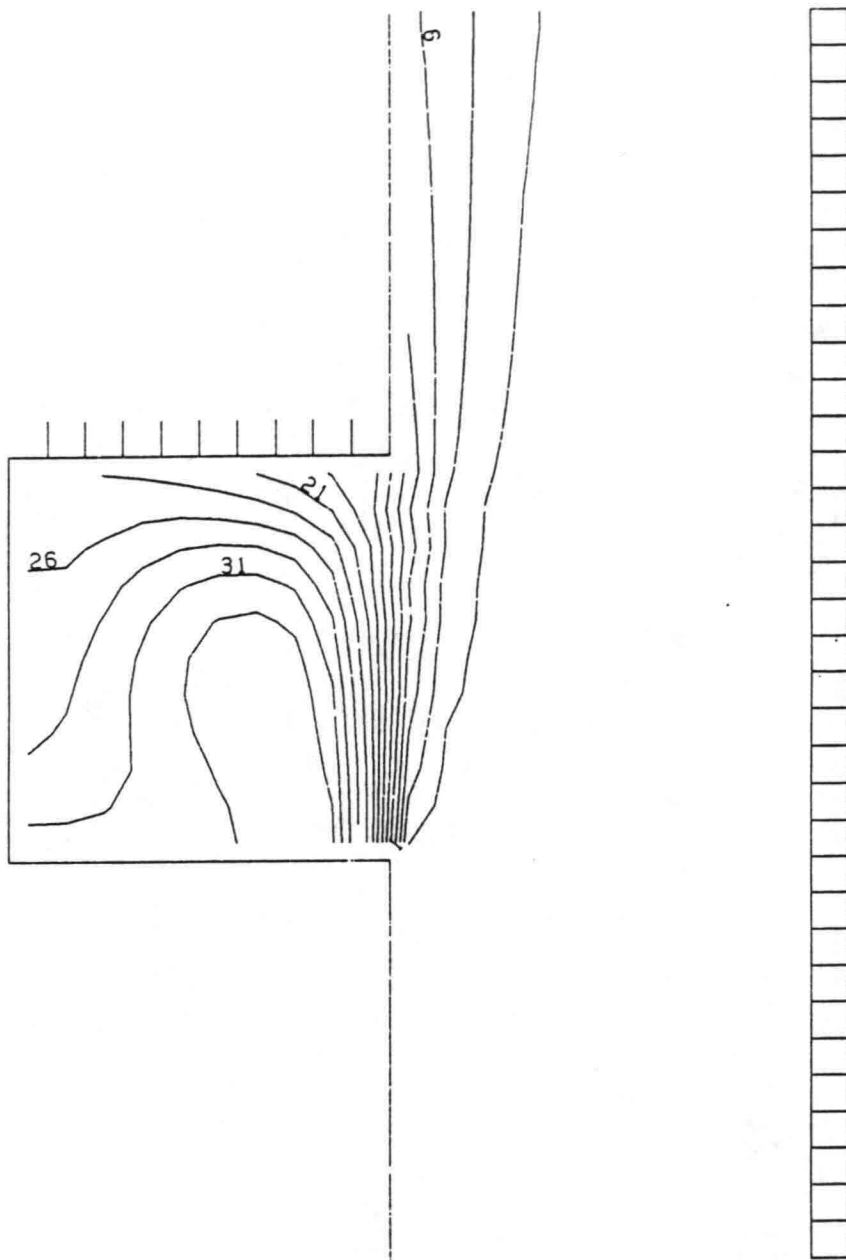
Isolines of the concentration (mg/l)
constant dispersion coefficient

TIME = 400.0 s
⊢——⊣ = 0.14 m
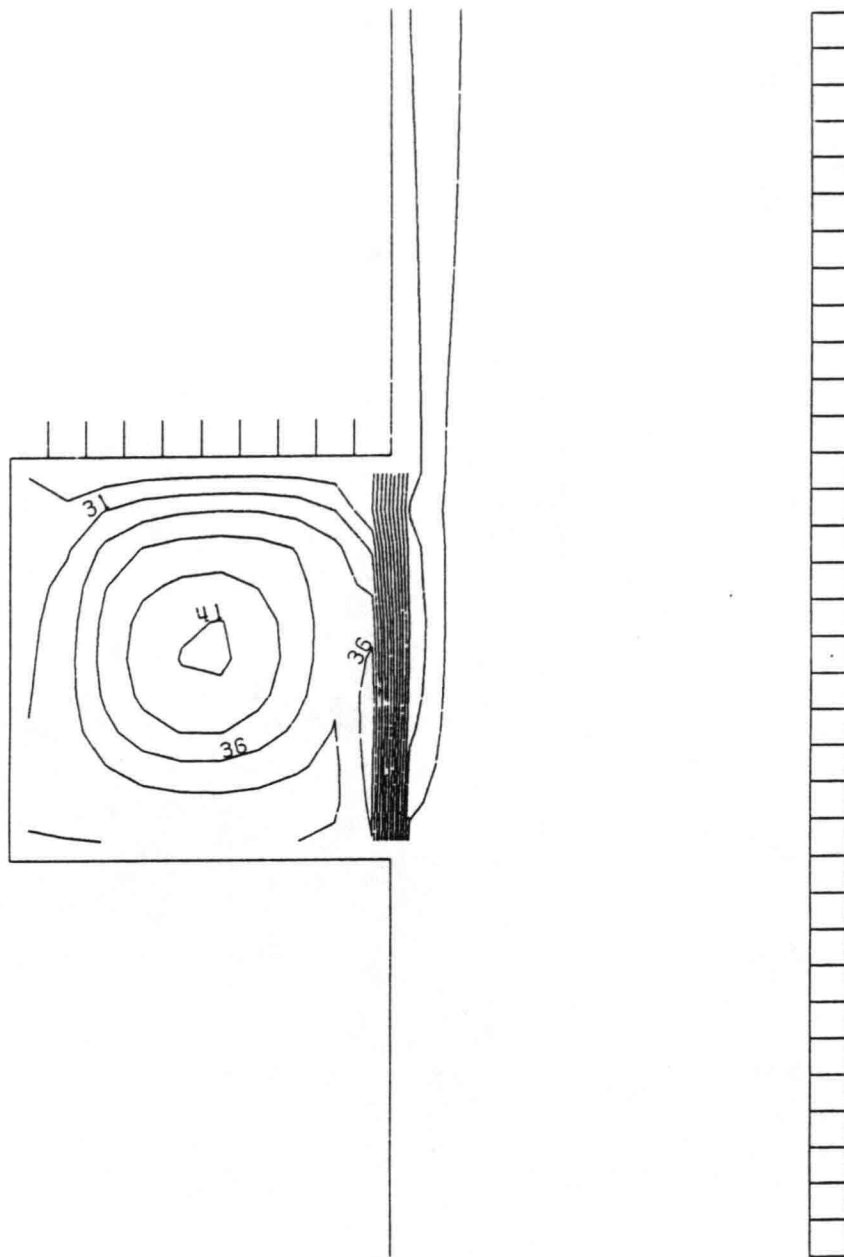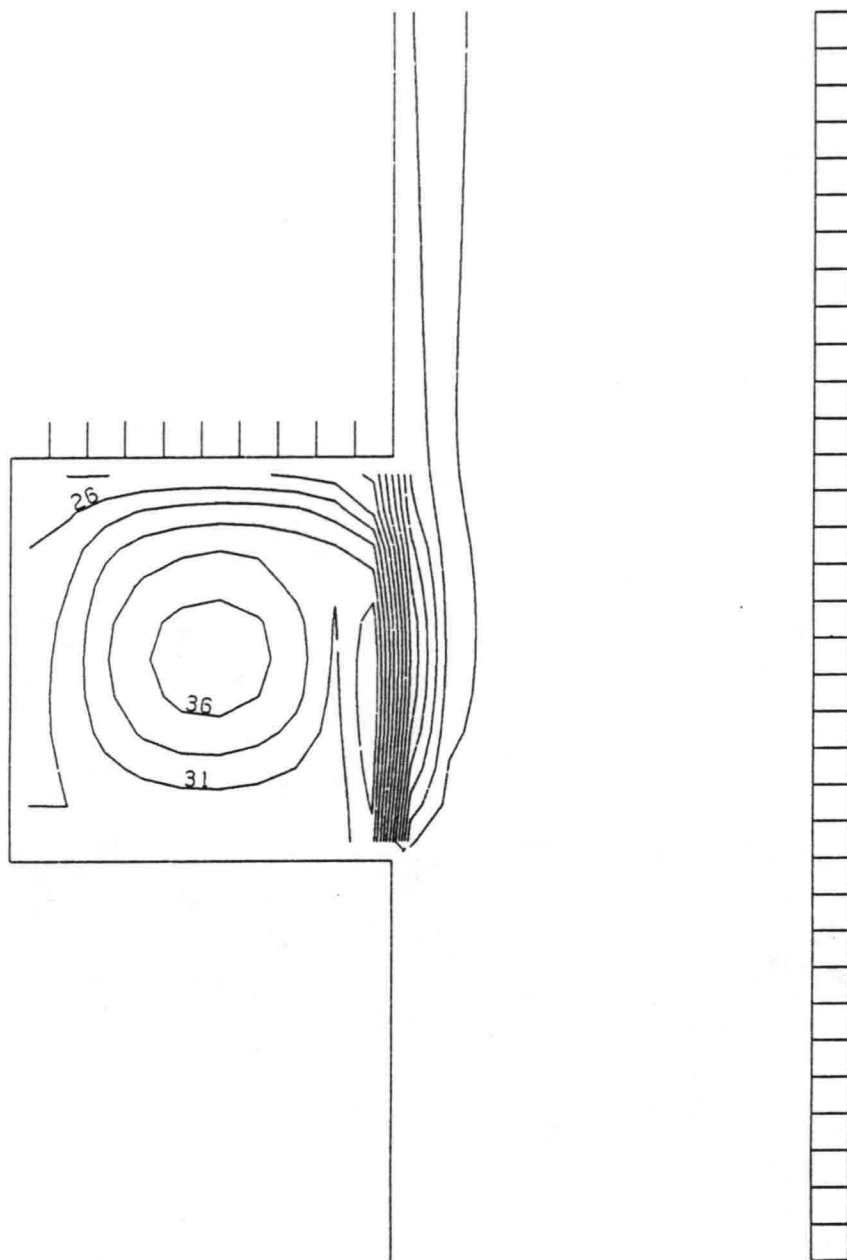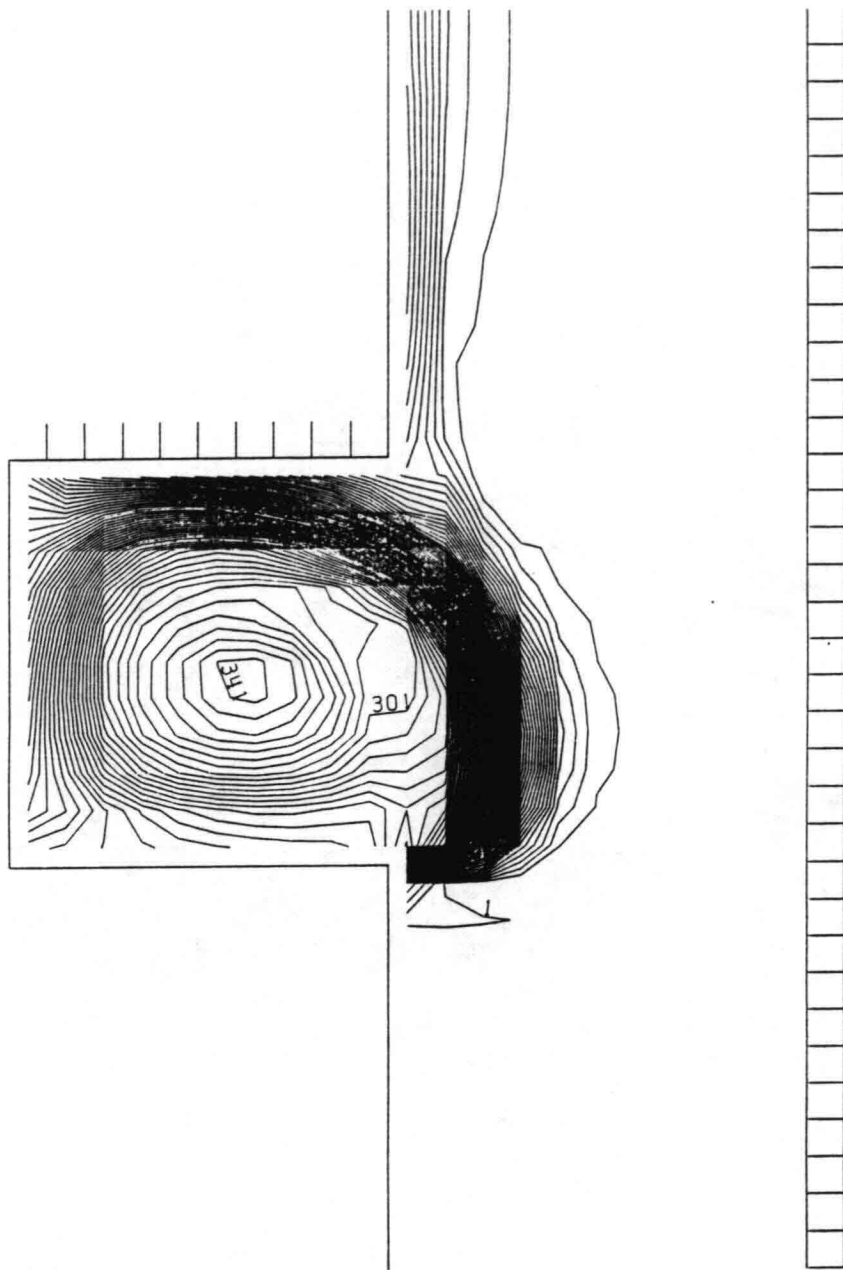△ = 2.5 mg/l

Delft University of Technology

Fig. 3.5.b
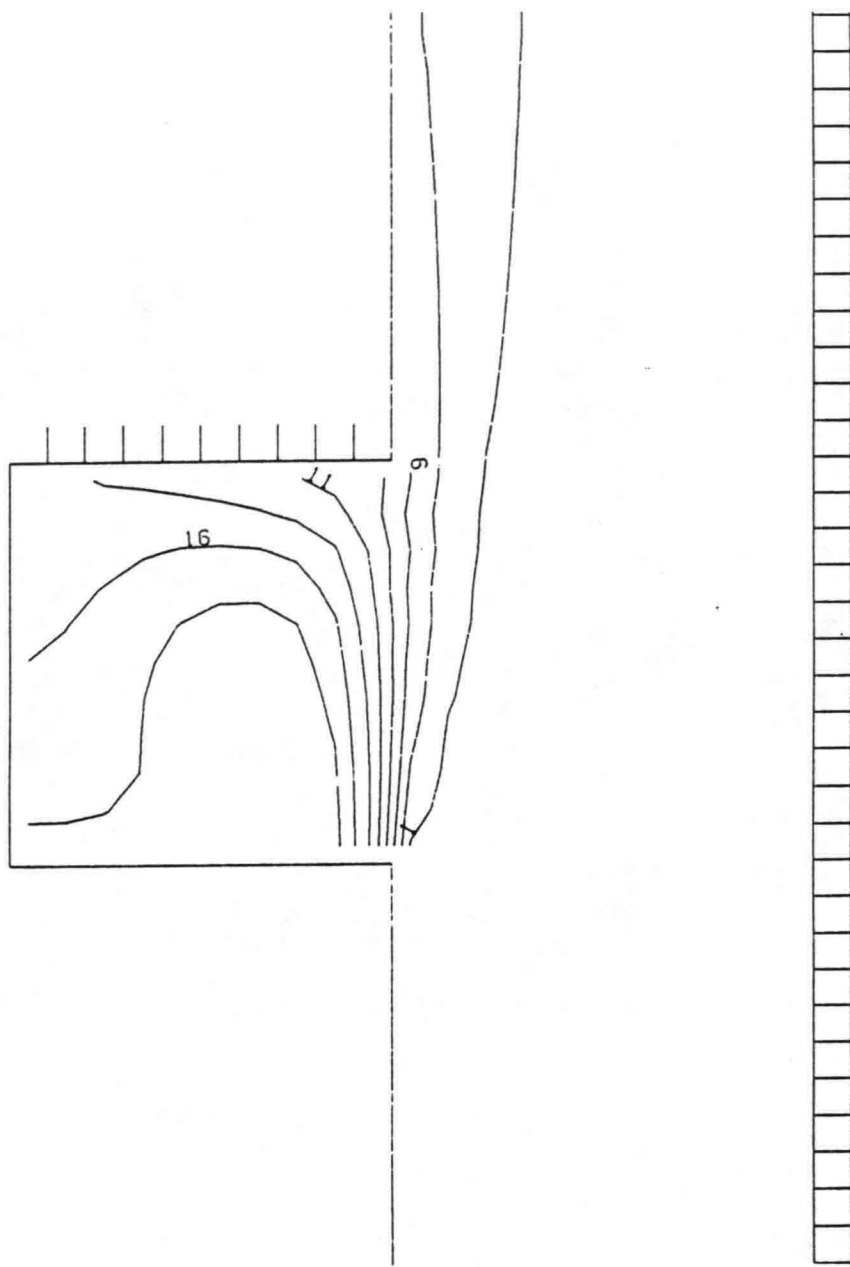
Isolines of the concentration (mg/l) constant dispersion coefficient	TIME = 425.0 s ├───┤ = 0.14 m △ = 2.5 mg/1
Delft University of Technology	Fig. 3.5.c
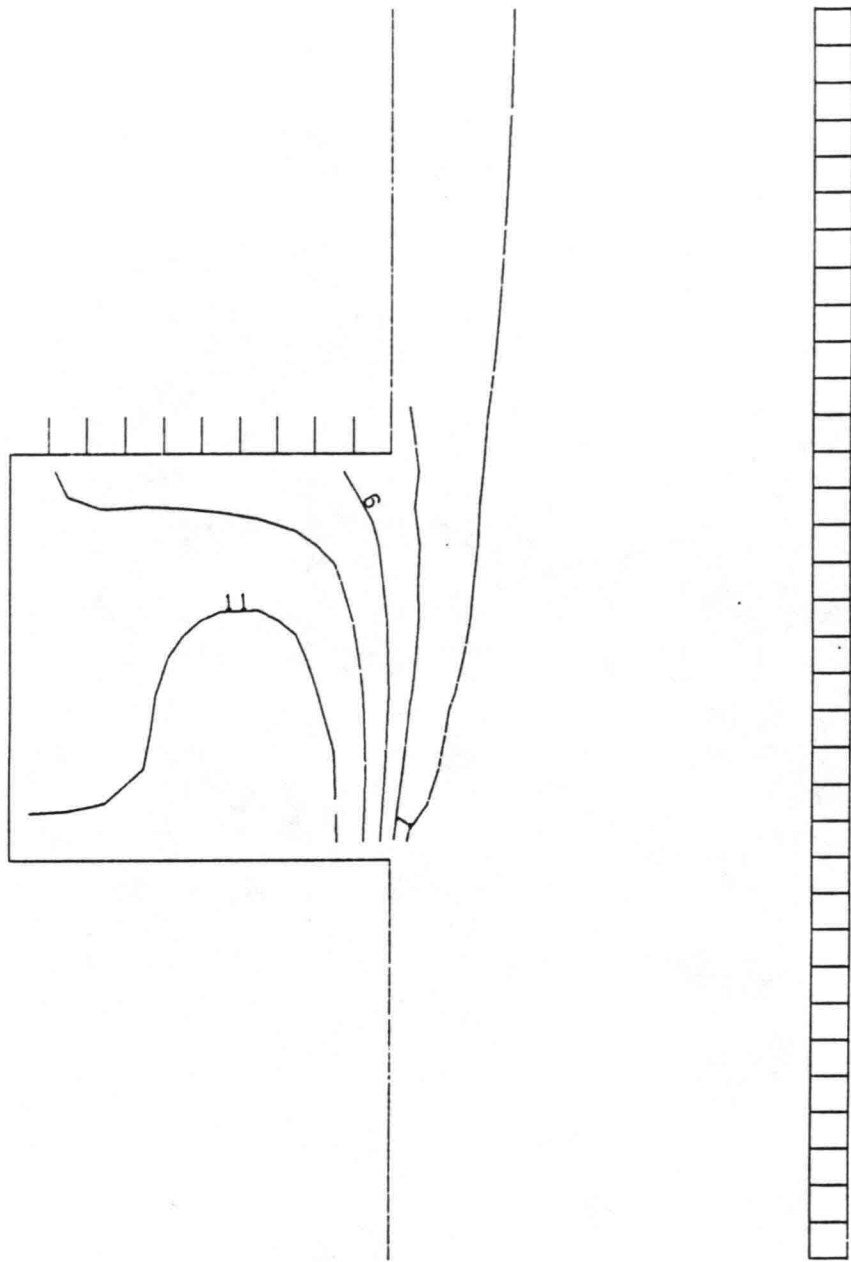
Isolines of the concentration (mg/l) constant dispersion coefficient	TIME = 450.0 s ├──┤ = 0.14 m △ = 2.5 mg/l
Delft University of Technology	Fig. 3.5.d
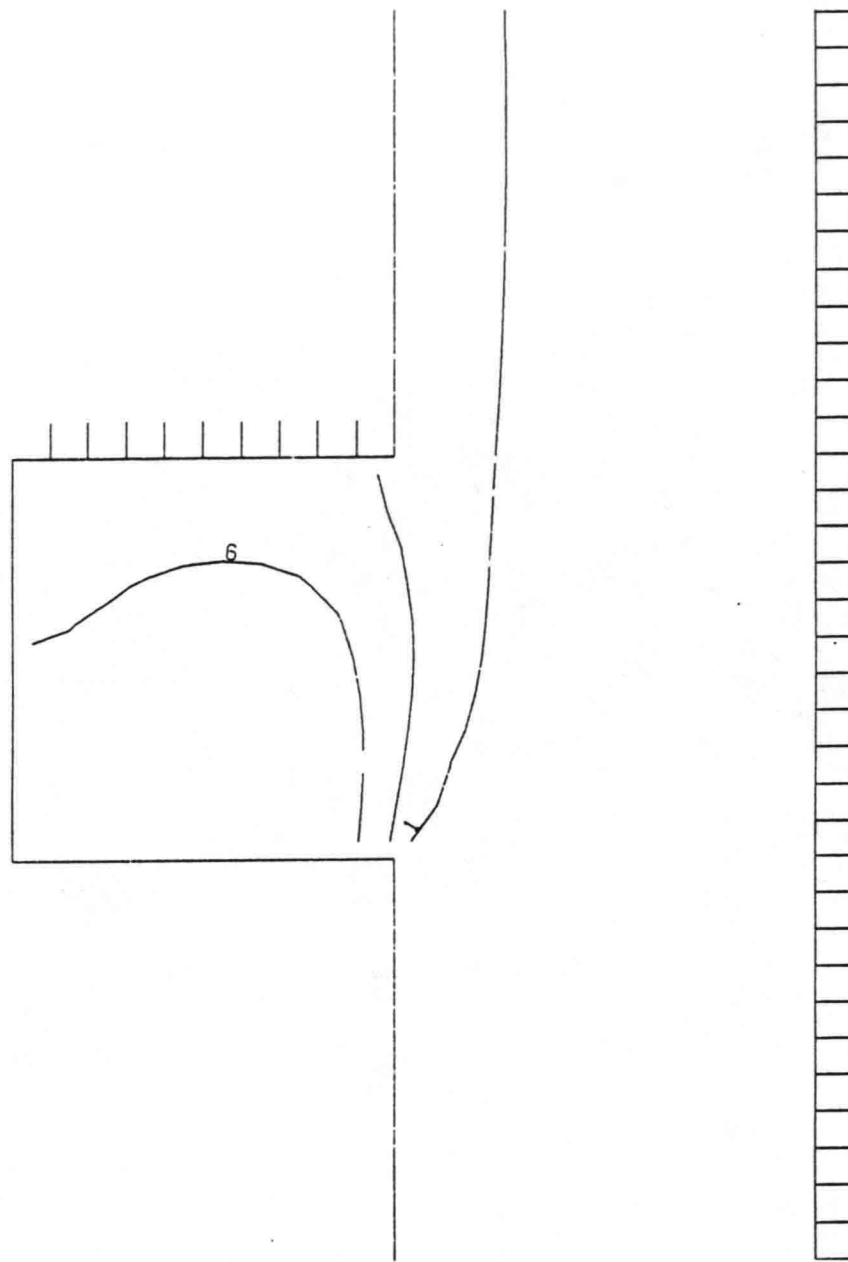
Isolines of the concentration (mg/l)
constant dispersion coefficient

TIME = 475.0 s
⊢——⊣ = 0.14 m
△ = 2.5 mg/l

Delft University of Technology

Fig. 3.5.e
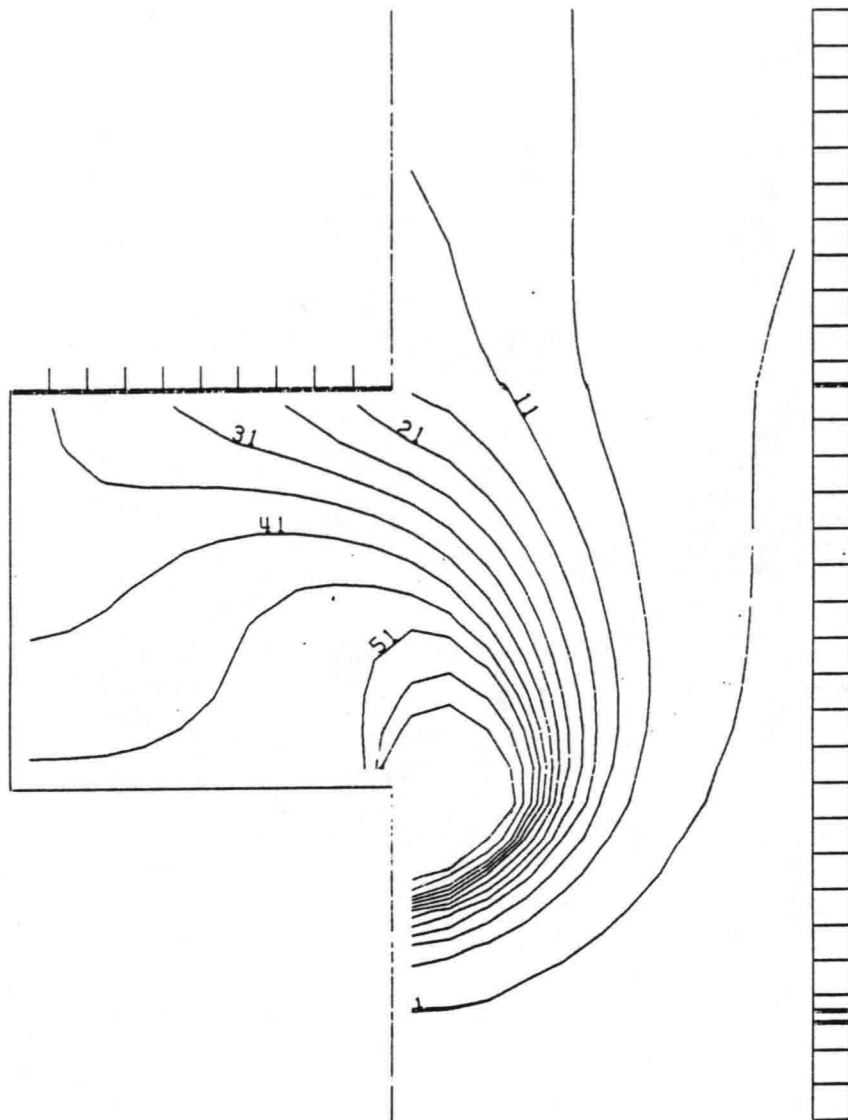
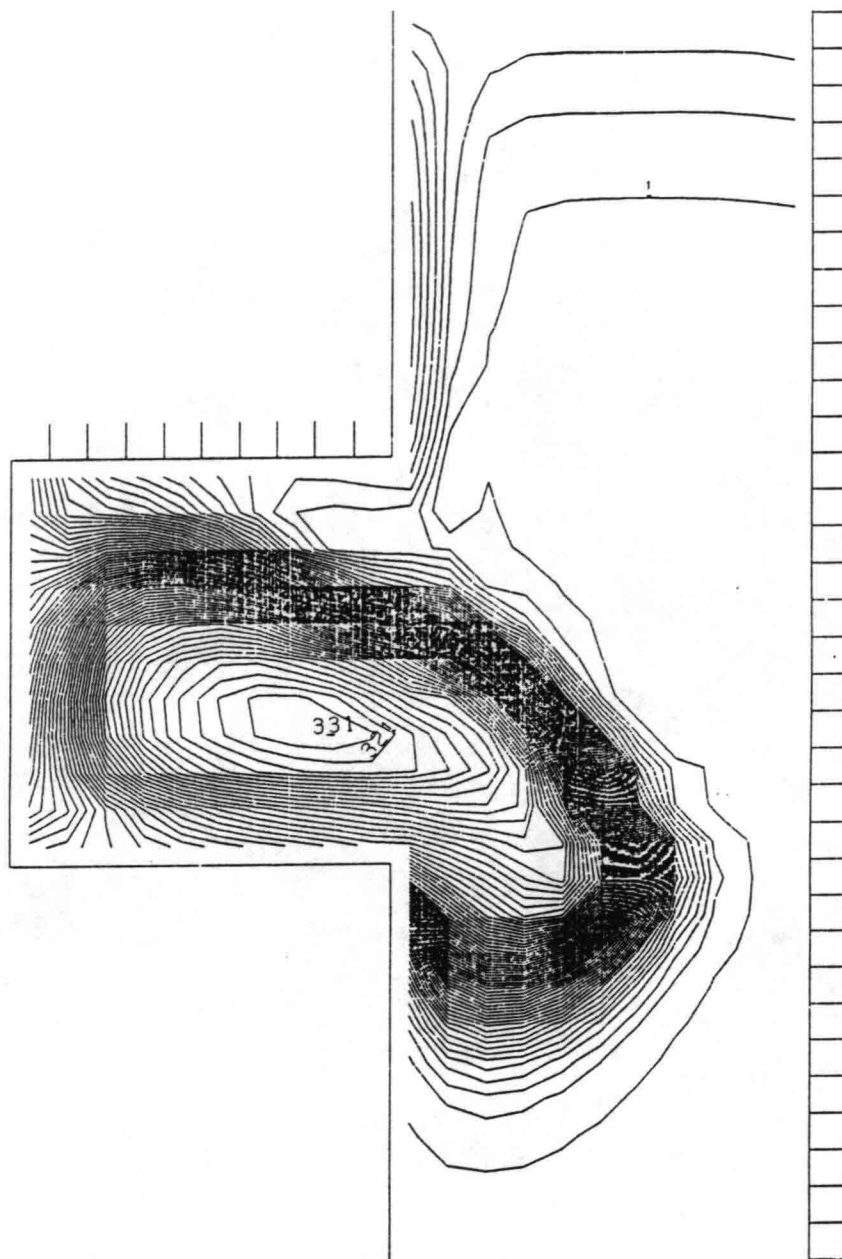|	
Isolines of the concentration (0.1 mg/l) constant dispersion coefficient	TIME = 0.0 s ⊢——⊣ = 0.14 m △ = 0.5 mg/l
Delft University of Technology	Fig. 3.5.f
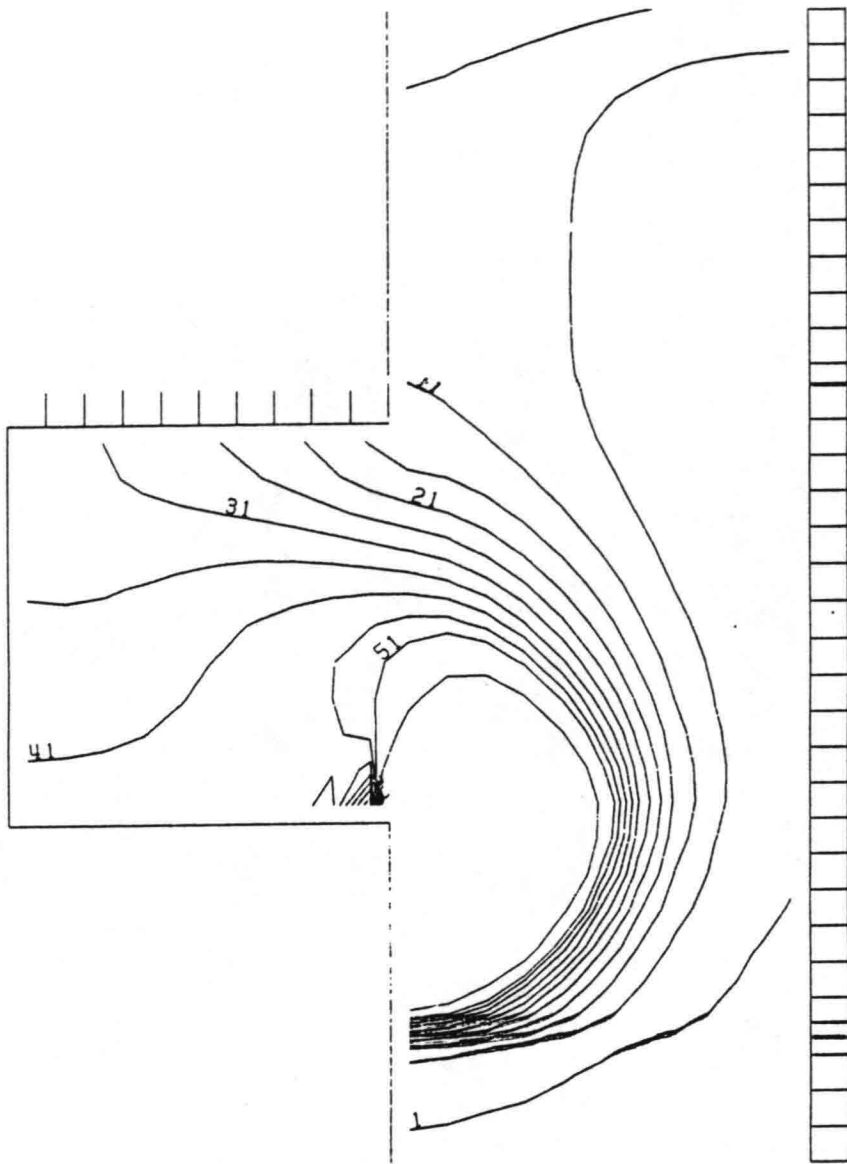
Isolines of the concentration (0.1 mg/l)
constant dispersion coefficient

TIME = 5.0 s
├─┤ = 0.14 m
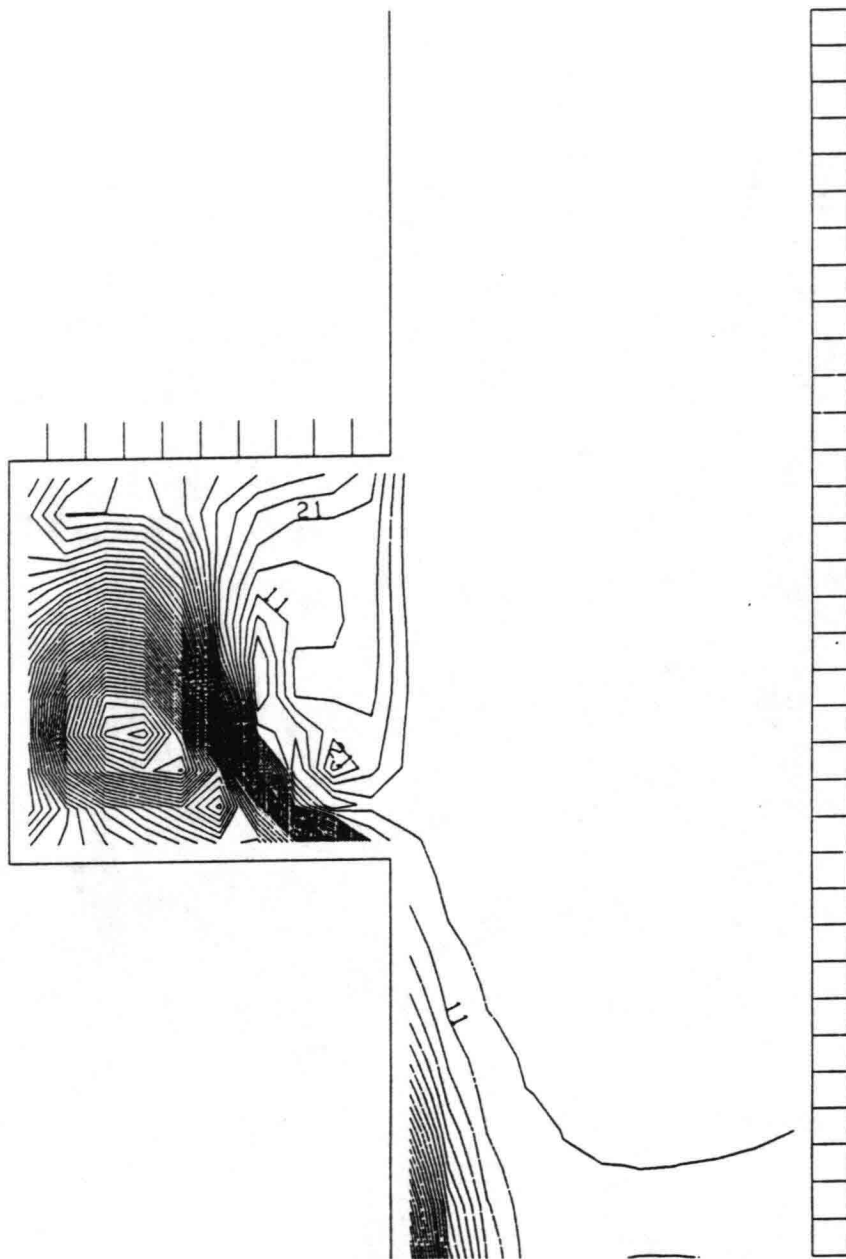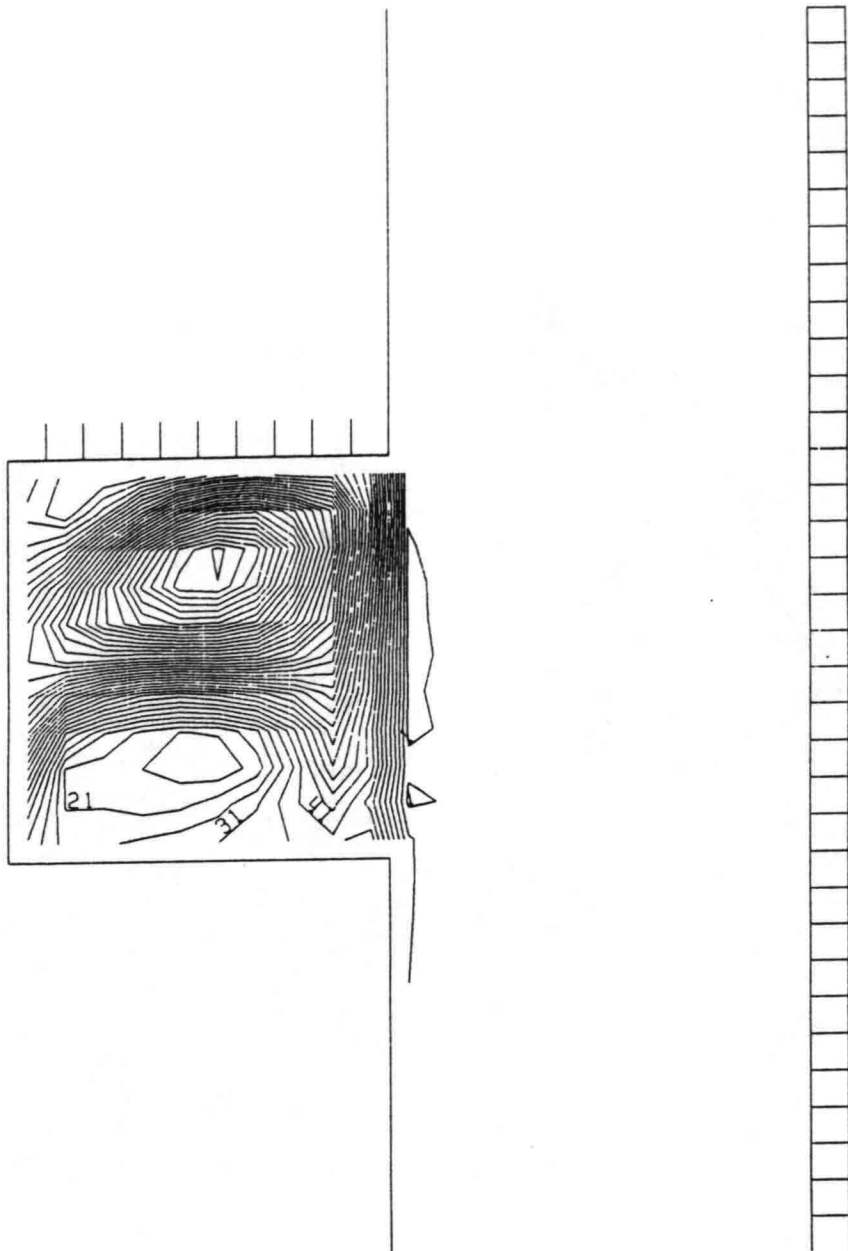△ = 0.5 mg/l

Delft University of Technology

Fig. 3.5.g
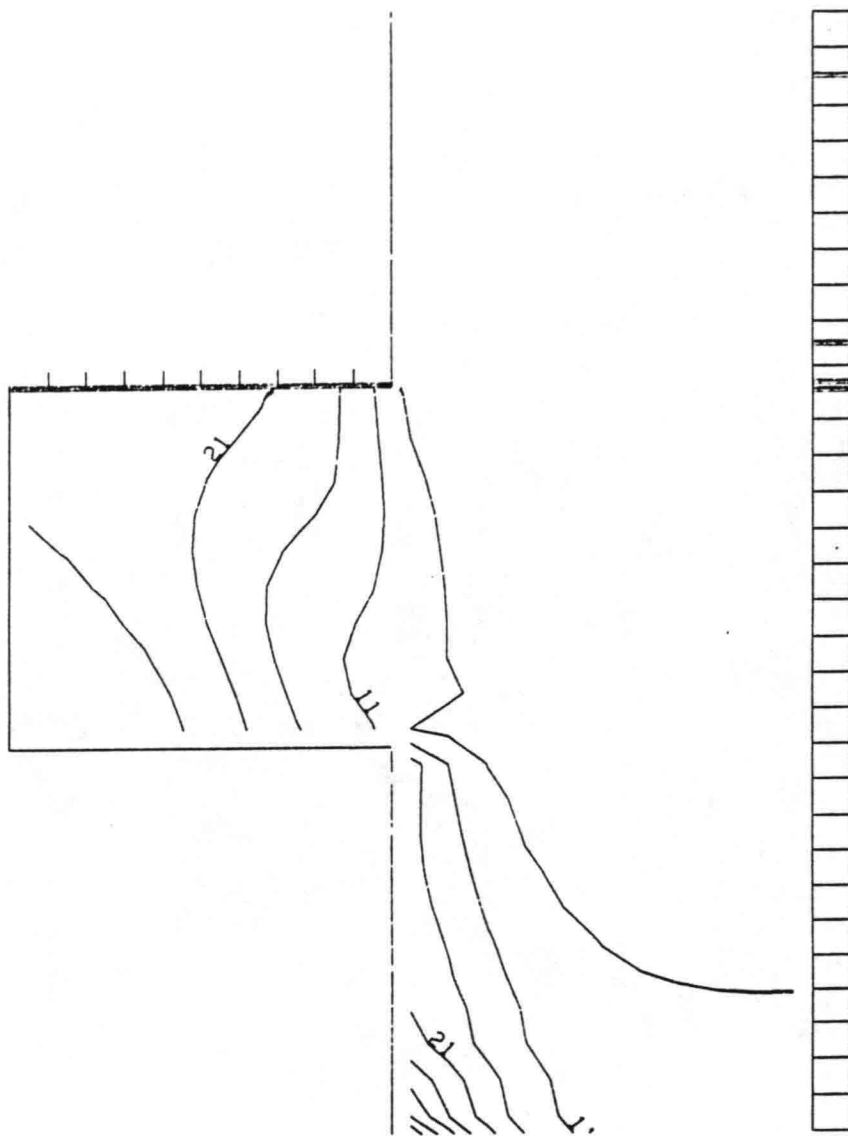
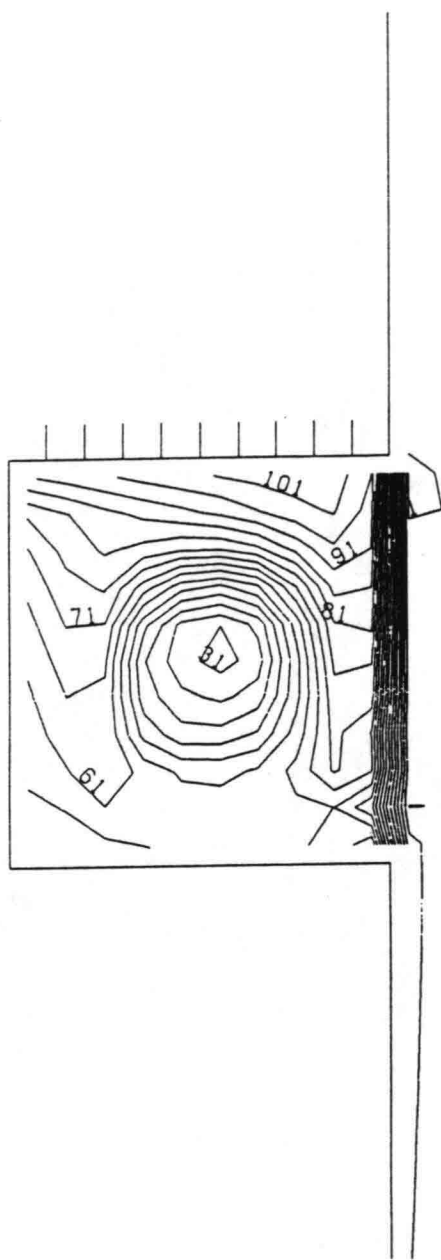| Isolines of the concentration (0.1 mg/l) constant dispersion coefficient	TIME = 35.0 s $\longmapsto$ = 0.14 m $\triangle$ = 0.5 mg/l
Delft University of Technology	Fig. 3.5.h
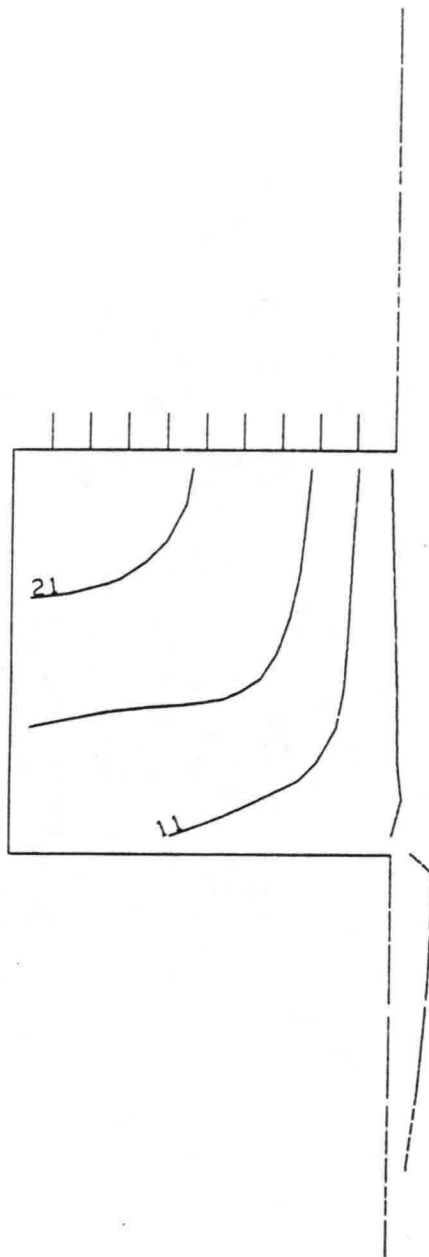
Isolines of the concentration (0.1 mg/l)
constant dispersion coefficient

TIME = 60.0 s
⊢——⊣ = 0.14 m
△ = 0.5 mg/l

Delft University of Technology

Fig. 3.5.i
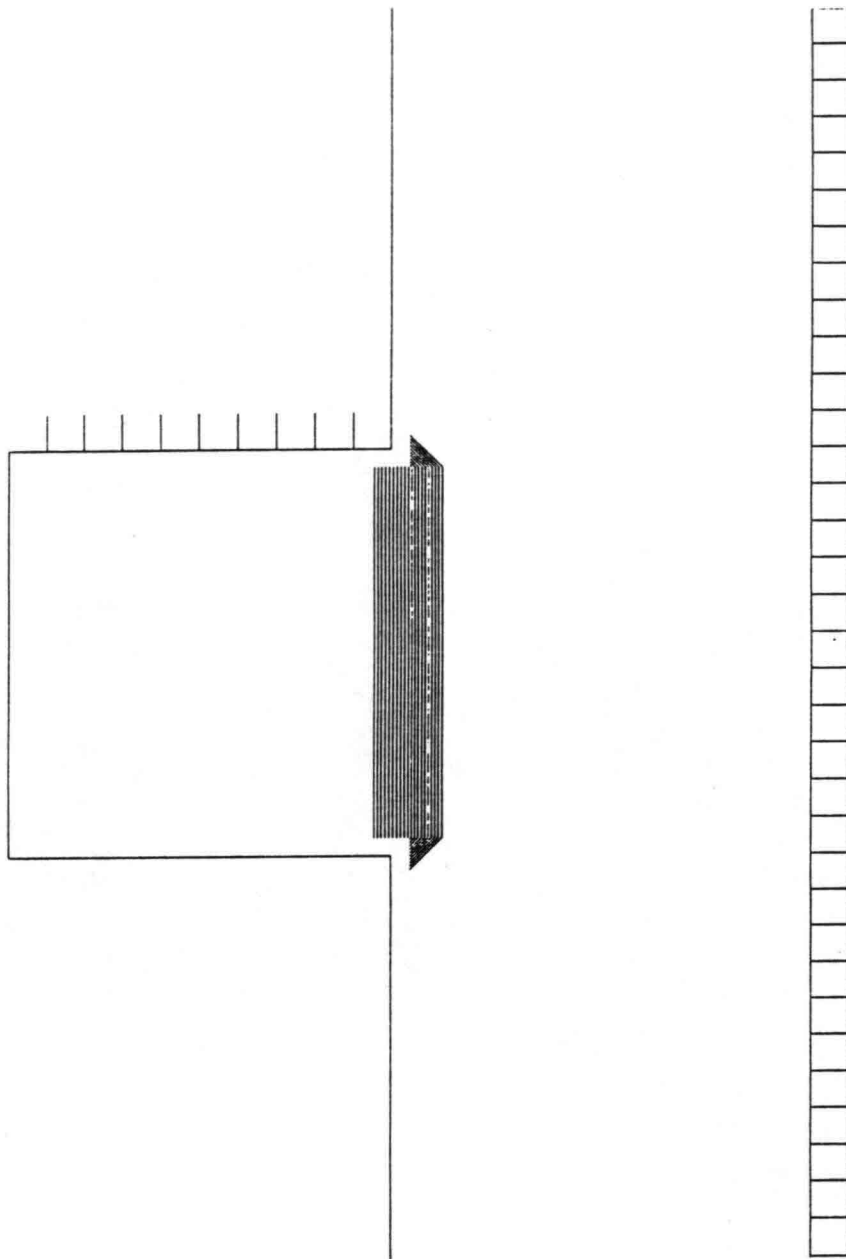
Isolines of the concentration (mg/l) dispersion coefficient according to Elder	TIME = 375.0 s ⊢——⊣ = 0.14 m △ = 2.5 mg/l
Delft University of Technology	Fig. 3.6.a
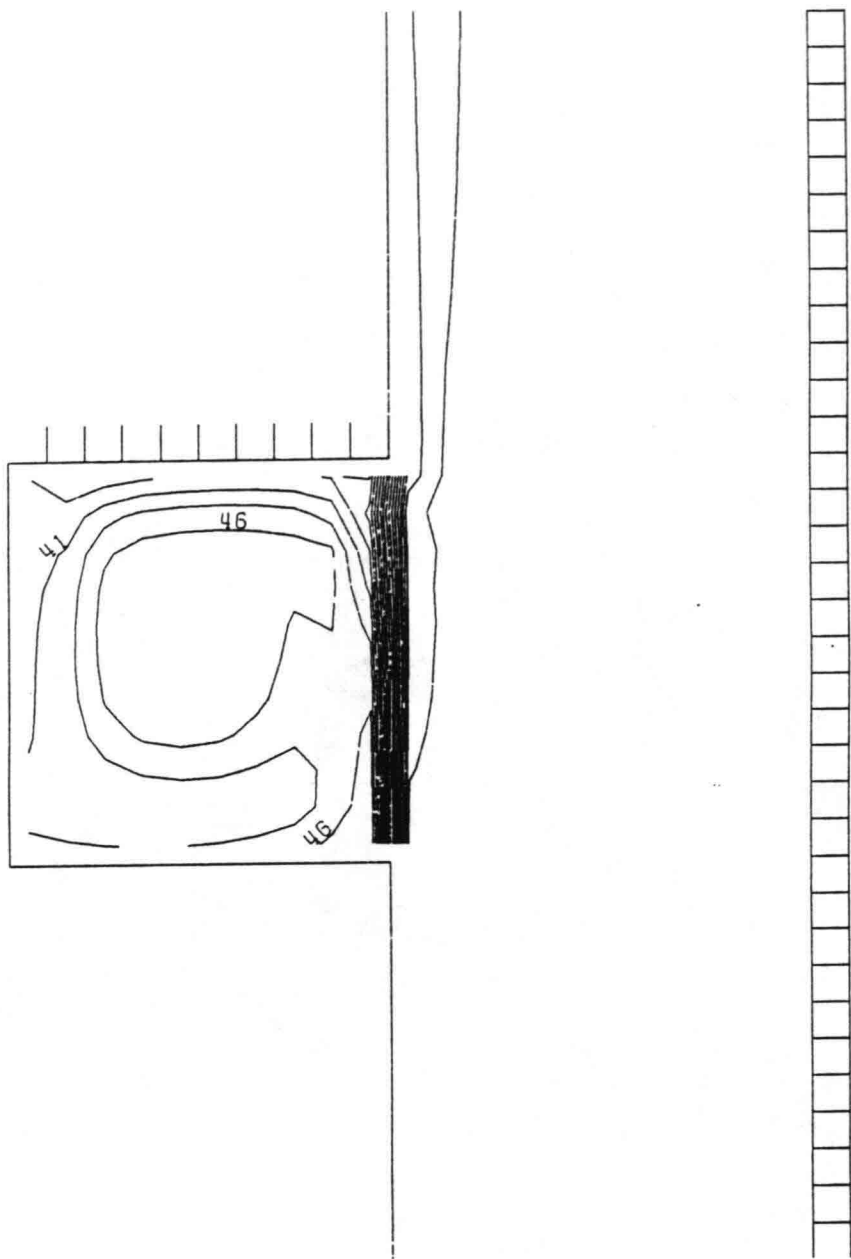
Isolines of the concentration (mg/l)
dispersion coefficient according to Elder

TIME = 400.0 s
⊢——⊣ = 0.14 m
△ = 2.5 mg/l

Delft University of Technology

Fig. 3.6.b
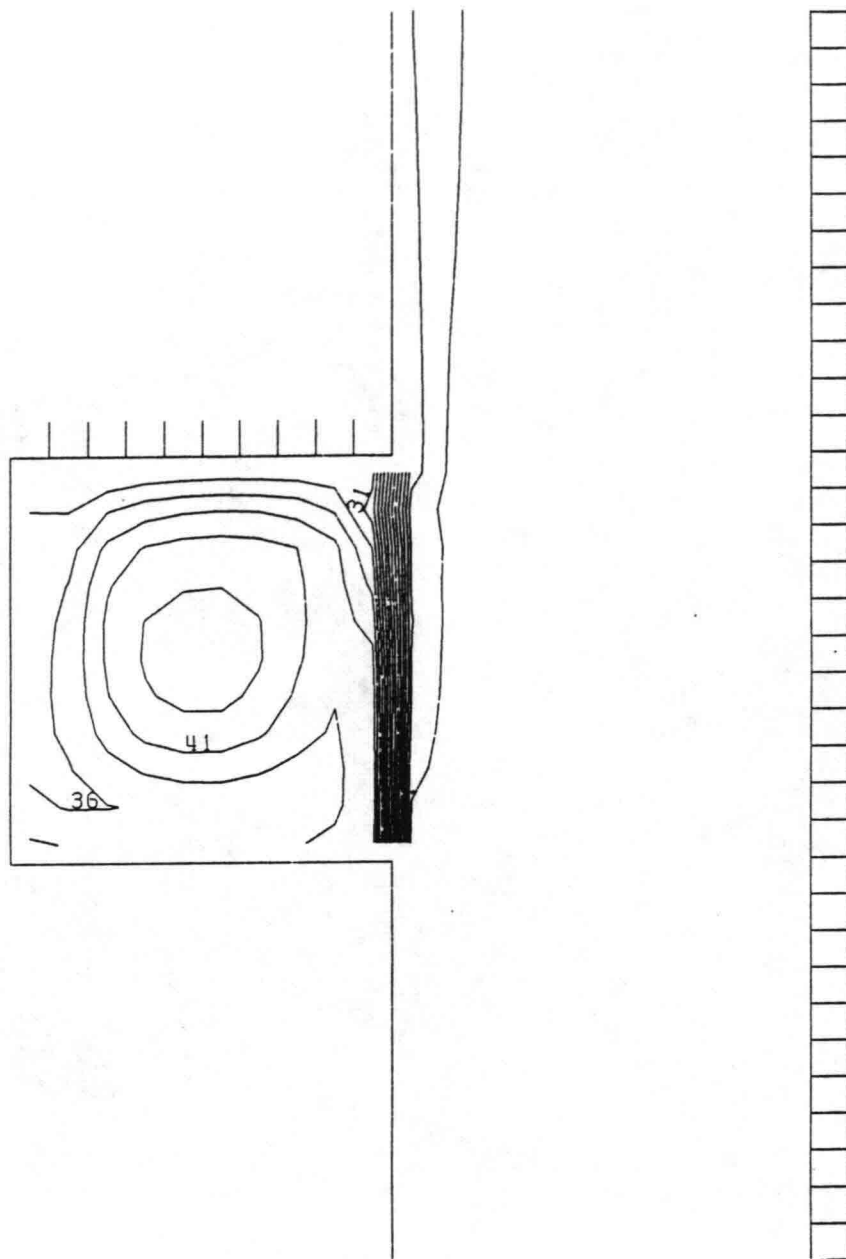
| Isolines of the concentration (mg/l) dispersion coefficient according to Elder	TIME = 425.0 s ⊢—⊣ = 0.14 m △ = 2.5 mg/l
Delft University of Technology	Fig. 3.6.c

Isolines of the concentration (mg/l) dispersion coefficient according to Elder	TIME = 450.0 s ⊢——⊣ = 0.14 m △ = 2.5 mg/l
Delft University of Technology	Fig. 3.6.d

| Isolines of the concentration (mg/l) dispersion coefficient according to Elder | TIME = 475.0 s
⊢——⊣ = 0.14 m
△ = 2.5 mg/l |
| Delft University of Technology | Fig. 3.6.e |

Isolines of the concentration (0.1 mg/l)
dispersion coefficient according to Elder

TIME =   0.0 s
├───┤ = 0.14 m
△ = 0.5 mg/l

Delft University of Technology

Fig. 3.6.f

Isolines of the concentration (0.1 mg/l)
dispersion coefficient according to Elder

TIME = 10.0 s
⊢——⊣ = 0.14 m
△ = 0.5 mg/l

Delft University of Technology

Fig. 3.6.g

Isolines of the concentration (0.1 mg/l) dispersion coefficient according to Elder	TIME = 35.0 s ⊢——⊣ = 0.14 m △ = 0.5 mg/l
Delft University of Technology	Fig. 3.6.h

Isolines of the concentration (0.1 mg/l)
dispersion coefficient according to Elder

TIME = 60.0 s
⊢——⊣ = 0.14 m
△ = 0.5 mg/l

Delft University of Technology

Fig. 3.6.i

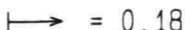| Isolines of the concentration (0.1 mg/l) dispersion coefficient according to Elder	TIME = 110.0 s ⊢——⊣ = 0.14 m △ = 0.5 mg/l
Delft University of Technology	Fig. 3.6.j
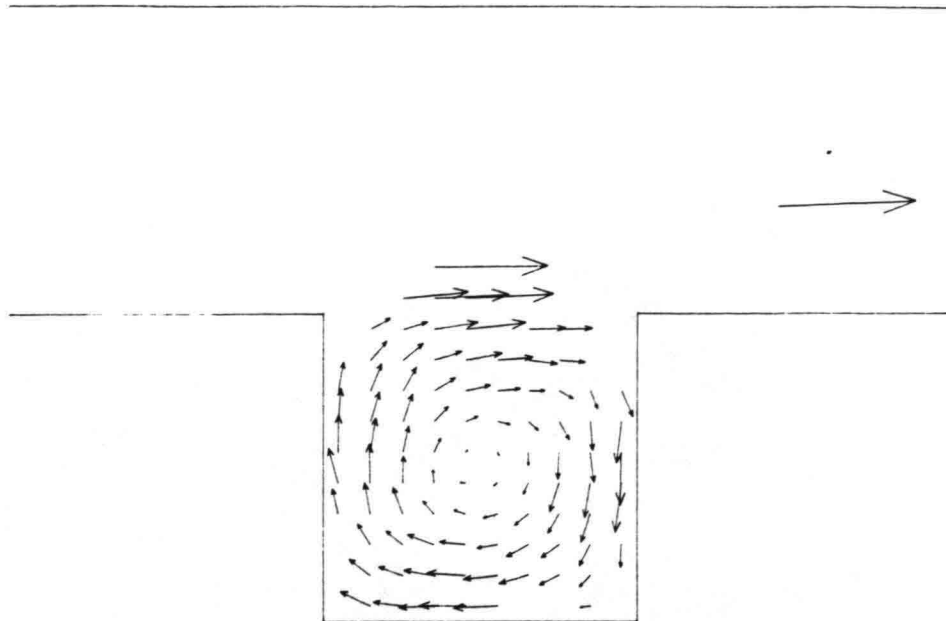
I) Physical model
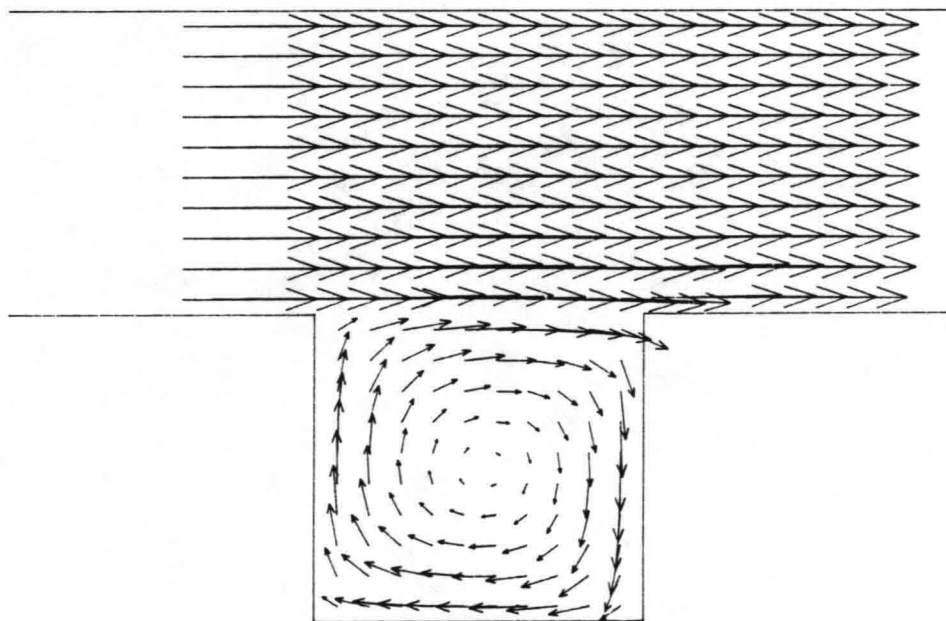
II) Mathematical model

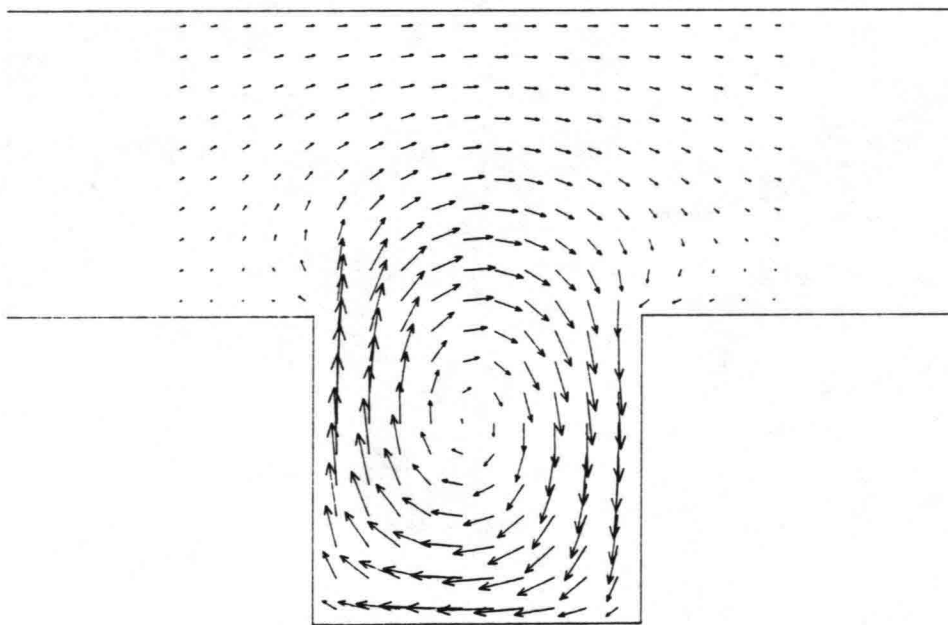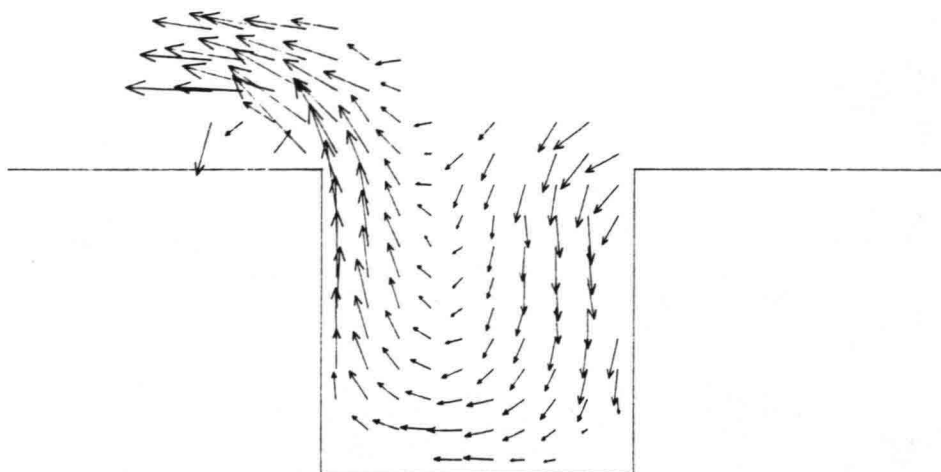| Normalized depth averaged flow patterns in physical and mathematical model.	TIME = 175.0 s ⊢——⊣ = 0.17 m ⊢——▶ = 0.32
Delft University of Technology	Fig. 4.1.a
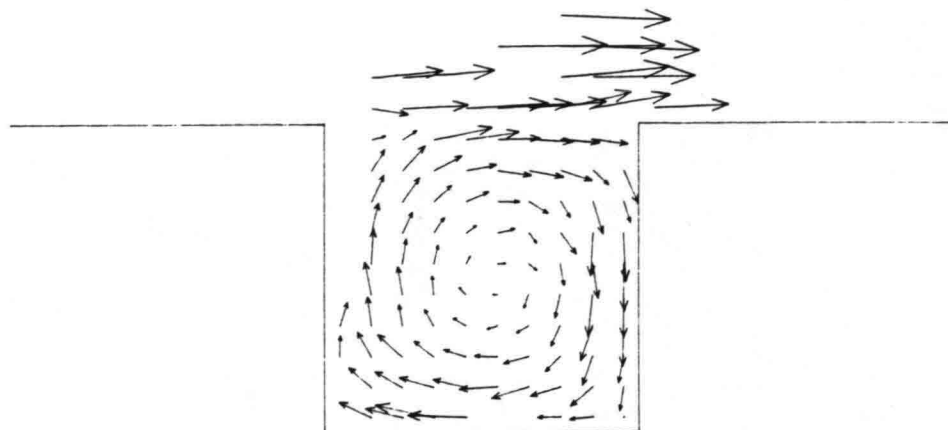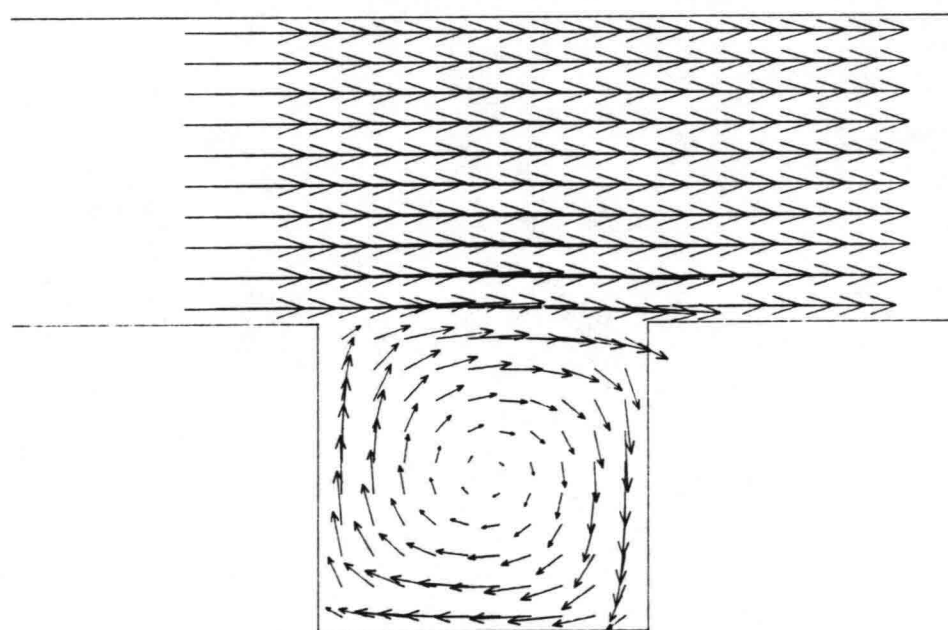
I) Physical model

II) Mathematical model

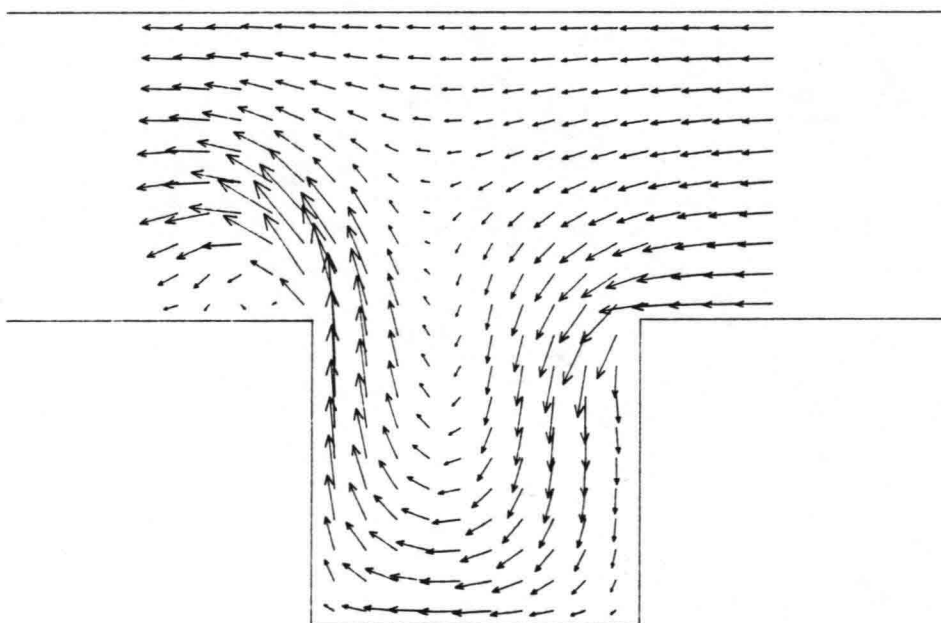| Normalized depth averaged flow patterns in physical and mathematical model.	TIME = 200.0 s ⊢——⊣ = 0.17 m ⊢——→ = 0.27
Delft University of Technology	Fig. 4.1.b
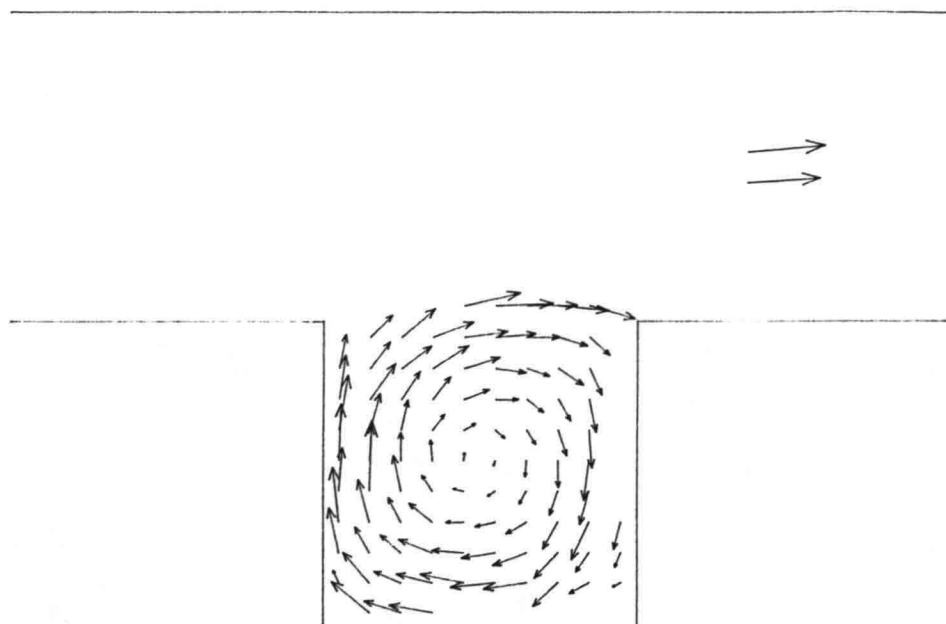
I) Physical model
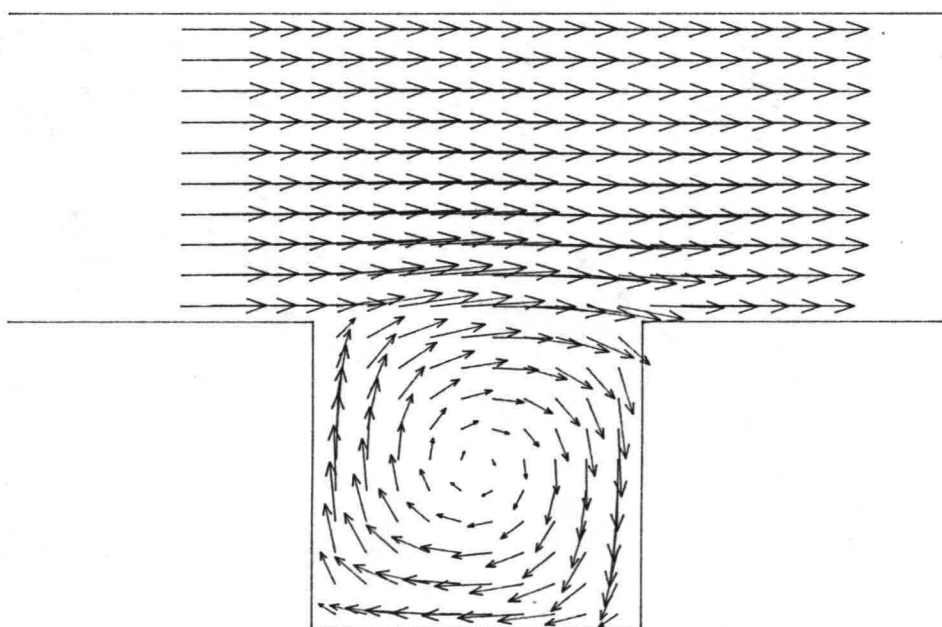
II) Mathematical model

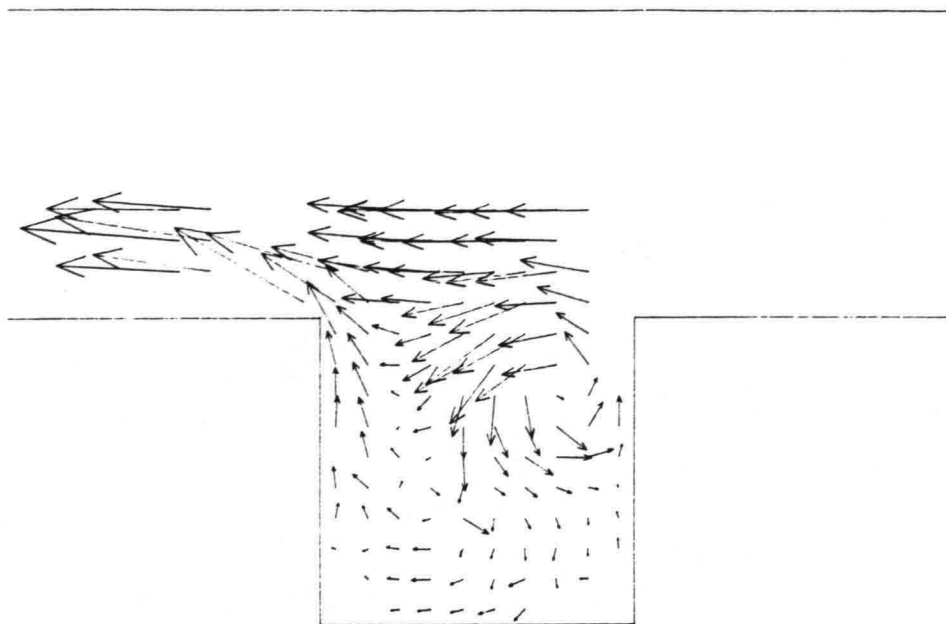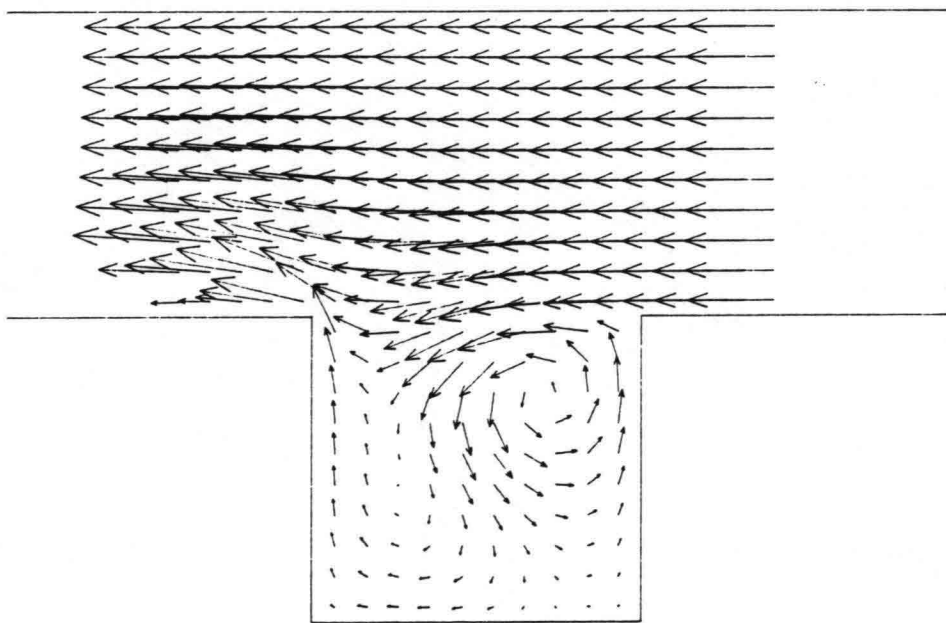| Normalized depth averaged flow patterns in physical and mathematical model.	TIME = 225.0 s ⊢——⊣ = 0.17 m ⊢——→ = 0.20
Delft University of Technology	Fig. 4.1.c
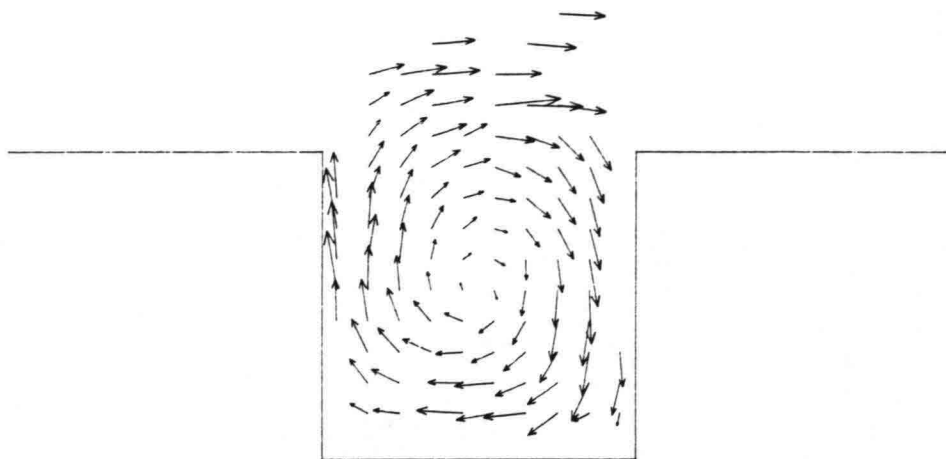
I) Physical model
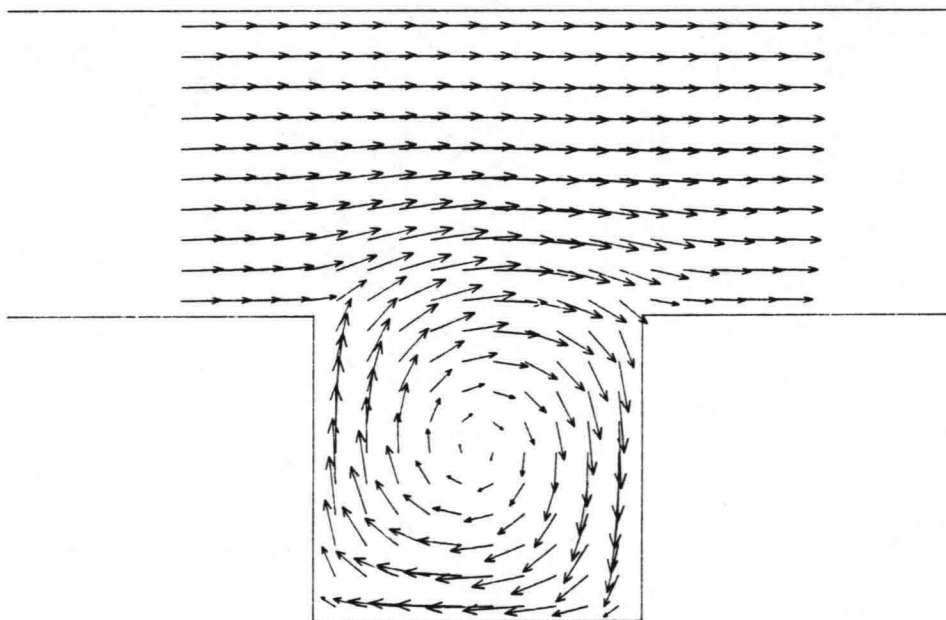
II) Mathematical model

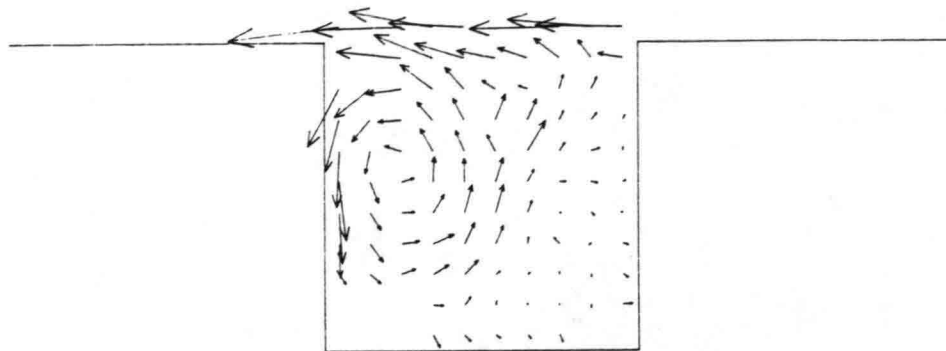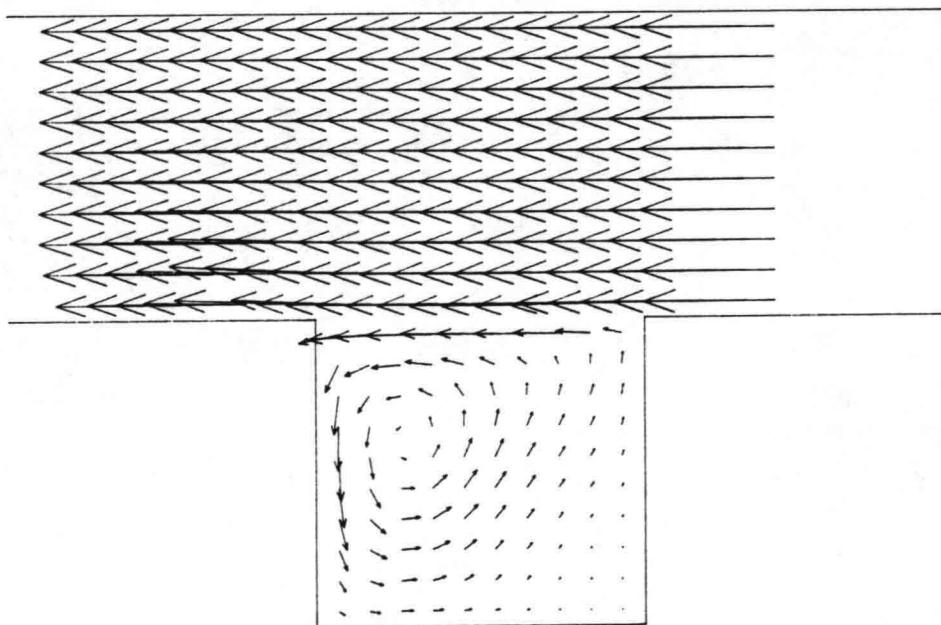| Normalized depth averaged flow patterns in physical and mathematical model.	TIME = 240.0 s
	⊢——⊣ = 0.17 m
	⊢——→ = 0.18
Delft University of Technology	Fig. 4.1.d
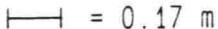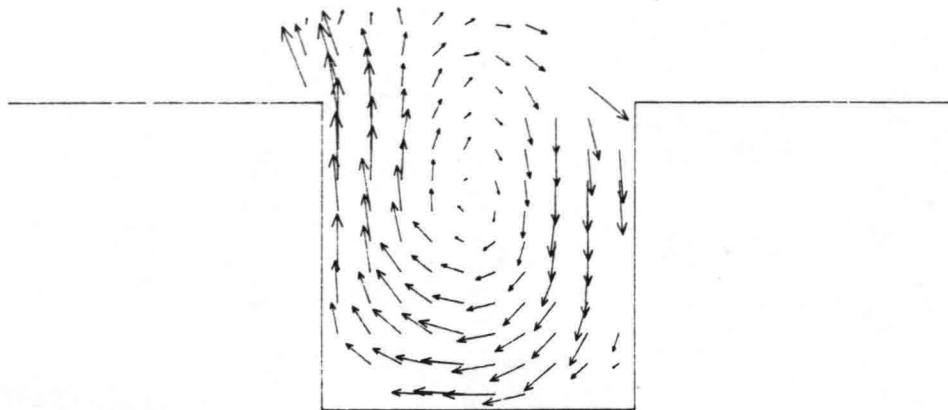
I) Physical model

II) Mathematical model

Normalized depth averaged flow patterns in physical and mathematical model.	TIME = 250.0 s
	⊢——⊣ = 0.17 m
	⊢——➝ = 0.18
Delft University of Technology	Fig. 4.1.e

I) Physical model

II) Mathematical model

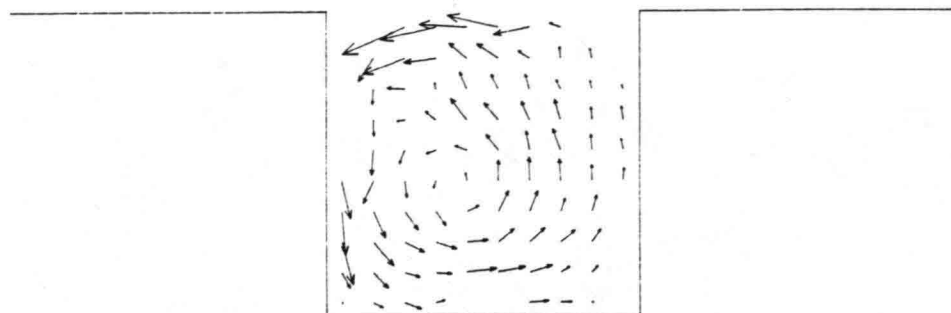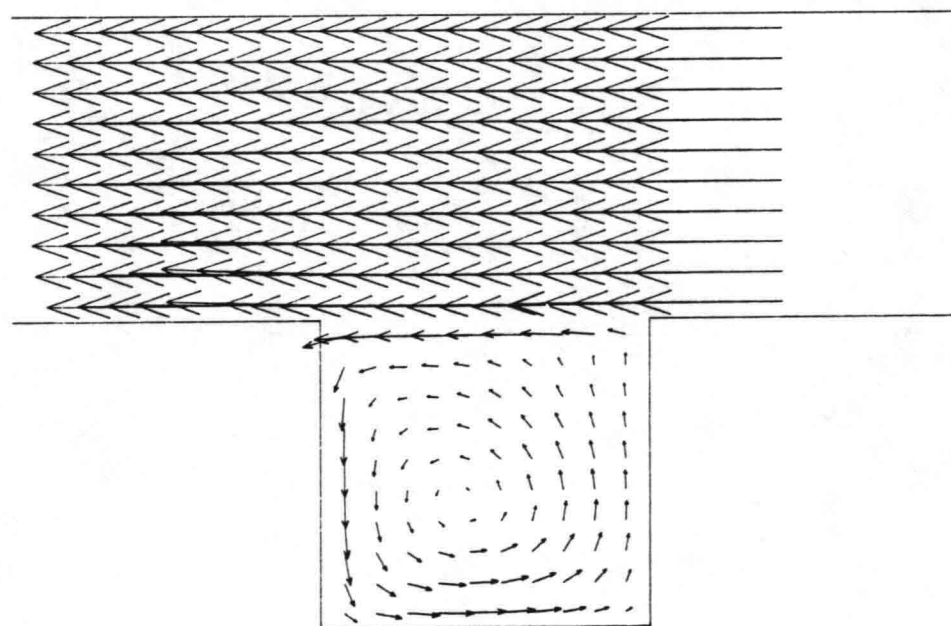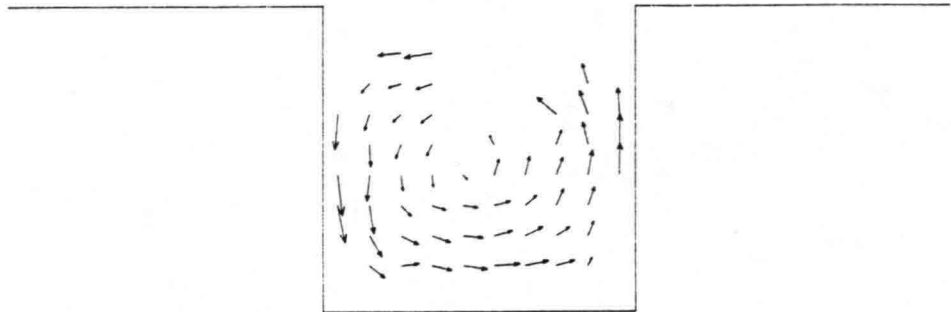| Normalized depth averaged flow patterns in physical and mathematical model.	TIME = 260.0 s ⊢——⊣ = 0.17 m ⊢——→ = 0.18
Delft University of Technology	Fig. 4.1.f

I) Physical model

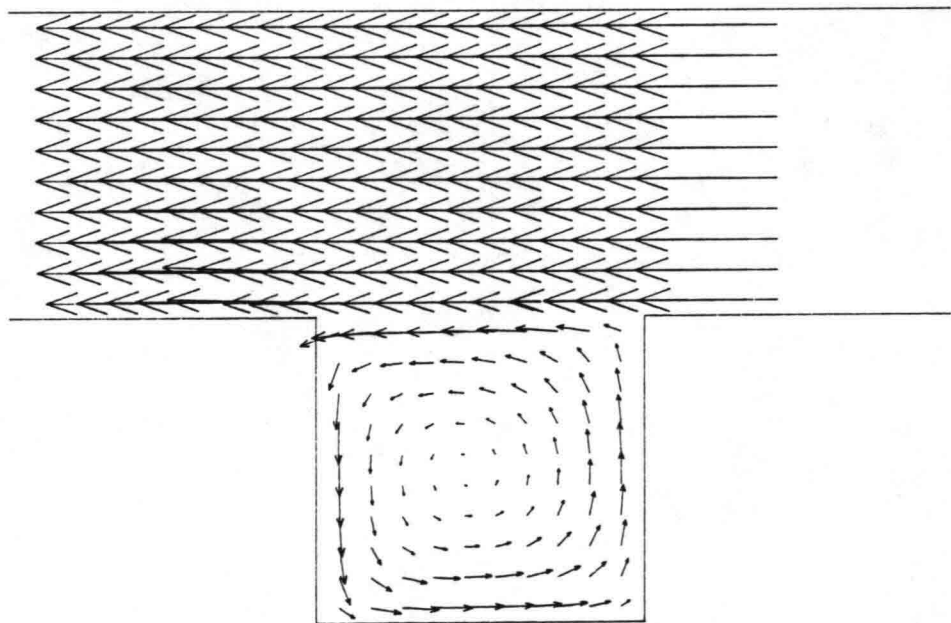II) Mathematical model

Normalized depth averaged flow patterns in physical and mathematical model.	TIME = 275.0 s ⊢——⊣ = 0.17 m ⊢——→ = 0.18
Delft University of Technology	Fig. 4.1.g

I) Physical model

II) Mathematical model

| Normalized depth averaged flow patterns in physical and mathematical model.	TIME = 300.0 s ⊢——⊣ = 0.17 m ⊢——→ = 0.23
Delft University of Technology	Fig. 4.1.h

I) Physical model

II) Mathematical model

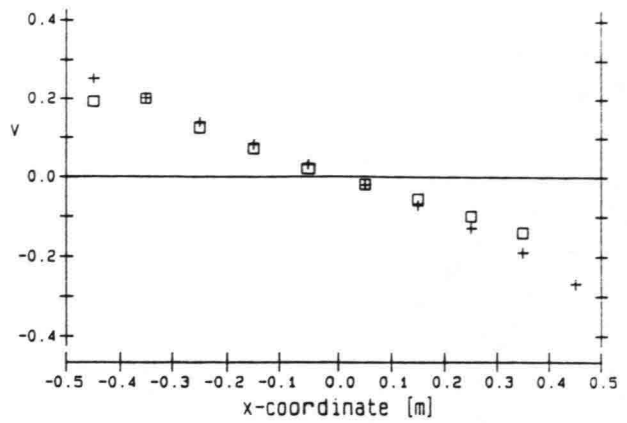| Normalized depth averaged flow patterns in physical and mathematical model.	TIME = 325.0 s ⊢——⊣ = 0.17 m ⊢——▶ = 0.29
Delft University of Technology	Fig. 4.1.i

I) Physical model

II) Mathematical model

Normalized depth averaged flow patterns in physical and mathematical model.	TIME = 350.0 s ⊢——⊣ = 0.17 m ⊢——▸ = 0.36
Delft University of Technology	Fig. 4.1.j
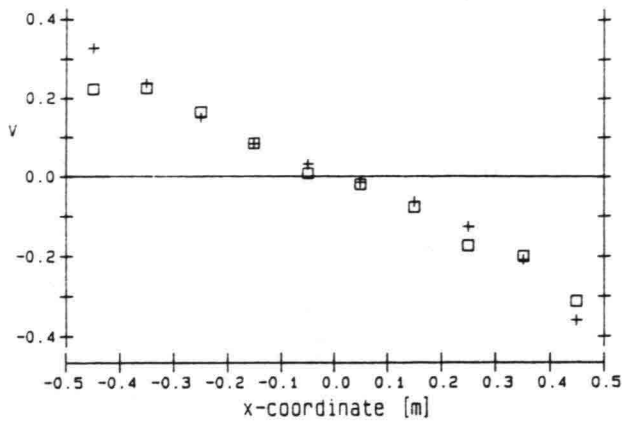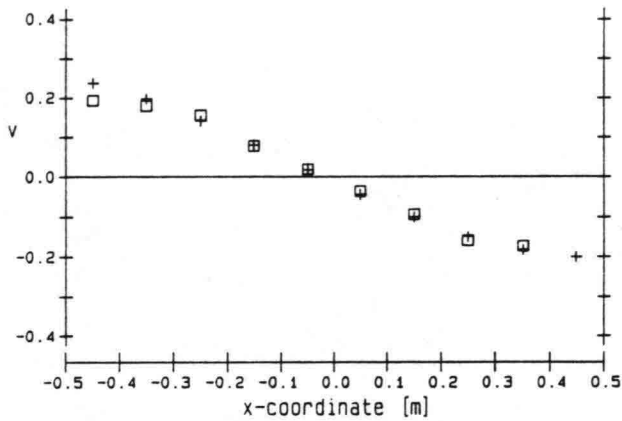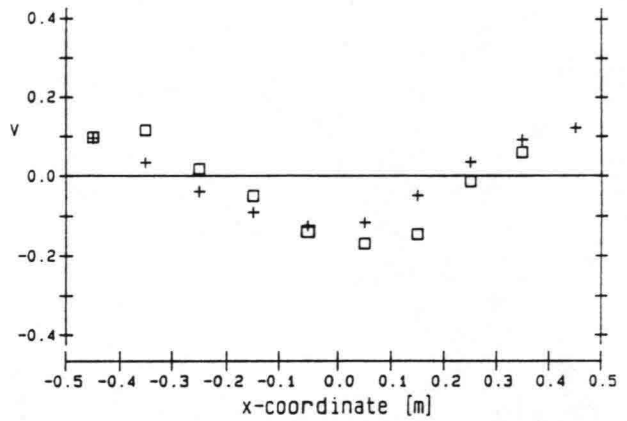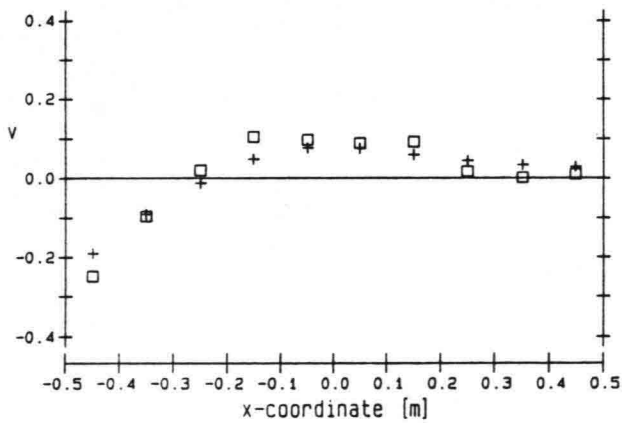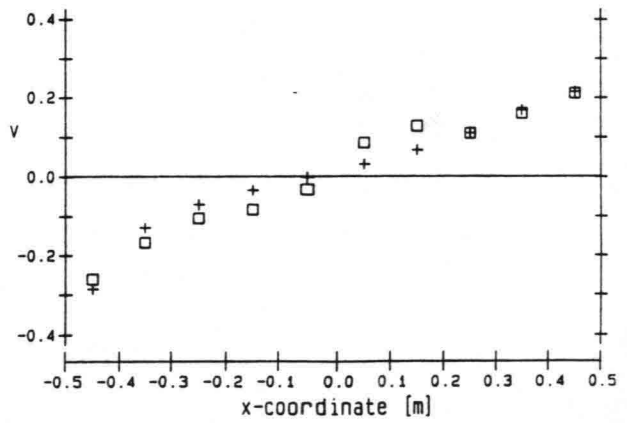
Normalized velocity profiles along a transect in x-direction through the center of the eddy.

□ = measured
+ = computed

Delft University of Technology

Fig. 4.2